A FIELD COMPARISON OF IN SITU METEOROLOGICAL SENSORS

J. C. Kaimal
J. E. Gaynor
P. L. Finkelstein
M. E. Graves
T. J. Lockhart

Report Number Six
December 1984

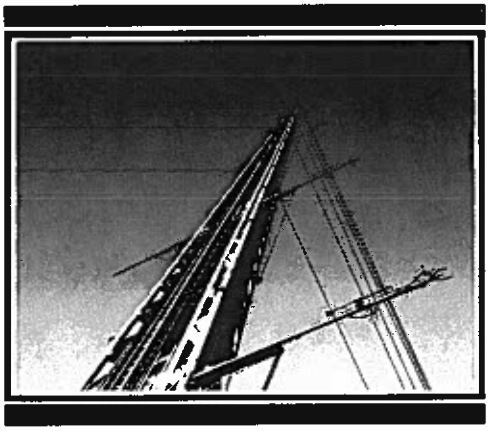

NOAA
Boulder Atmospheric Observatory

U.S. Department of Commerce
National Oceanic and Atmospheric Administration
Environmental Research Laboratories

A NOAA publication available from NOAA/ERL, Boulder, CO 80303.

A FIELD COMPARISON OF IN SITU METEOROLOGICAL SENSORS

by

J. C. Kaimal and J. E. Gaynor
NOAA/ERL/Wave Propagation Laboratory
Boulder, Colorado 80303

P. L. Finkelstein*
Environmental Protection Agency
Research Triangle Park, North Carolina 27711

M. E. Graves
Northrop Services, Inc.
Research Triangle Park, North Carolina 27709

T. J. Lockhart**
Meteorology Research, Inc.
Altadena, California 91001

This study was conducted for
U.S. Environmental Protection Agency
under Interagency Agreement No. DW1-3F2A059

Wave Propagation Laboratory
Environmental Research Laboratory
U.S. Department of Commerce
Boulder, Colorado 80303

* On assignment from National Oceanic and Atmospheric Administration

** Present Affiliation: Meteorological Standards Institute
Fox Island, Washington 98333

NOTICE

Acquisition of information provided in this document was funded in part by the United States Environmental Protection Agency under Interagency Agreement No. DW1-3F2A059. This study was conducted jointly by NOAA/Environmental Research Laboratory and the Environmental Protection Agency.

Mention of a commercial company or product does not constitute an endorsement by NOAA/Environmental Research Laboratories or the Environmental Protection Agency.

CONTENTS

ABSTRACT

Measurements of wind speed, wind direction, and the vertical wind component from five conventional in situ meteorological systems were compared with similar measurements from a fast-response sonic anemometer. The systems tested were an orthogonal three-axis propeller anemometer, a light bivane and cup anemometer, a bivane propeller anemometer, a light cup and vane with a vertical propeller, and a vane-mounted propeller anemometer with a vertical propeller. Computed accuracy and field precision variables measured by each system are presented. The response characteristics of the sensors tested are discussed.

FIGURES

TABLES

ACKNOWLEDGMENTS

The authors acknowledge the valuable contributions made by David McSorley, Janet Lockhart, Joan Hart, Jim Newman, Daniel Wolfe, Norbert Szczepczynski, Leslie Mosley, and Mary Sue Phillips to the field experiment and to the analysis of the data. The experiment and the data analysis were sponsored by the U.S. Environmental Protection Agency under Interagency Agreement No. DW1-3F2A059.

1. INTRODUCTION

It has recently become clear through advances in both theoretical and experimental meteorology, that improvements in modeling the transport and dispersion of pollutants will require on-site measurements of the atmosphere. This requirement has in turn generated questions about our ability to make such measurements. To help answer these questions the Environmental Protection Agency sponsored at NOAA's Boulder Atmospheric Observatory (BAO) an experiment designed to assess the ability of in situ and remote sensors to measure the mean and turbulent properties of the lower atmosphere. The tests were carried out over a 3 week period in September 1982. They were designed and conducted with the goal of gaining a knowledge of the accuracy, precision, and general performance characteristics of a variety of meteorological sensors that are commonly used in environmental studies. The results should prove valuable in designing experiments, understanding data from field studies, and interpreting the inherent limits of accuracy and precision possible in transport and diffusion models.

The BAO was chosen as the site for the experiment because of the availability of precise profile and turbulence data from accurate fast-response sensors on a 300 m tower, as well as comprehensive data-logging facilities (Kaimal and Gaynor, 1983). Two categories of sensors were tested. One consisted of lightweight in situ sensors of types that have been frequently used in the recent past for boundary layer studies. The other category consisted

of four commercially available Doppler sodars, with the capability to measure wind speed, wind direction, and vertical component of turbulence, all at various heights above the ground. The sodar comparison has been described by Kaimal et al. (1984). This report deals only with the in situ instrument comparison.

2. DESCRIPTION OF THE FIELD EXPERIMENT

The sensors were selected to provide a measure of turbulence in addition to mean speed and direction at 10 m above the ground. The systems compared in this study (see Table 1) were selected because they represent types commonly used in meteorological monitoring programs related to air pollution. The selection was also made to include all usual configurations of instruments capable of describing three-dimensional flow. The reference standard for comparison was the BAO three-axis sonic anemometer, noted as SONIC throughout this report and placed on Tower 4.

Table 1. Instrument selection summary

Tower no.	Designation	Sensor type	Manufacturer
1	U-V-W	Gill UVW propeller	R.M. Young Co.
2	C-BIV	Bivane and cup	Meteorology Research, Inc.
3	P-BIV	Propeller bivane	R.M. Young Co.
4	SONIC	Sonic anemometer	Applied Technology, Inc.
5	C-V-W	Cup and vane Vertical propeller	Climatronics, Inc. R.M. Young Co.
6	P-V-W	Propeller vane Vertical propeller	R.M. Young Co. R.M. Young Co.

The instruments were mounted on 10 m towers, erected in a line to the west of the 300 m BAO tower (see Figs. 1 and 2). Each tower held a different

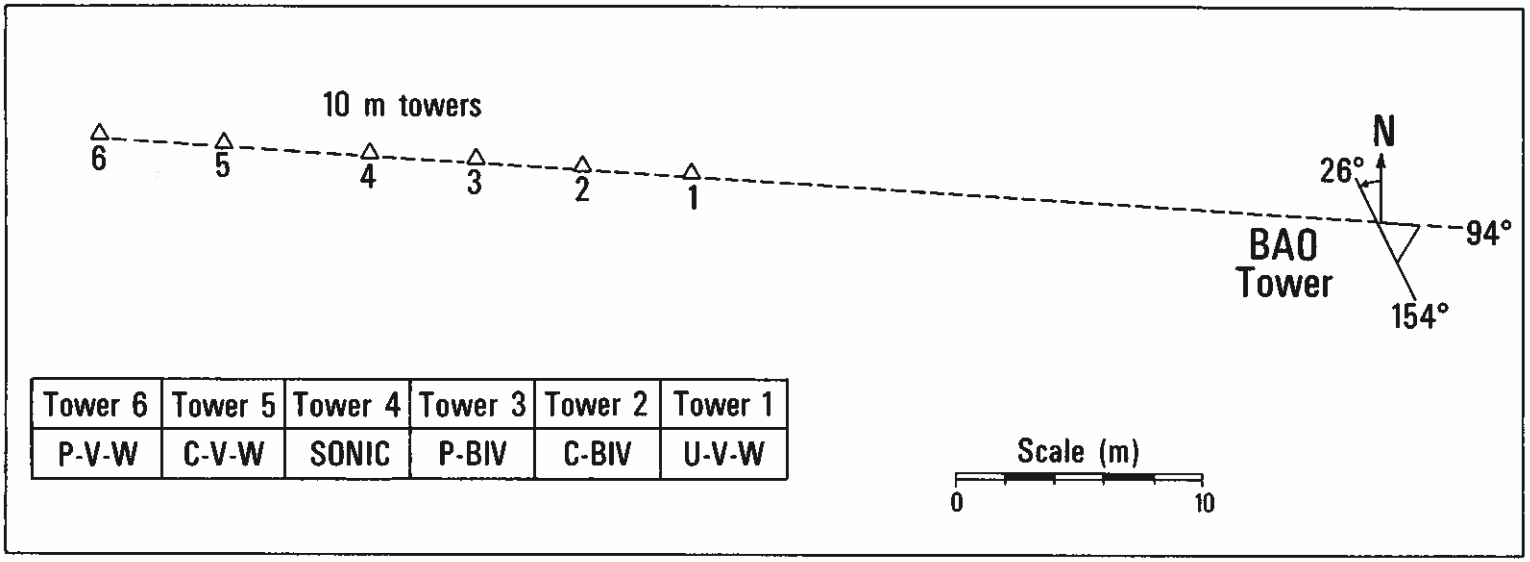

Figure 1. Location of the 10-m towers at the BAO site and the in situ wind sensors they support.

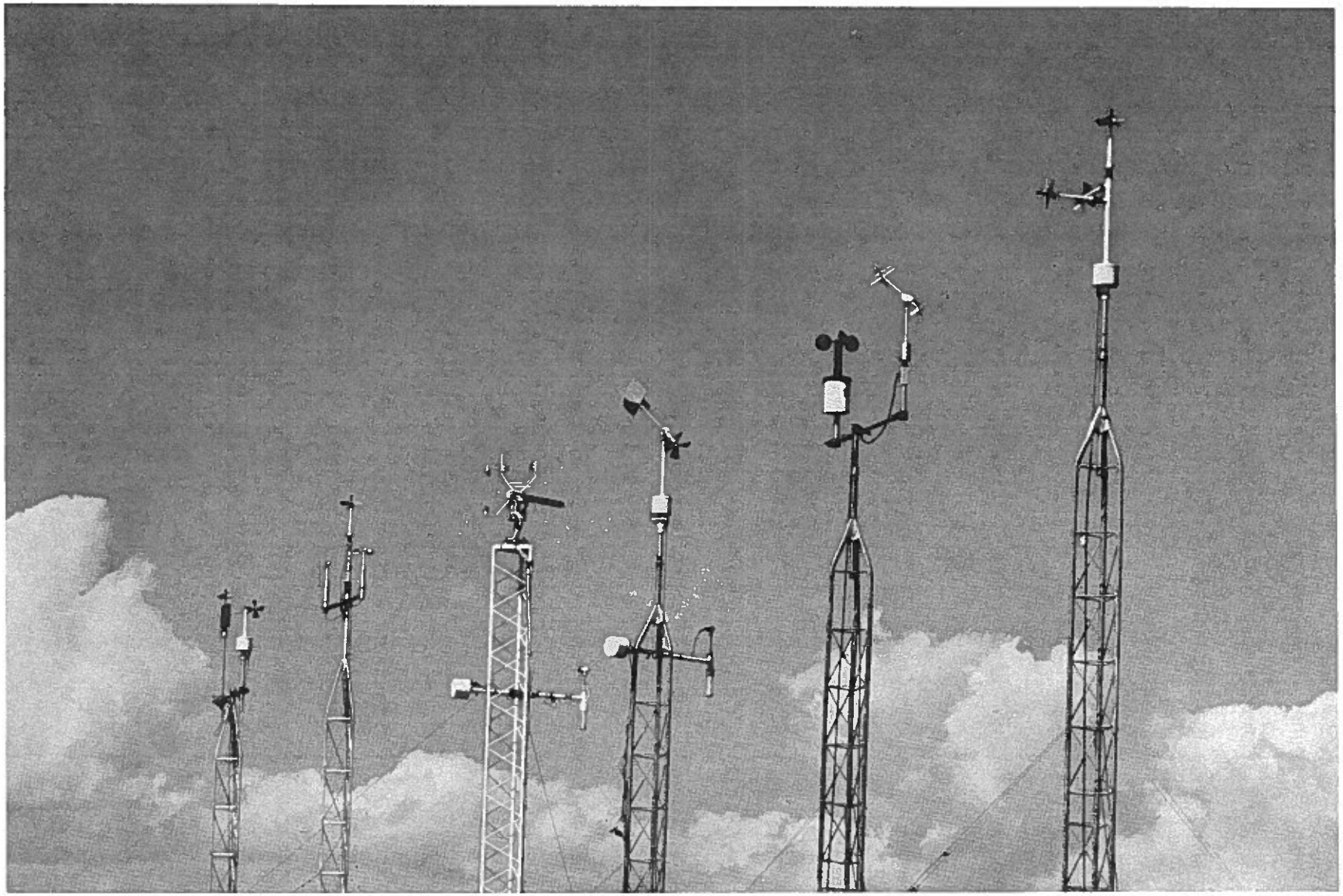

Figure 2. Sensors on the 10 m tower, viewed from the east.

instrument set. The installation of the instruments was intended to simulate the best practice found in operational field programs and not the best possible practice if money were of no concern. Various levels of quality control checks were used to achieve the best practical results, including daily review of instrument performance. One benefit of the program was the evaluation of the quality control procedures, calibration checks, and operational methods.

The sensors on the towers, going from east to west, are described in detail below.

2.1 Tower 1

The sensor mounted on this tower was a Gill UVW (U-V-W) anemometer (Fig. 3) manufactured by the R. M. Young Company, Traverse City, Michigan. It has three helicoid propeller anemometers oriented north-south, east-west, and up-down. The implied assumption when fixed propellers are used is that they have a nearly cosine response and will respond linearly to the component of the wind vector parallel to their axis of rotation. How well they perform is one of the questions to be answered by this study.

The propeller selected was made of polystyrene with 19 cm diameter and 0.30 m pitch. This propeller offers a good compromise between response and durability. The distance constant is listed by the manufacturer as 0.8 m (63% recovery) and the starting threshold as 0.3 m/s. It should be remembered that the starting threshold relates to the component of wind parallel to the turning axis of the propeller and not to the wind speed. Each propeller is flexibly coupled to a small d.c. generator. The output voltage was carried to

the BAO instrument trailer (about 42 m away) through signal cables, which were connected to a standard R. M. Young translator. Here the sensor signal was noise filtered and amplified to provide a linear output of 0.100 volts per m/s. The W propeller was scaled to a different pitch than the U or V propeller, even though the propellers are identical, in order to compensate for the non-cosine response when the wind is nearly perpendicular to the axis of rotation. This practice is recommended by the manufacturer.

2.2 Tower 2

This tower held two instruments (C-BIV) manufactured by Meteorology Research, Inc. of Altadena, California (see Fig. 4). The wind vane was a Model 1041 bivane with freedom to turn 360 degrees in azimuth and ±60 degrees in elevation. The bivane has a front damping vane to improve performance. The manufacturer lists a damping ratio of 0.6 for this instrument and a delay distance (50% recovery) of 0.3 m. The sensor output is a resistance proportional to the vane shaft position.

The anemometer was a Model 1074 speed and direction sensor from which the direction vane had been removed. This cup anemometer provided the mean horizontal wind speed measurement with which the azimuth and elevation wind direction measurements could be transformed to vector components. It has rather large cups, which have a response distance (63% recovery) of about 5 m. The sensor output is a pulse train from a 132 slot light-chopper disc. Both sensors were connected by a 47 m cable to standard signal-conditioning circuits in the BAO instrument trailer.

2.3 Tower 3

This tower supported a single instrument, the Gill Anemometer Bivane (P-BIV), manufactured by the R. M. Young Company (see Fig. 5). It provides the two directions and speed necessary to define the three-dimensional flow. The helicoid propeller mounted at the front of the bi-directional wind vane provides some damping of the vane. The manufacturer lists a damping ratio of 0.63 and a delay distance (50% recovery) of 1.0 m. The 23 cm diameter × 0.30 m pitch propeller has a response distance (63% recovery) of 1.0 m.

The vane position is measured by two potentiometers. The propeller is flexibly coupled to a d.c. generator for the speed measurement. The sensor is connected by a 52 m cable to a standard translator unit in the trailer. The speed measurement is noise filtered and scaled to 0.100 volts per m/s. The azimuth range is 1 to 351 degrees and the elevation range is ±45 degrees.

2.4 Tower 4

The sonic anemometer (SONIC) installed on this tower (Fig. 6) was one of the three-axis anemometers used for routine wind measurement at each of the eight levels on the BAO 300 m tower. It measures the wind component along each of its three orthogonal acoustic paths (vertical and two horizontal). For convenience of data handling and processing, the acoustic array was oriented in the same direction (approximately SSE) as the anemometers on the BAO tower. The high-frequency response of the sonic anemometer is limited by the attenuation introduced by line averaging along the acoustic paths. The response function for line averaging has its half-power at a wavelength roughly the length of the path which, for these arrays, is 25 cm. In a linear

first-order system the equivalent distance constant would be smaller by a factor of 2π, or roughly 4 cm.

An important source of error in a sonic anemometer is the systematic underestimation in the measured horizontal velocity components from partial shadowing of the acoustic path by the transducers as the wind direction approaches the array axes (Kaimal and Gaynor, 1983). A simple algorithm in the data acquisition software corrects this error in real time.

2.5 Tower 5

Three instruments (C-V-W) were mounted on this tower (Fig. 7). Wind speed and direction were measured by a Model F460 sensitive cup and vane set manufactured by Climatronics, Inc., of Bohemia, New York. The vertical wind component was measured by an R. M. Young propeller anemometer, similar to that on Tower 1. The vane position is measured by a potentiometer. The manufacturer lists the damping ratio of the vane to be 0.4 at a 10 degree initial angle of attack, and the distance constant to be 1.1 m. The rate of rotation of the cup wheel is measured by a pulse train from a 32 slot light chopper. The sensor distance constant is listed as 2.4 m for the stainless steel cup wheel. A 62 m cable carried the instrument outputs to standard signal conditioners (Climatronics and Young) in the BAO trailer. The signal conditioner for the F460 normally has a built-in 10 s averaging circuit, but for this experiment it was removed by the manufacturer at our request so that we could observe the full response of the instrument.

2.6 Tower 6

The sensors (P-V-W) on this tower (Fig. 8) were a Gill Propeller Vane for the horizontal wind speed and direction measurement, and a vertical propeller identical to those on Towers 1 and 5, both made by R.M. Young Co. The propeller and vane were changed slightly after the tower was knocked down by high winds on 9/13/82. Before the accident the Model 35005 with aluminum vane and polypropylene propeller was used. The damping ratio of this vane is listed by the manufacturer as 0.45 with a delay distance (50% recovery) of 1.3 m. The distance constant (63% recovery) for the propeller is 3.3 m. The tower was reinstalled on 9/16/82 with a polystyrene tail and propeller, making the sensor a Model 35003. The damping ratio of this vane is 0.54 with a delay distance of 1.2 m. The distance constant of the propeller is 1.0 m. The sensor outputs were connected through a 67 m cable to standard R.M. Young signal-conditioning circuits.

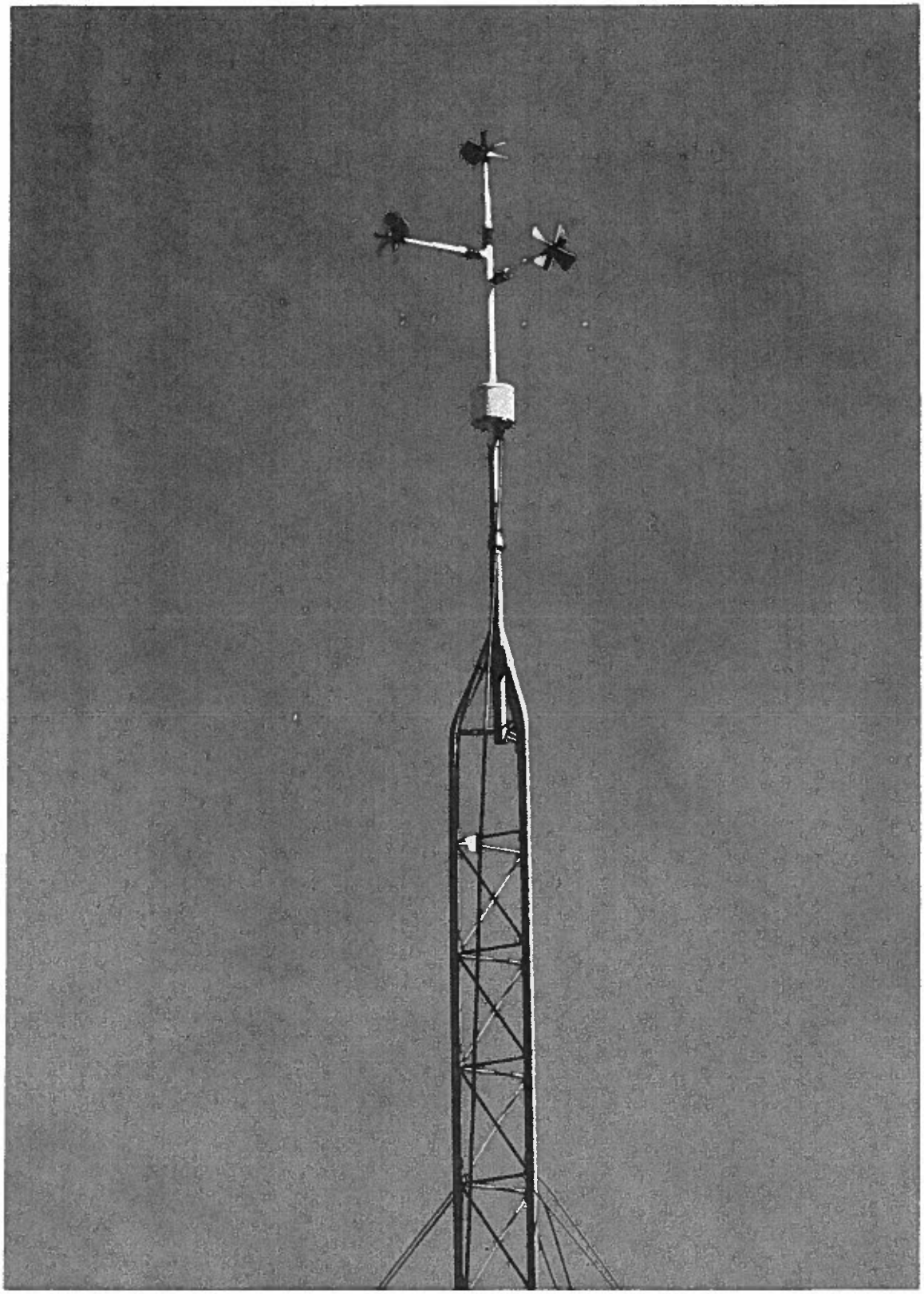

Figure 3. Gill UVW anemometer on Tower 1.

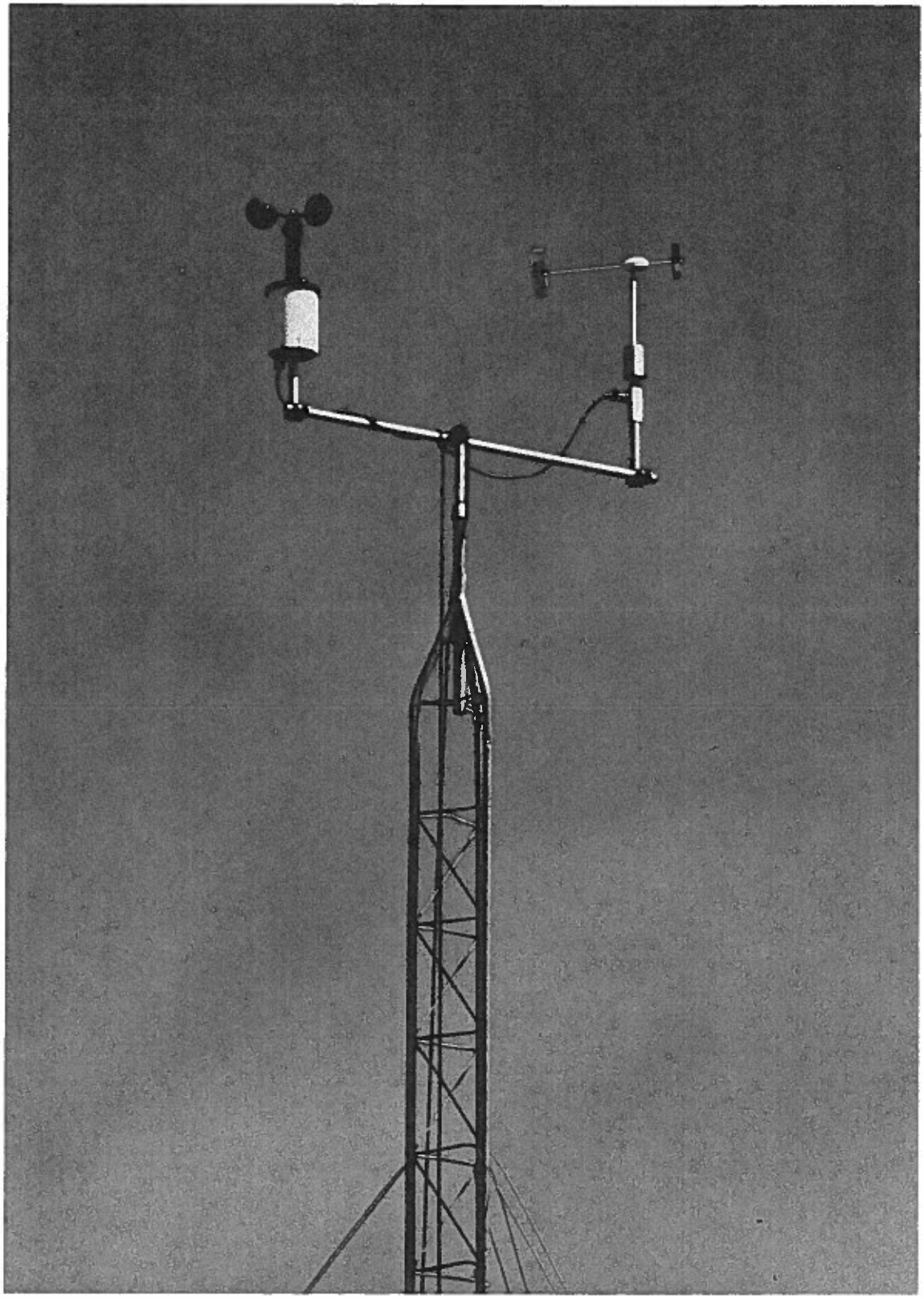

Figure 4. Cup anemometer and bivane on Tower 2.

Figure 5. Propeller bivane on Tower 3.

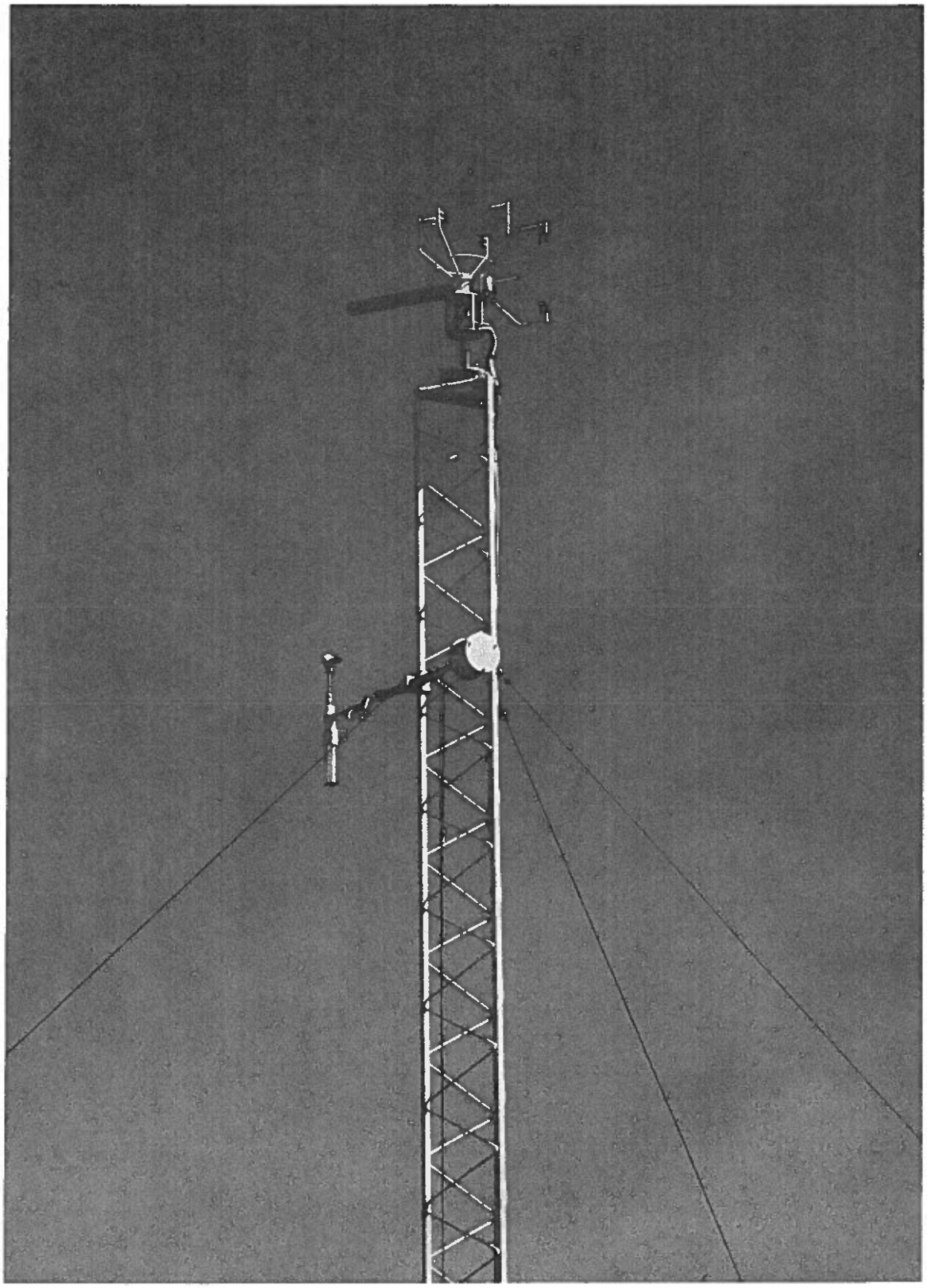

Figure 6. BAO sonic anemometer on Tower 4.

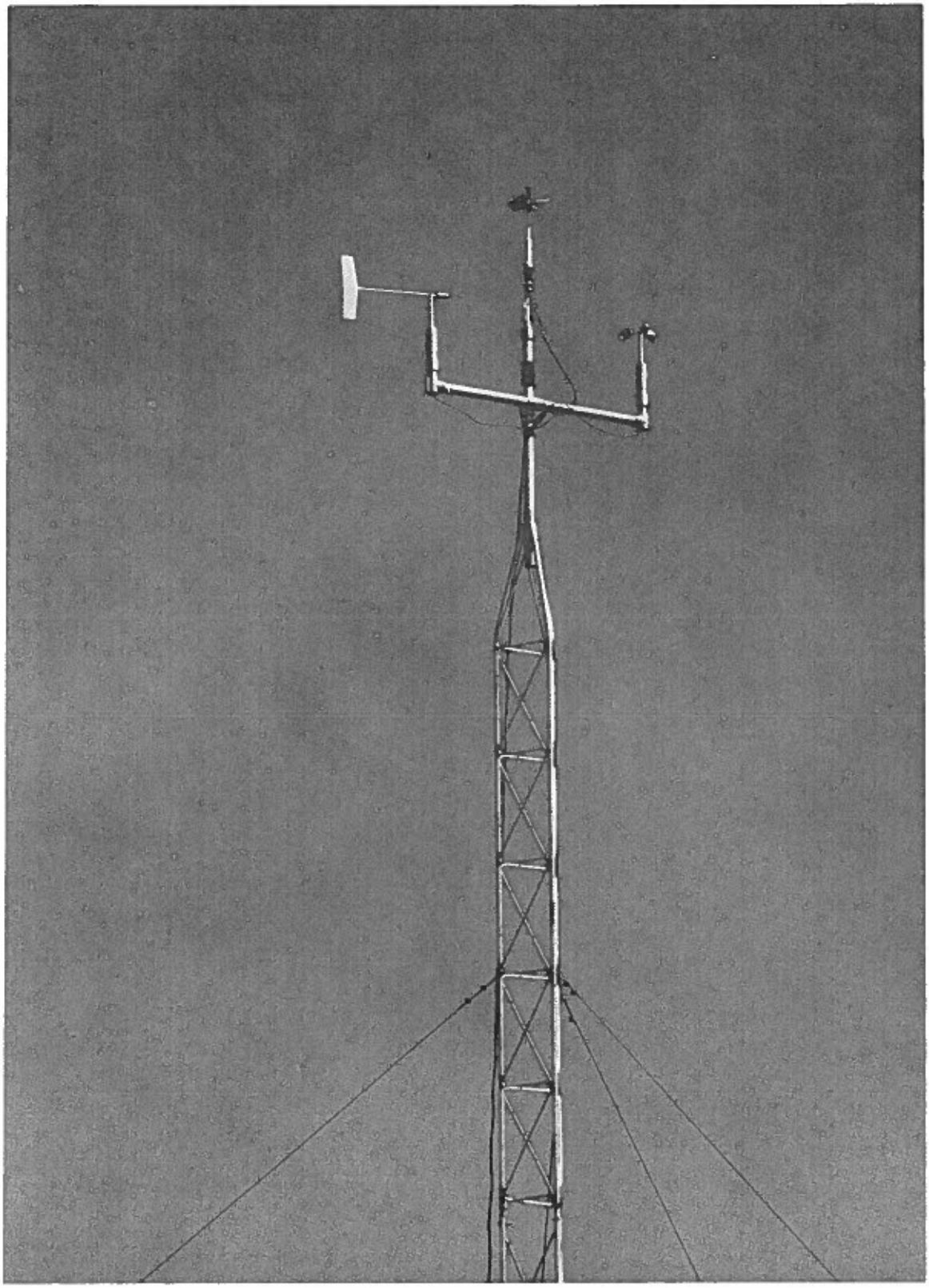

Figure 7. Cup and vane with vertical propeller on Tower 5.

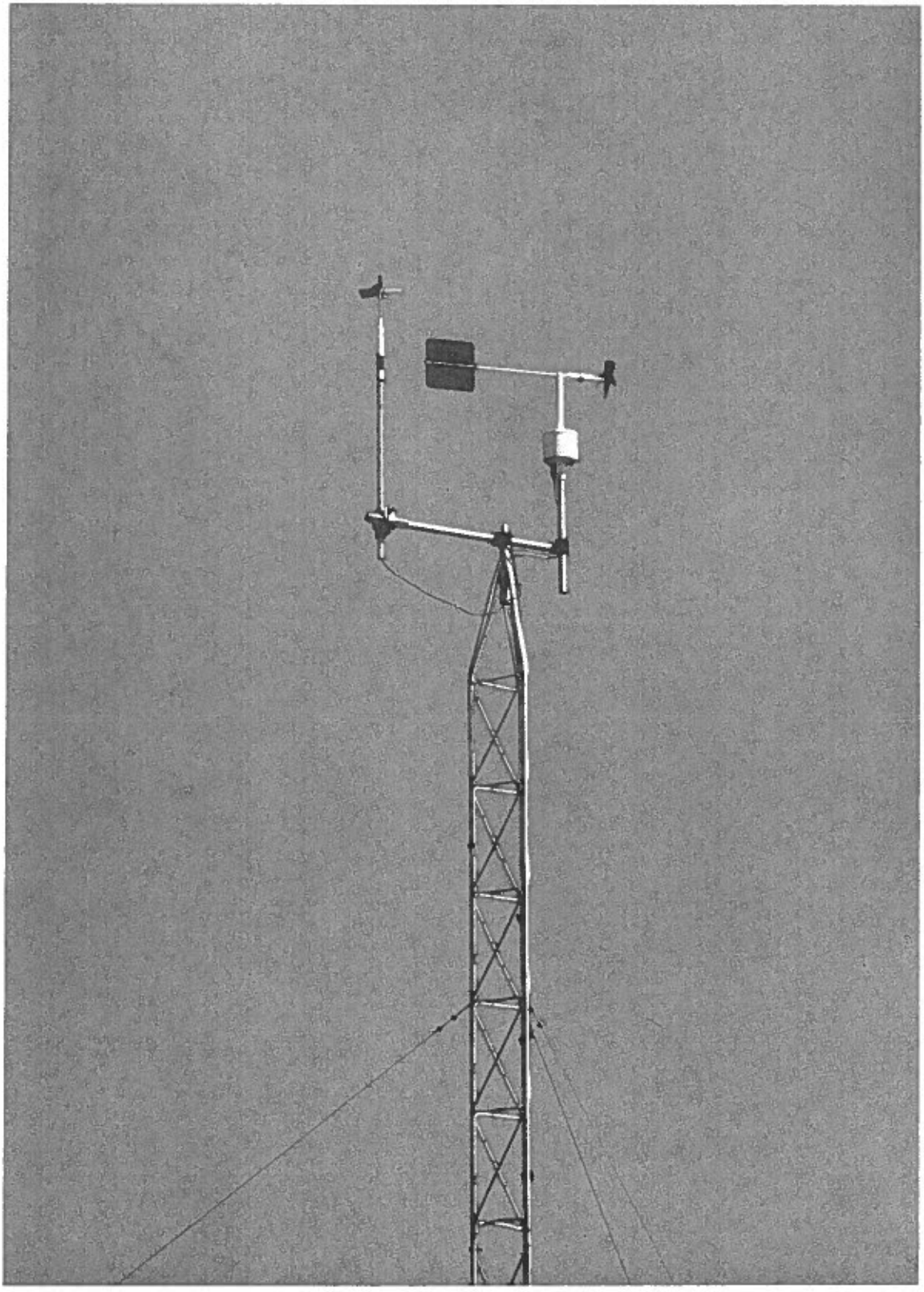

Figure 8. Propeller-vane and vertical propeller on Tower 6.

3. DATA ACQUISITION, PROCESSING, AND ANALYSIS

The output signals from the anemometers were connected through shielded cables to their signal conditioners located in an instrument trailer at the base of the tower. The outputs of the signal conditioners were sampled, digitized, and processed by the BAO data acquisition system, along with all the signals from the standard sensors on the 300 m tower. The sonic anemometer signals were processed in exactly the same manner as all the other sonic anemometer signals from the tower. All the channels were sampled ten times per second. See Kaimal and Gaynor (1983) for details of the BAO operation. The data acquisition computer calculates in real time the means and variances of samples of the outputs, converts them into meteorological units, and prints out the results at the end of every 20 min non-overlapping averaging period. For selected periods the complete time series (10 samples/s) can be recorded on magnetic tape. The rest of the time only 10 s non-overlapping averages are saved. From each of the 10 s periods a grab sample (one of these instantaneous values) is also saved. These grab samples are needed especially for computing standard deviations since they retain the high-frequency information inherent in the data sample. Thus, we have 120 grab samples for calculating each 20-min standard deviation.

Scalar averages and standard deviations were computed for all variables. For U-V-W and SONIC, the instantaneous direction was computed from the measured horizontal wind components. For the 20 min periods in which there were major shifts in wind direction, and for which the scalar average direc-

tion would be meaningless, the wind direction values were edited out of the data set. Data were excluded when the wind was parallel to the line of the towers to avoid any shadowing effect. Care was also taken to ensure that misleading values were not generated when the wind was from the north. Northerly winds cast a shadow on the SONIC w axis and also caused errors in some vane direction readings from their discontinuities at 0 deg. The entire data set was also carefully edited to remove spurious values caused by instrument malfunction, line noise, birds, rain, and the like.

The intercomparisons of first and second moments (means and standard deviations) are made against the SONIC measurements, which are considered the reference or true values. The statistics of comparison are the bias, b, and comparability, c, as defined by Hoehne (1971) and as used by Kaimal et al. (1984). They are defined as

$$b = \frac{1}{N} \sum_{i=1}^{N} (Y_i - S_i) \tag{1}$$

$$c = \left[\frac{1}{N} \sum_{i=1}^{N} (Y_i - S_i)^2\right]^{1/2} \tag{2}$$

where N = number of 20 min observations

Y_i = ith observation of the test instrument

S_i = ith observation of the reference instrument.

The field observations for the experiment extended from 1 to 22 September. Two periods were selected for recording data at the 10 samples/s rate. The first period, 0800-1540 MST recorded on 9 September, represents typical convective conditions encountered at the BAO, while the second period, 1600-2320 MST recorded on 18 September, represents neutral and stable conditions. These rapidly sampled data are used in subsequent sections to explore details of the

sensor response to the turbulence in the flow. In the sections to follow, we will examine first comparisons of the means and standard deviations of wind speed and wind direction (derived from the 20 min observations) and then examine how the response characteristics of the various sensors contribute to the observed performance.

4. OPERATIONAL MAINTENANCE AND QUALITY CONTROL

A field monitoring program from which data of known quality are required should be planned with a quality assurance effort aimed toward that goal. The quality assurance plan for this experiment required that the data gathering period be bracketed by calibrations and that an independent audit be conducted during the field program. The ideal time for an audit is at the beginning of the field measurement program so that errors can be corrected before too many data have been collected. An independent audit serves two purposes. (1) The expectation that someone else will check to be sure things have been done right inspires the person responsible for the operation of the system to be sure everything is done and documented within the planned methodology. (2) The auditor gives another layer of authority to the claim that data are valid and representative. His report and the records kept for calibration are an important part of the data history.

Since this program was short (3 weeks), it was important to monitor the operations daily. When problems arose, corrective action was taken at once. When, for example, a strong wind blew down Tower 4 (because of rain-softened soil and inadequate anchors for such conditions) and Tower 4 fell across the guy wires of Tower 5, causing Tower 5 to fall across the guy wires of Tower 6, our daily presence allowed immediate action. Towers were repaired and re-erected with stronger anchors. Sensors were inspected and the necessary parts for replacement ordered. Towers down on noon of the 13th were back on line on

the 16th with new parts from Traverse City, Mich., and Bohemia, N.Y. Such fast action could happen only with maximum cooperation from both vendors and field personnel. A normal monitoring program with weekly visits would have lost 2 or 3 weeks of data.

The initial calibration documented the response of the system elements to artificial known conditions, such as rate of rotation for speed shafts and position change for wind vane shafts. Because we monitored the 20 min average data on hard copy continuously, we were able to detect consistent differences in wind direction that led us to correct the orientation before the measurement program began officially. Normally a monitoring program does not have redundant sensors, so differences are not there to see. It would be prudent to have the orientation checked by a different person than the one who did the orientation initially. This may be the most important field task and perhaps the most difficult.

The final calibration marks the termination of the data gathering period. It remains for the data themselves to support the claim that the instruments performed the same between calibrations as they did during calibrations. When collocated instruments are used, the data may show that the instruments are performing more accurately than the calibration suggests. Calibration methods have their own assumptions and uncertainties and it is difficult to know sometimes whether the error reported in a calibration comes from the measurement instruments or from the calibrator. In field calibrations of meteorological instruments, it is unusual to have the luxury of test equipment ten times as accurate as the instrument, as is usually required in routine quality control programs. The best quality control in a field monitoring program is to have an experienced meteorologist looking at the data streams in as near real time

as the budget will allow.

As technology advances, new problems advance in parallel. For instance, in the decades of analog strip chart recording it was not necessary to filter high-frequency noise spikes from the output signals since the recorders could not respond to them. Now that high speed digital data loggers are becoming less expensive and more common, it is necessary to look at the output signals with an oscilloscope to be sure that the value being recorded represents the measurement output and not some combination of measurement and high frequency noise. Since the BAO system can detect frequencies as high as 5 Hz, it was necessary to look at all outputs (from the signal conditioner--input to the data logger) to be sure they were free of noise. Where noise was present, filtering was used but at frequencies higher than the sensors could produce so that no data were lost or distorted.

During this experiment initial and final calibrations were conducted by one of the authors (Lockhart). The independent audit was conducted by Dr. Fred V. Brock of the National Center for Atmospheric Research (see Appendix). We believe the quality of data collected for this study to be as good as anything one can achieve under field conditions. Accuracies and precisions reported are illustrative of what one might expect with careful attention given to calibration and installation of the sensors.

5. COMPARISON OF WIND SPEED MEASUREMENTS

Speed readings from U-V-W and SONIC are scalar averages of the instantaneous resultant speeds from two horizontal velocity measurements. All the other anemometers measure scalar speed directly. Bias and comparability of wind speed for the five anemometer systems compared are given in Table 2. The most striking fact here is the substantial negative bias in U-V-W. The other sensors show a smaller bias. The non-cosine response in the propellers is the most likely reason for this underestimation. No corrections were made at any stage in the acquisition and processing of the data to correct for this effect. Another point of interest is the large positive bias in P-BIV. Upon reviewing the calibration data, we found that this instrument had a small, uncorrected error of +0.3 m/s, which accounts for this positive bias. P-V-W, which has a propeller similar to P-BIV, but attached to a vane fixed in the horizontal plane, had a rather small bias.

Table 2. Bias and comparability for wind speed

Instrument	b (m/s)	c (m/s)	N
U-V-W	-0.43	0.53	1279
C-BIV	-0.13	0.35	760
P-BIV	0.33	0.48	760
C-V-W	-0.13	0.36	760
P-V-W	-0.16	0.34	760

b = bias
c = comparability
N = number of observations

The two cup anemometers compared in this experiment are very different in size. C-BIV cups were rather large, while the C-V-W cups were small and light. However, they showed almost identical performance in measuring wind speed, both in terms of bias and comparability. The latter figure is a measure of the degree of scatter in the data. The results indicate that the overspeeding problem attributed to cups (Izumi and Barad, 1970; Busch and Kristensen, 1976) is not a problem here.

6. COMPARISON OF WIND DIRECTION MEASUREMENTS

Bias in wind direction measurements is usually an indication of our inability to align the sensor properly, since we have no reason to suspect that the vanes do not line up with the wind. In the experiment, great care was taken to line up the instruments, and they were checked several times by independent observers under field conditions. Therefore these bias data provide a measure of the expected absolute accuracy possible from any wind direction observation under normal conditions. The bias, b, and comparability, c, for the measurements of wind direction, θ, and standard deviation of the wind direction, σ_θ, are given in Tables 3 and 4.

Table 3. Bias and comparability for θ

Instrument	b (deg)	c (deg)	N
U-V-W	-1.47	5.40	1035
C-BIV	-2.69	5.54	1057
P-BIV	-0.16	4.61	1055
C-V-W	1.44	4.48	819
P-V-W	-0.31	4.03	897

Table 4. Bias and comparability for σ_θ

Instrument	b (deg)	c (deg)	N
U-V-W	-0.18	3.29	1024
C-BIV	-0.86	2.63	1045
P-BIV	0.26	3.46	1041
C-V-W	-0.28	2.25	810
P-V-W	0.11	2.92	879

With the exception of P-BIV and P-V-W, the observed biases in Table 3 are larger than the sensor resolution. The comparability figures in the same table are somewhat disturbing. They indicate that the scatter in the observations is about 5°. This scatter is a measure of the confidence one can place in any one or small group of wind direction observations. These results should be of interest, and concern, to those involved in such fields as diffusion model verification, where a 5° difference in wind direction can cause a considerable difference in the prediction of ground level concentrations.

The values of σ_θ bias in Table 4 show, on average, good agreement of σ_θ with SONIC. The scatter in the measurements, represented by c in Table 4, is small, about 3°, and there is not much difference between instruments. The lightest vanes (in C-BIV and C-V-W) did have the least scatter with respect to the reference. It is to be expected that all these instruments will measure a slightly smaller σ_θ than the reference instrument because of their insensitivity to very small turbulent eddies. This is indeed the case, except for the vanes that have a propeller mounted on the front (in P-BIV and P-V-W), which show slightly higher values of σ_θ. It is possible that the propeller configuration is causing some underdamping. This matter is discussed in Sec. 10.

To see if stability had an effect on the measurement of σ_θ, the data were divided into day and night categories. (Other stability-related categories, such as lapse rate, were tried and gave similar results, so this classification scheme was used for simplicity.) The results are given in Tables 5 and 6. In all but one case the bias and comparability are smaller at night than during the day. During the day the propeller vane (P-V-W) and propeller bivane (P-BIV) again seem to be underdamped, measuring a σ_θ that is higher than the sonic anemometer, but at night they show a slight negative bias.

Table 5. Bias and comparability for σ_θ during the day (0600 - 1800 MST)

Instrument	b (deg)	c (deg)	N
U-V-W	-0.23	3.54	469
C-BIV	-1.07	3.07	481
P-BIV	0.60	4.20	475
C-V-W	-0.27	2.71	383
P-V-W	0.32	3.59	405

Table 6. Bias and comparability for σ_θ at night (1800 - 0600 MST)

Instrument	b (deg)	c (deg)	N
U-V-W	-0.14	3.06	555
C-BIV	-0.69	2.20	564
P-BIV	-0.02	2.70	566
C-V-W	-0.30	1.74	427
P-V-W	-0.08	2.19	474

Figures 9-13 contain plots of θ bias for the various instruments as a function of wind direction. The pattern in Fig. 9 for the U-V-W is most striking. It is obviously a sinusoidal wave with minima at 0°, 100°, 180°, 270°, and 360°, and with maxima in between. This pattern may be caused by two factors, the slight departure from cosine response of the propellers, and the fact that when the wind is not perpendicular to the propellers, the threshold response speed is higher. Both factors cause the bias to be more negative for wind directions along either axis. Interference from the sensor-supporting arms is not the cause since that would tend to produce maxima along those directions. For P-BIV and P-V-W, Figs. 11 and 13 show a rapid increase in b near 360° when the readings are left in the data set. This is caused by the

small dead band in the direction potentiometer at this position.

Figures 10-13 show what might be a pattern of noise, which persists in almost the same form in all the plots. There is no symmetry about 180° but a faint one around 154°, the direction in which the sonic anemometer is pointed. Although the pattern is not the same on either side of 154°, the minima at 134° and 185° point to possible residual errors in the SONIC correction for transducer shadowing as the likely cause of the deviations.

Figures 14-18 show plots of σ_θ comparability as a function of wind speed. As expected, all the instruments show more scatter at lower wind speeds. The secondary peak in Fig. 16 (P-BIV) is not understood.

Figures 19-28 are plots of σ_θ bias and comparability as a function of σ_θ itself (as measured by SONIC). This is roughly equivalent to plotting it as a function of stability. The bias stays close to zero for σ_θ up to 30°, but falls off rapidly above that, approaching -4° at σ_θ = 50°. The comparability becomes larger with increasing σ_θ (or with increasing instability), implying that the sensors are less well able to follow the large-amplitude fluctuations.

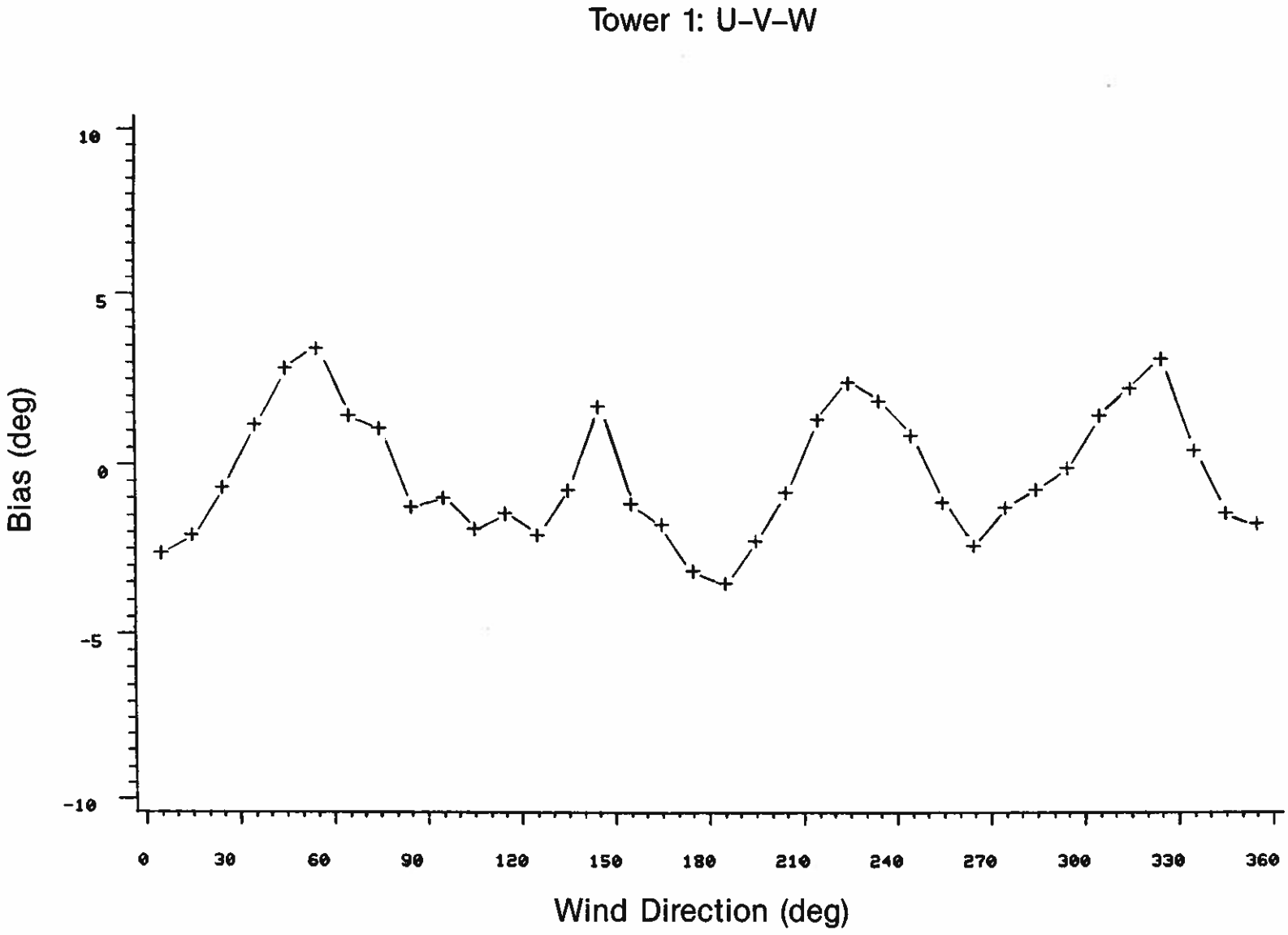

Figure 9. Bias in U-V-W wind direction shown as a function of wind direction.

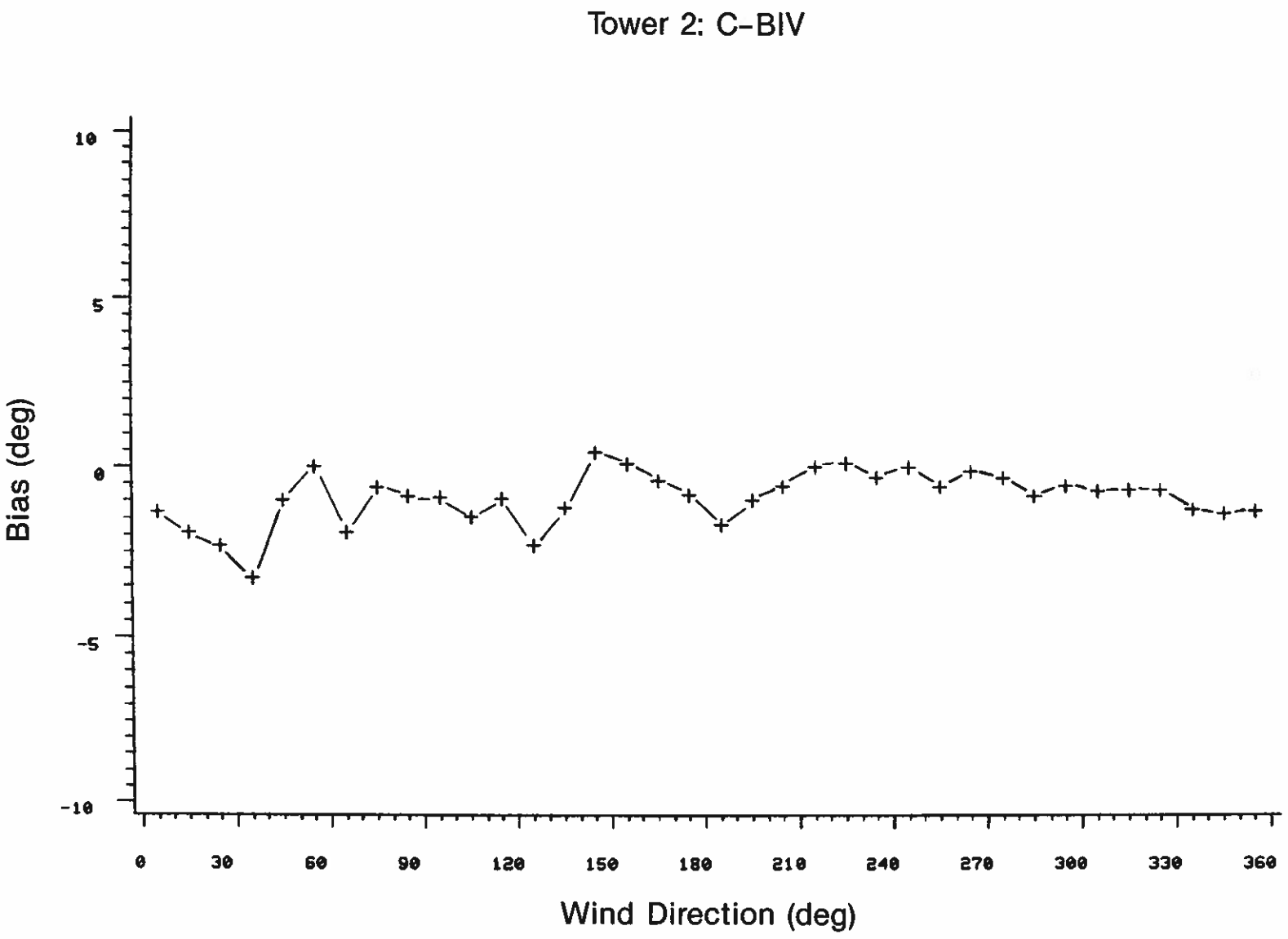

Figure 10. Bias in C-BIV wind direction shown as a function of wind direction.

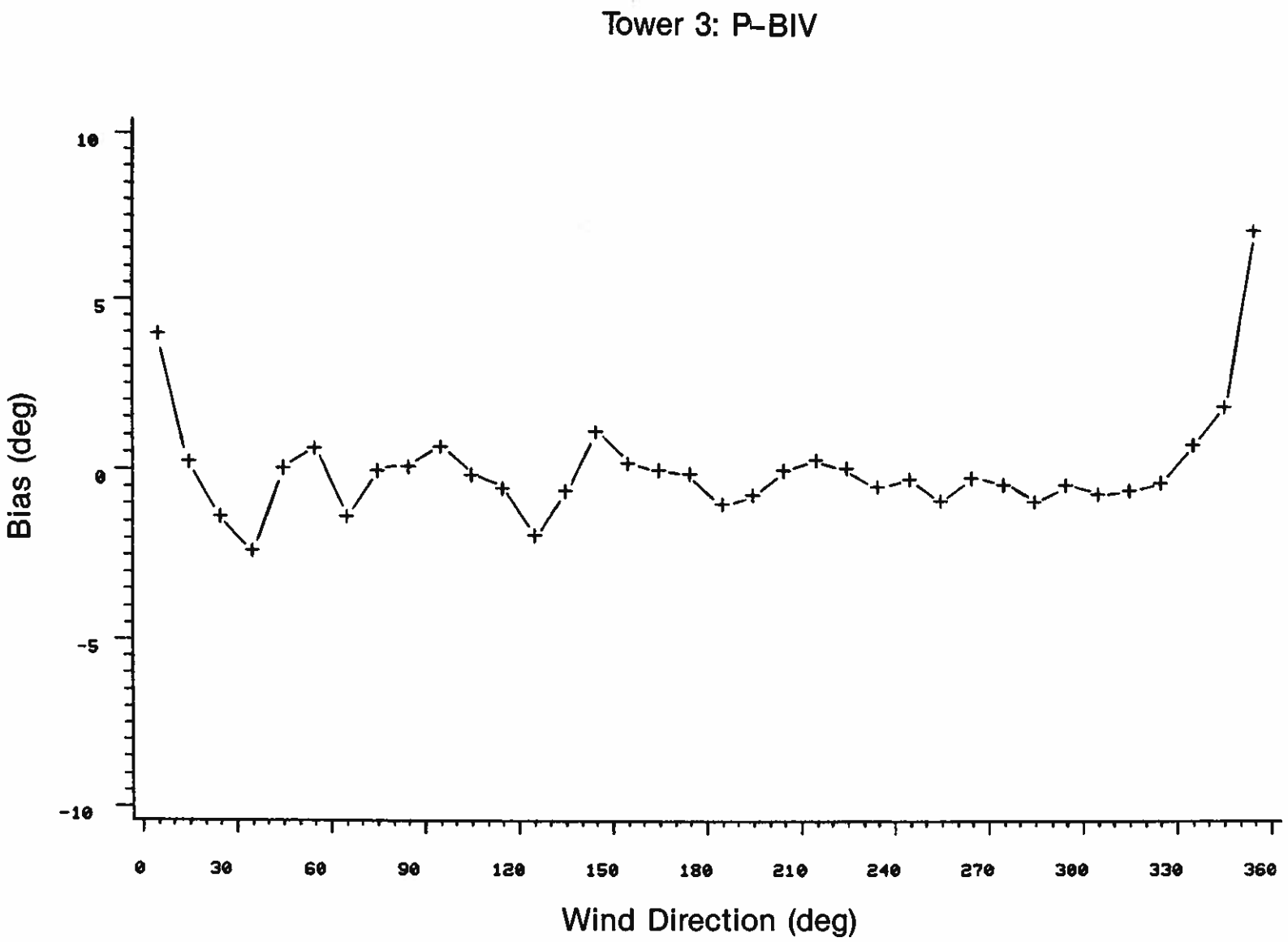

Figure 11. Bias in P-BIV wind direction shown as a function of wind direction.

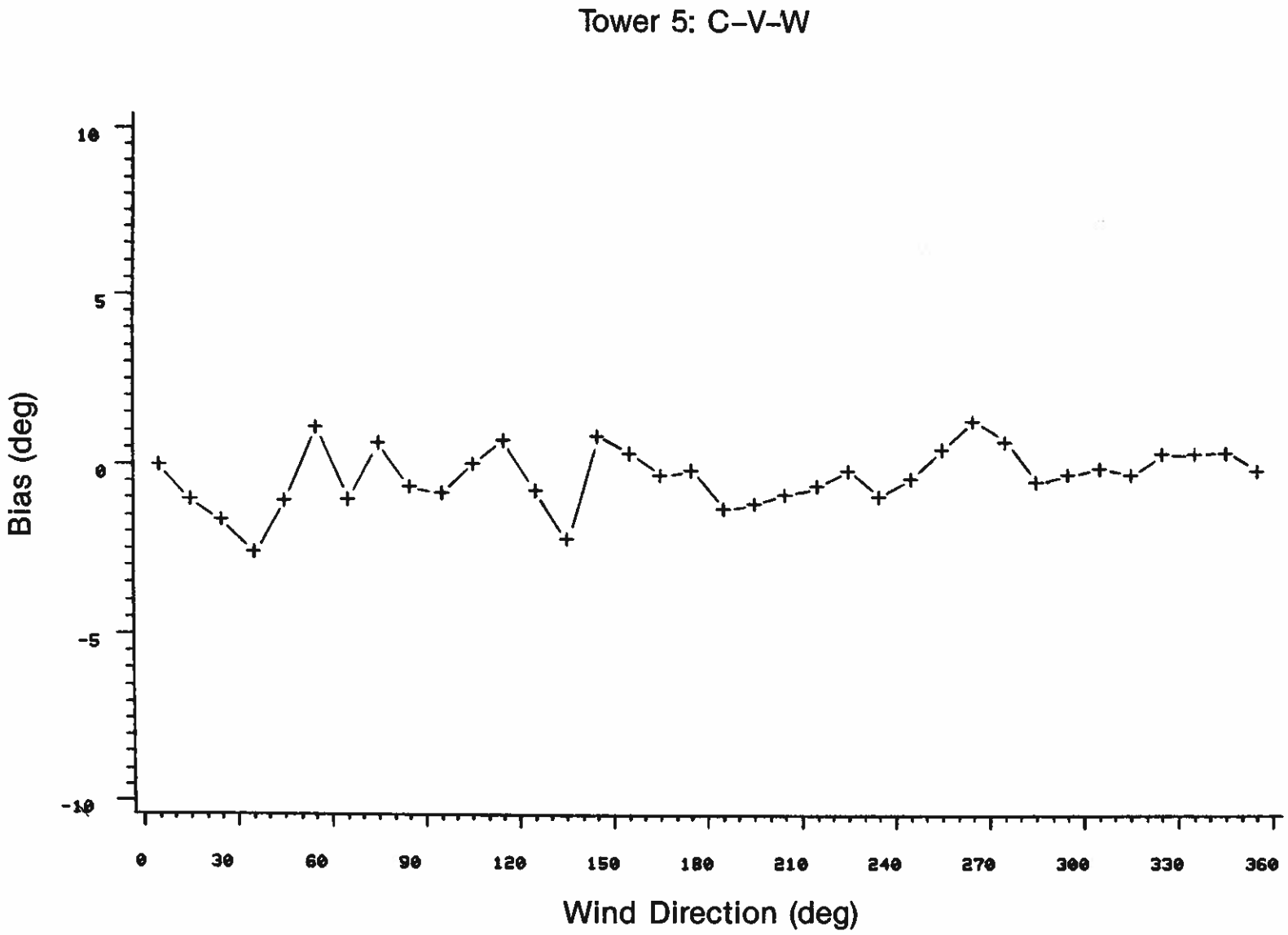

Figure 12. Bias in C-V-W wind direction shown as a function of wind direction.

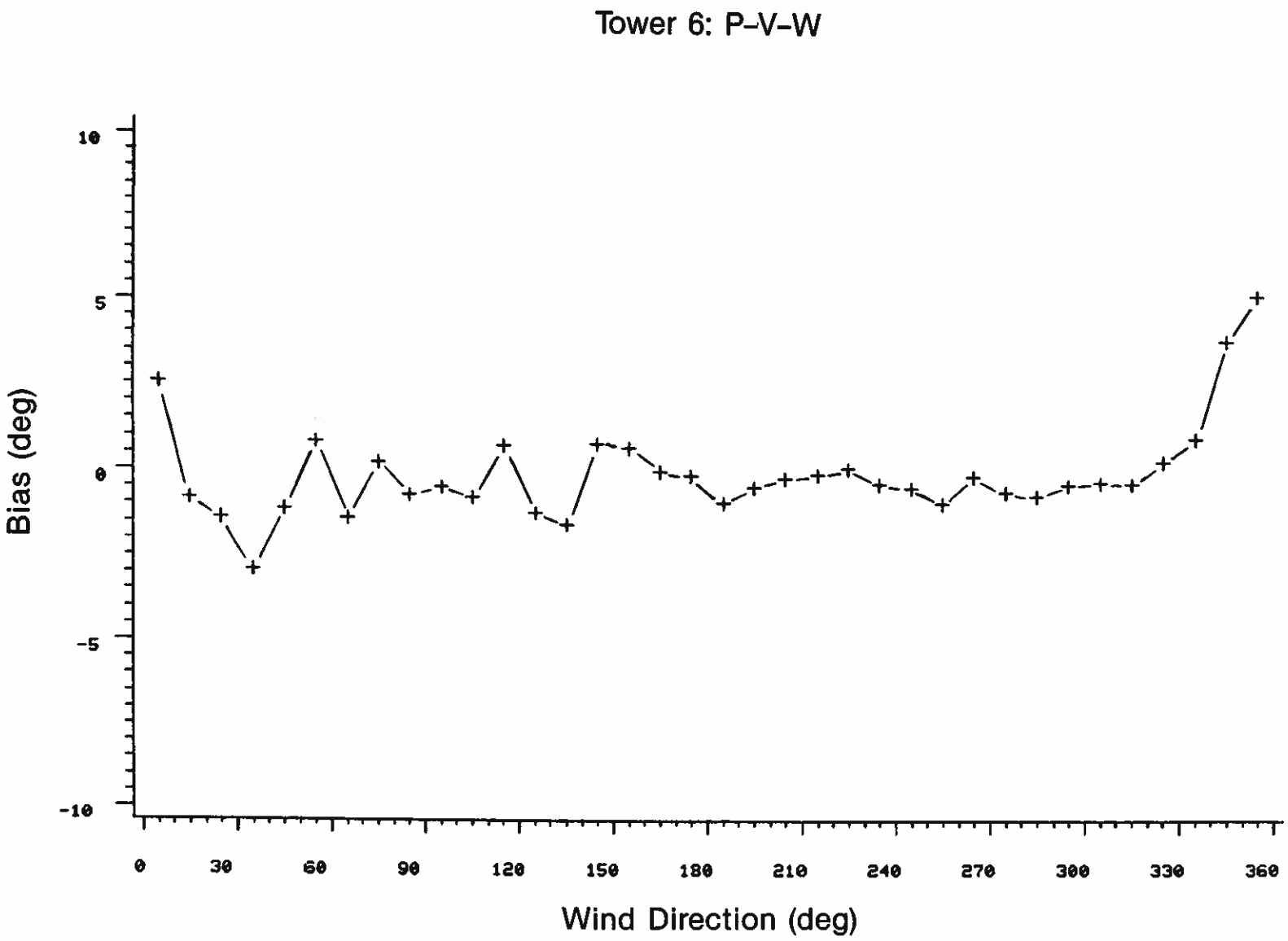

Figure 13. Bias in P-V-W wind direction shown as a function of wind direction.

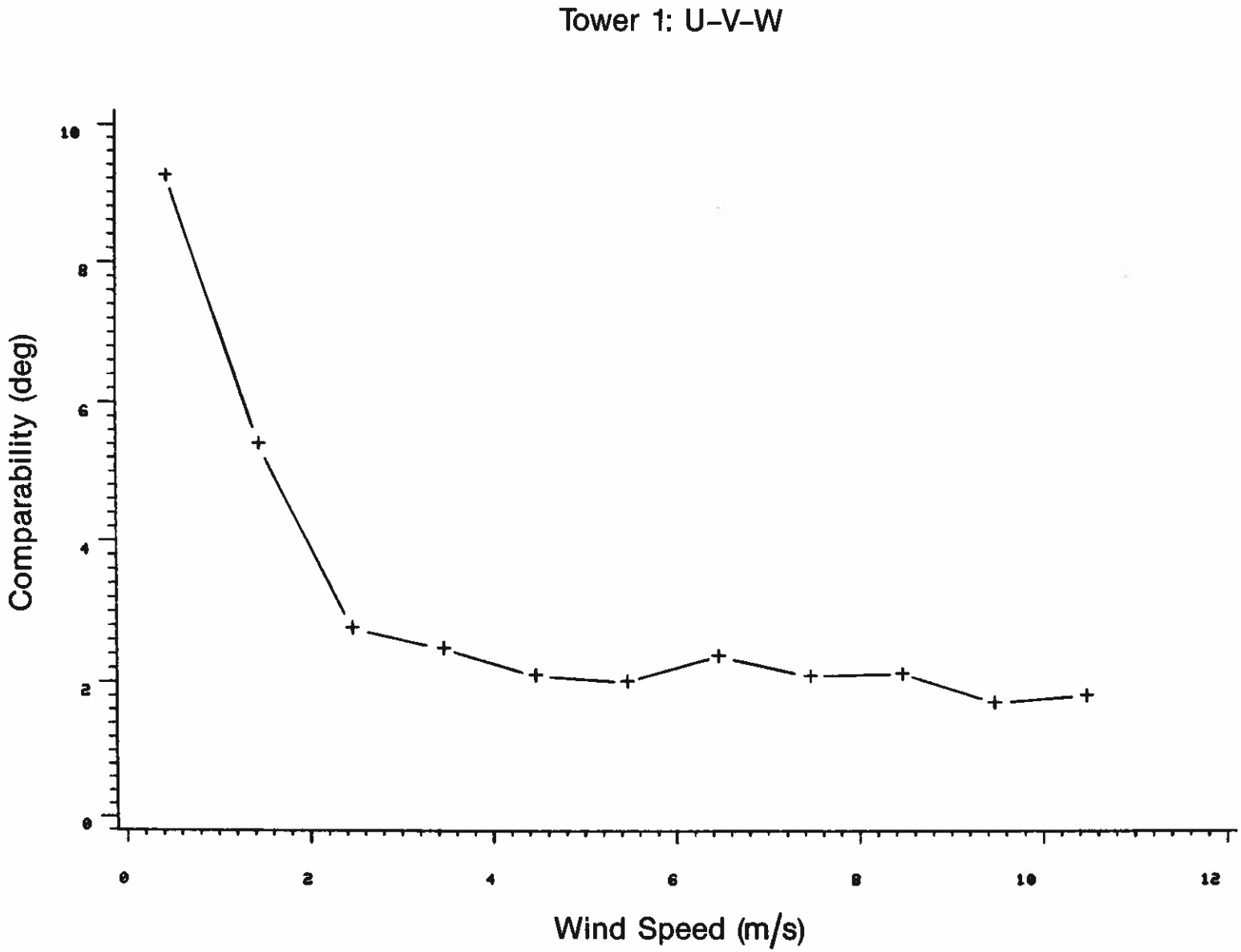

Figure 14. Comparability in σ_θ from U-V-W shown as a function of wind speed.

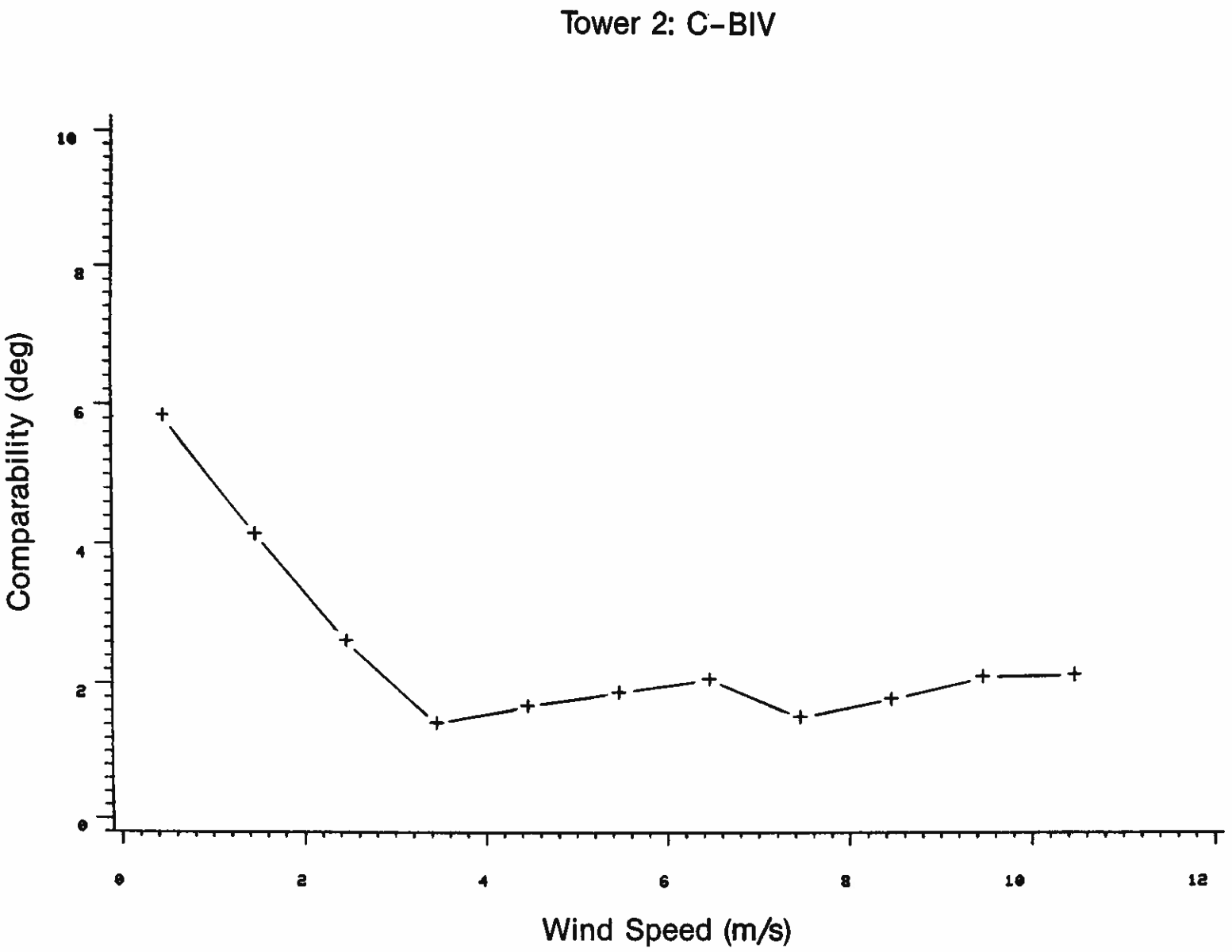

Figure 15. Comparability in σ_θ from C-BIV shown as a function of wind speed.

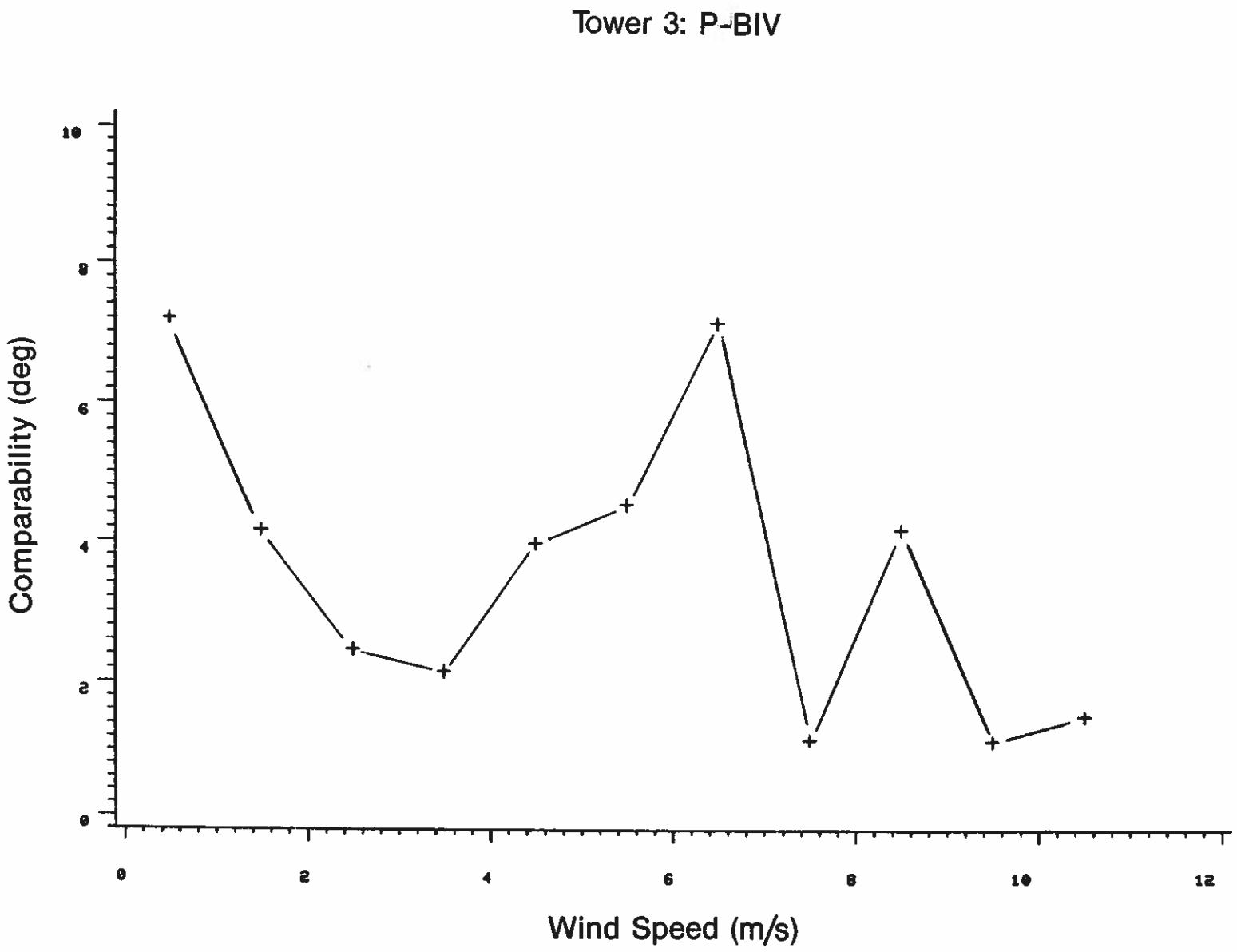

Figure 16. Comparability in σ_θ from P-BIV shown as a function of wind speed.

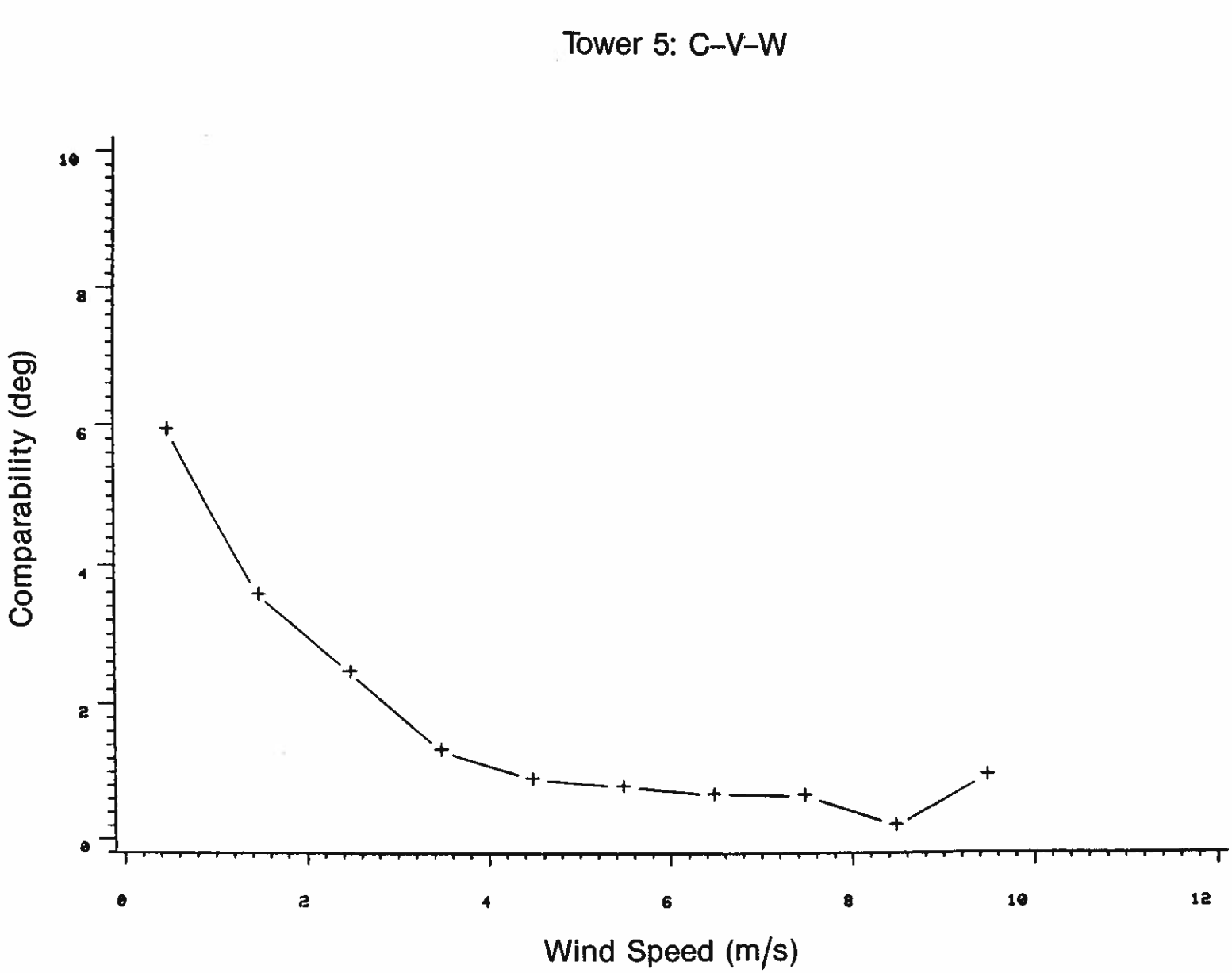

Figure 17. Comparability in σ_θ from C-V-W shown as a function of wind speed.

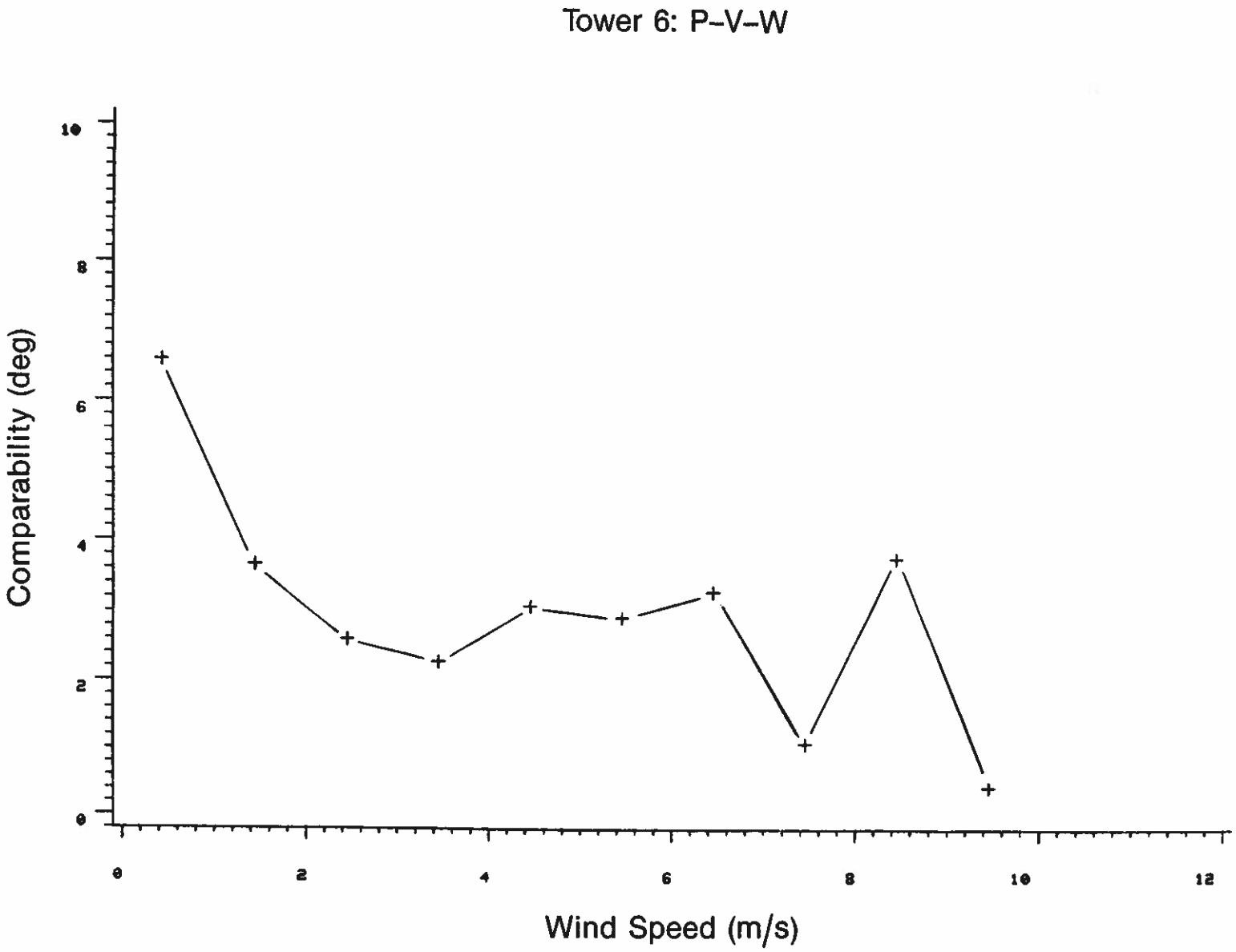

Figure 18. Comparability in σ_θ from P-V-W shown as a function of wind speed.

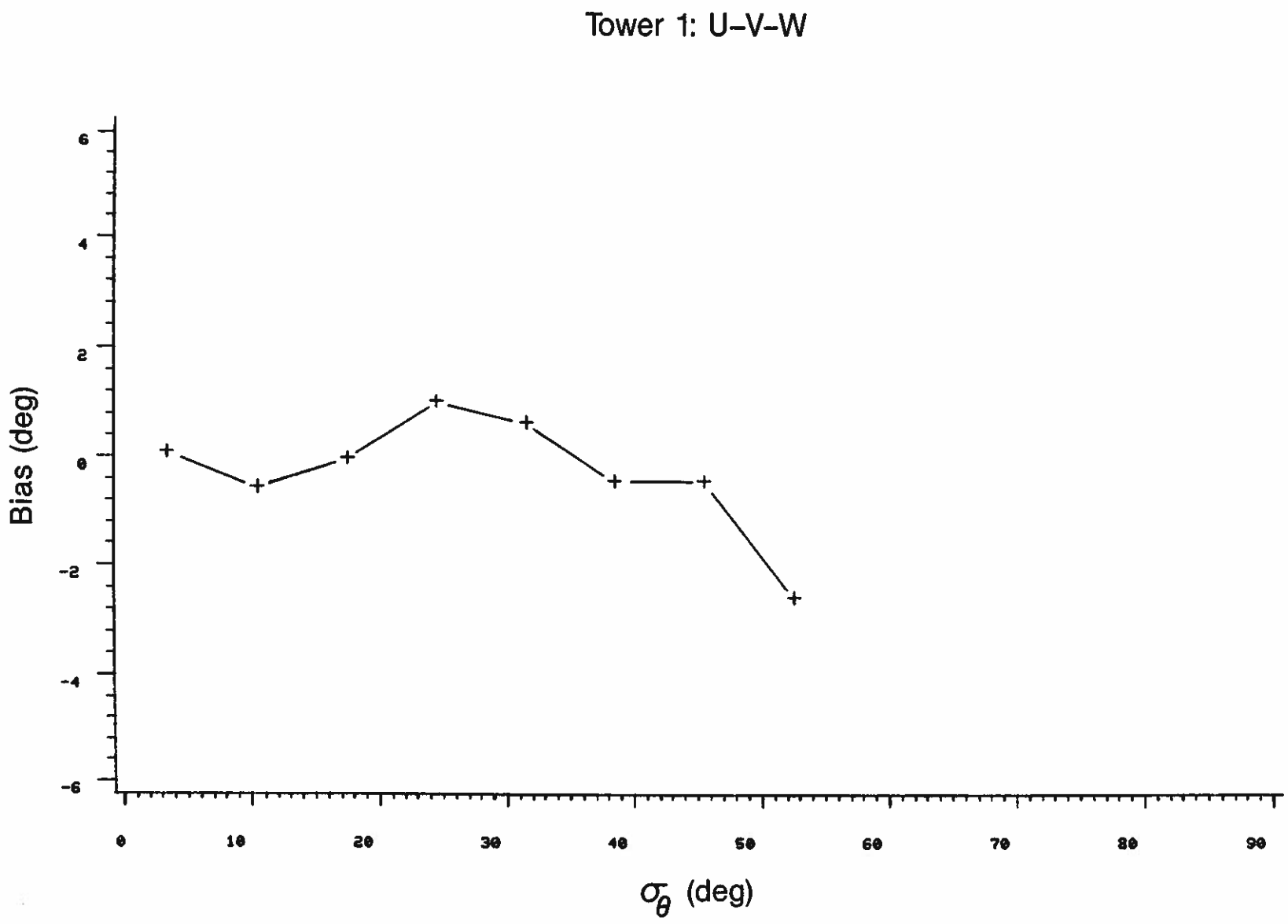

Figure 19. Bias in σ_θ from U-V-W shown as a function of σ_θ.

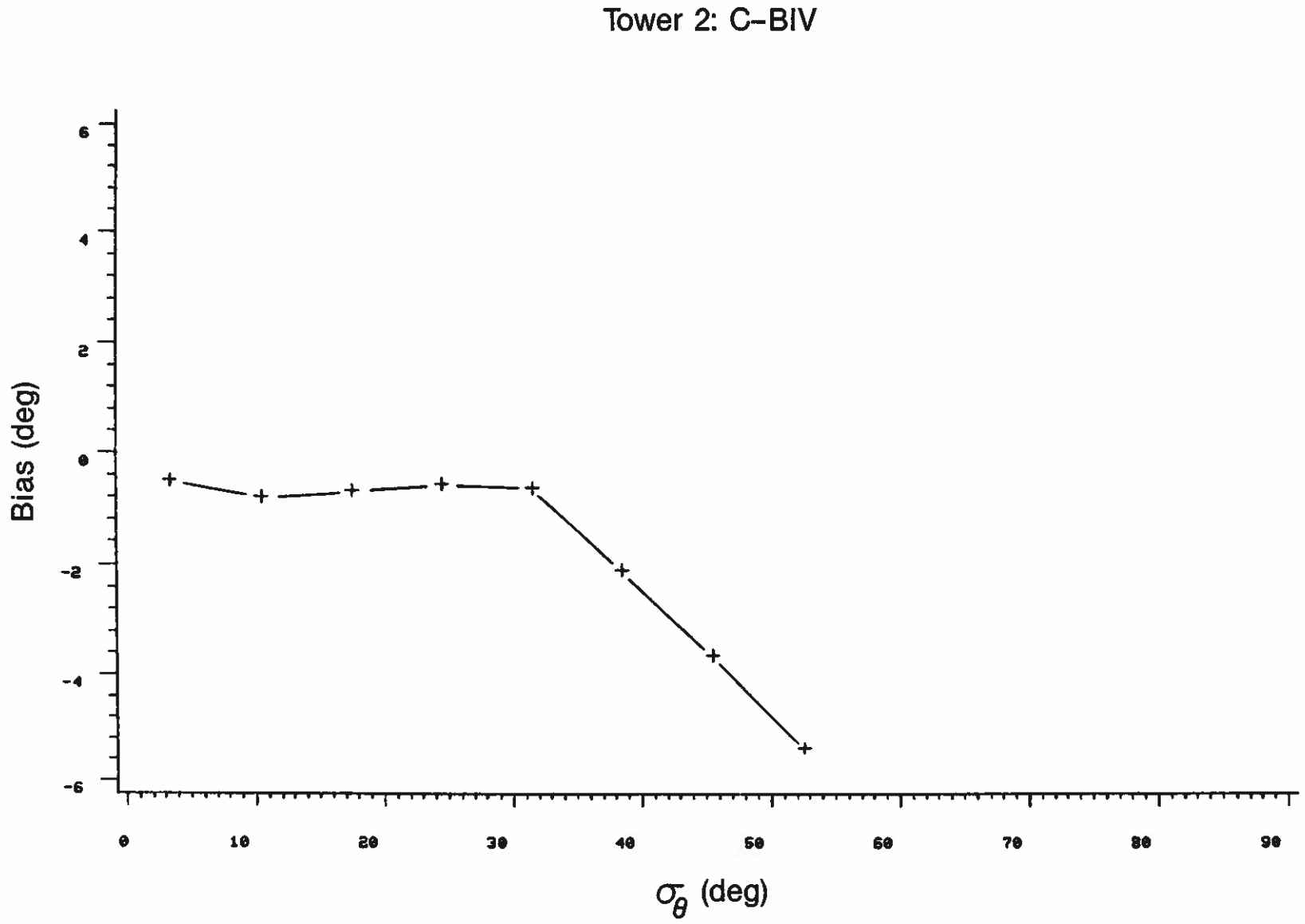

Figure 20. Bias in σ_θ from C-BIV shown as a function of σ_θ.

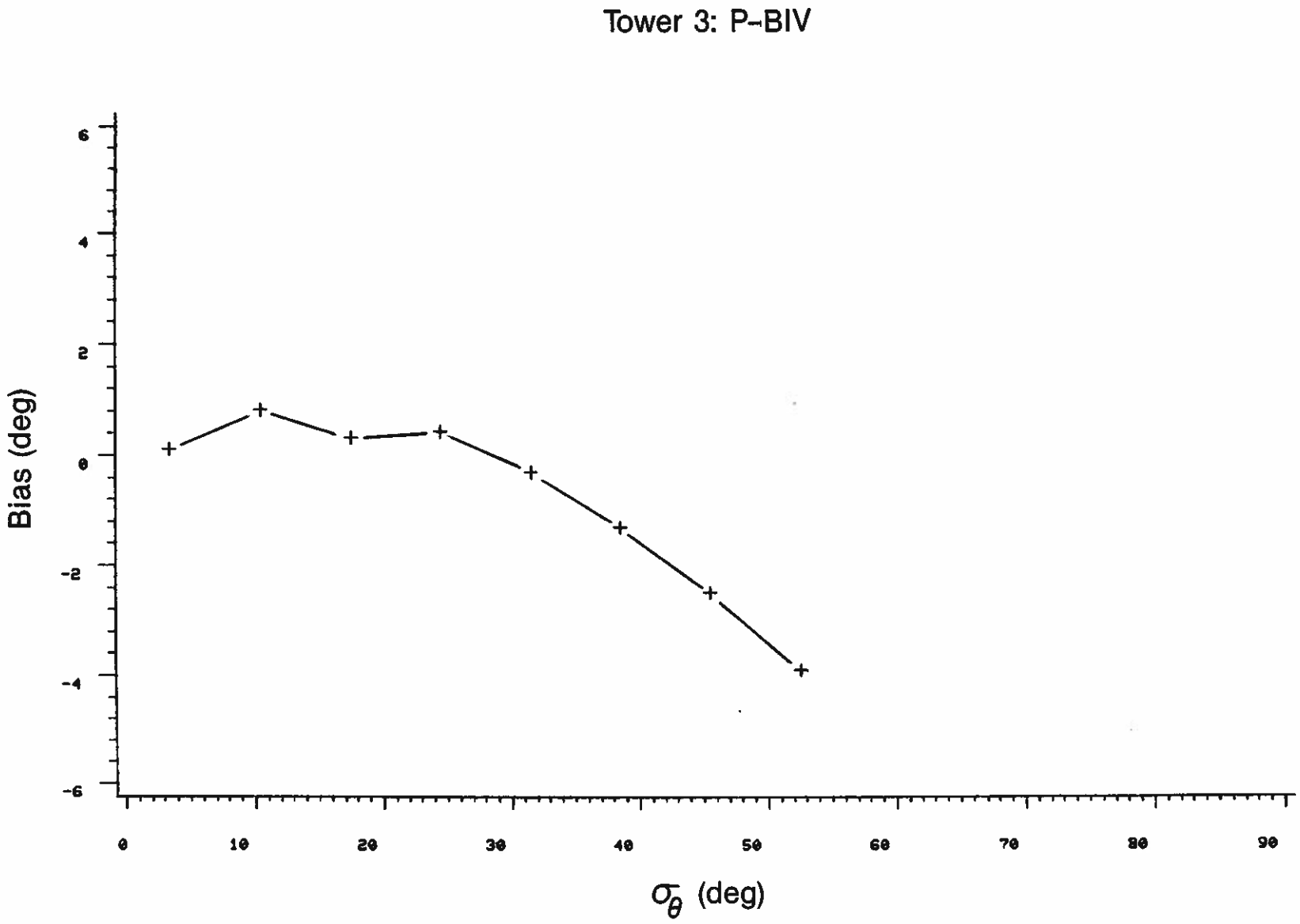

Figure 21. Bias in σ_θ from P-BIV shown as a function of σ_θ.

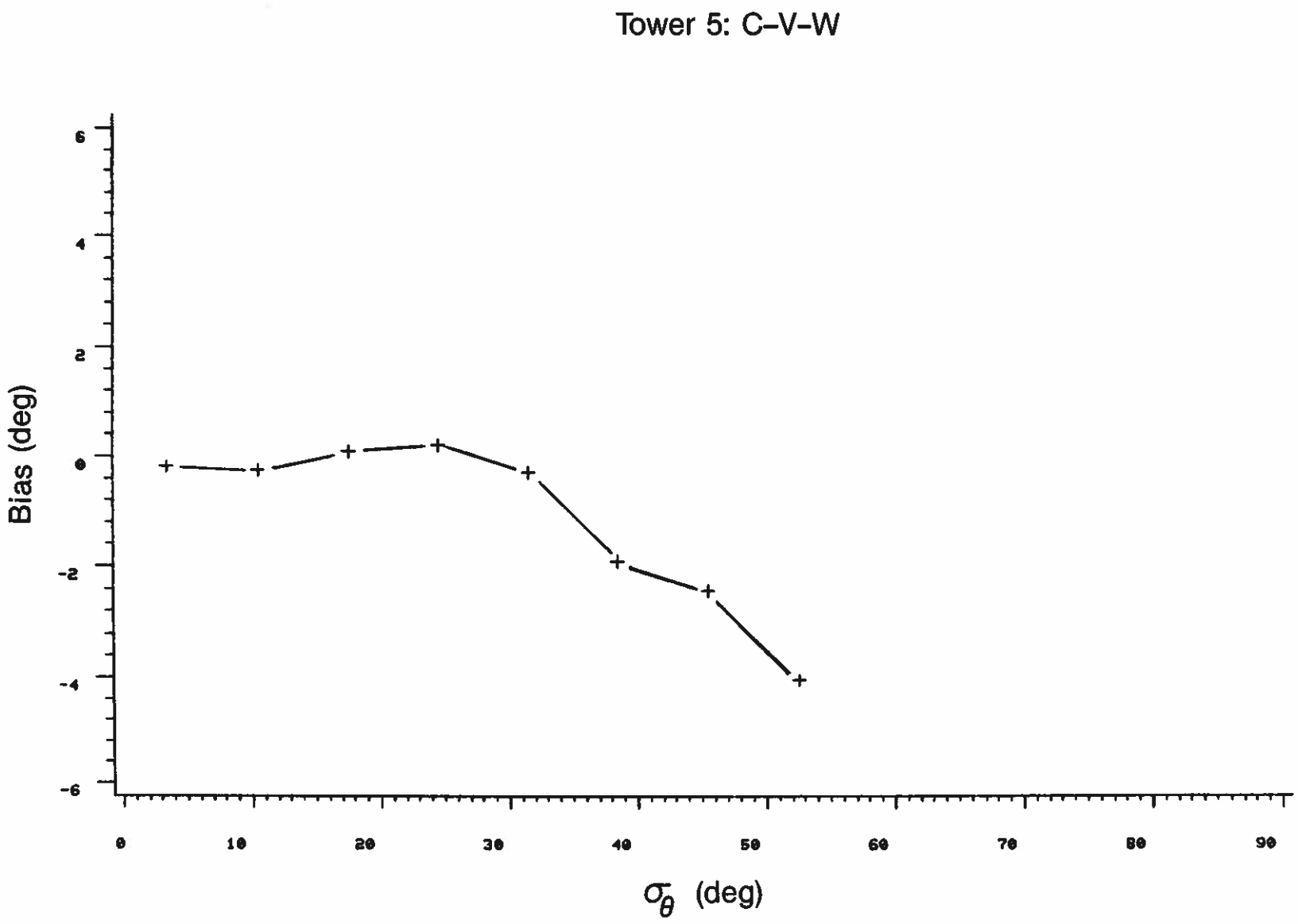

Figure 22. Bias in σ_θ from C-V-W shown as a function of σ_θ.

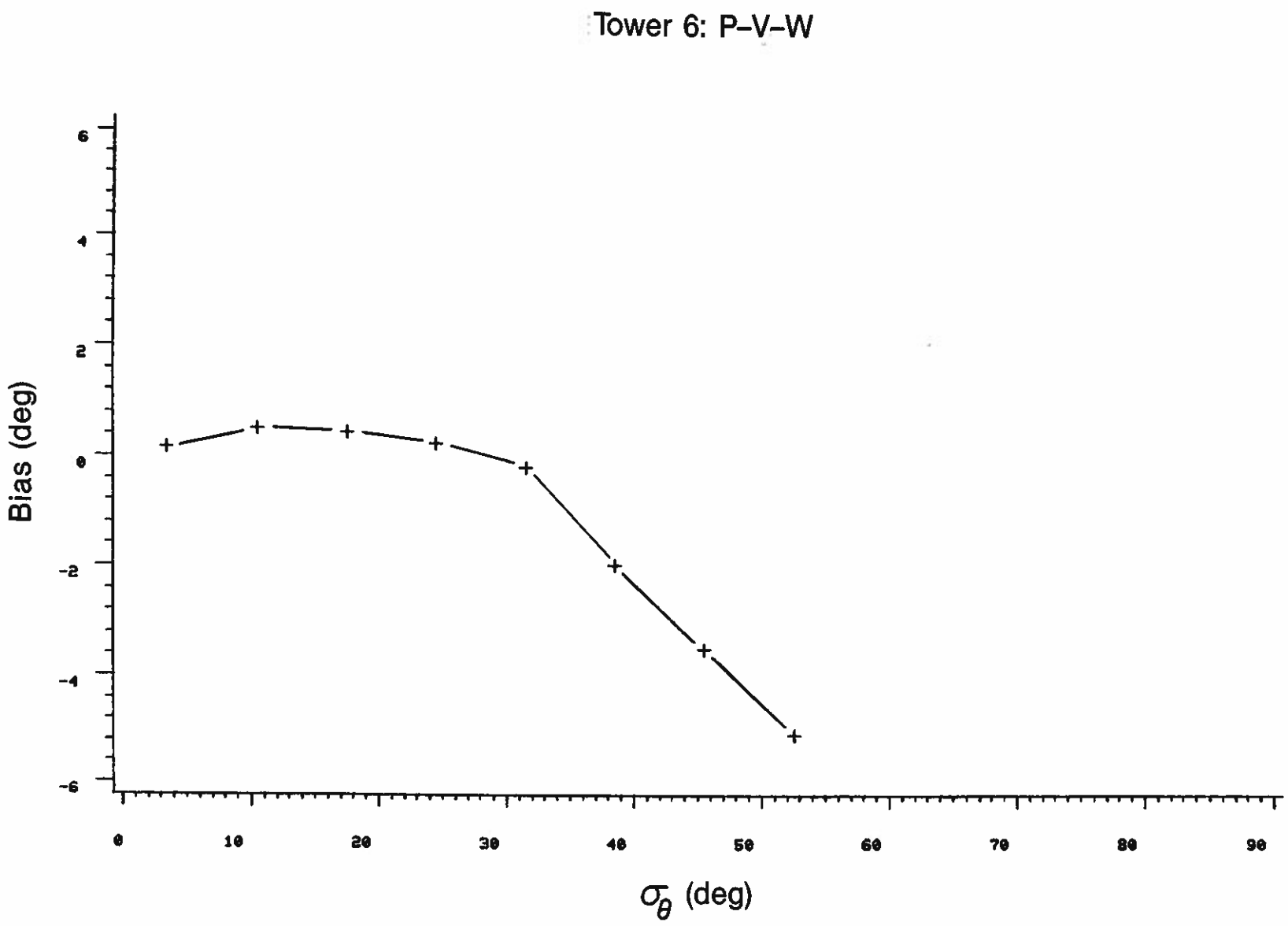

Figure 23. Bias in σ_θ from P-V-W shown as a function of σ_θ.

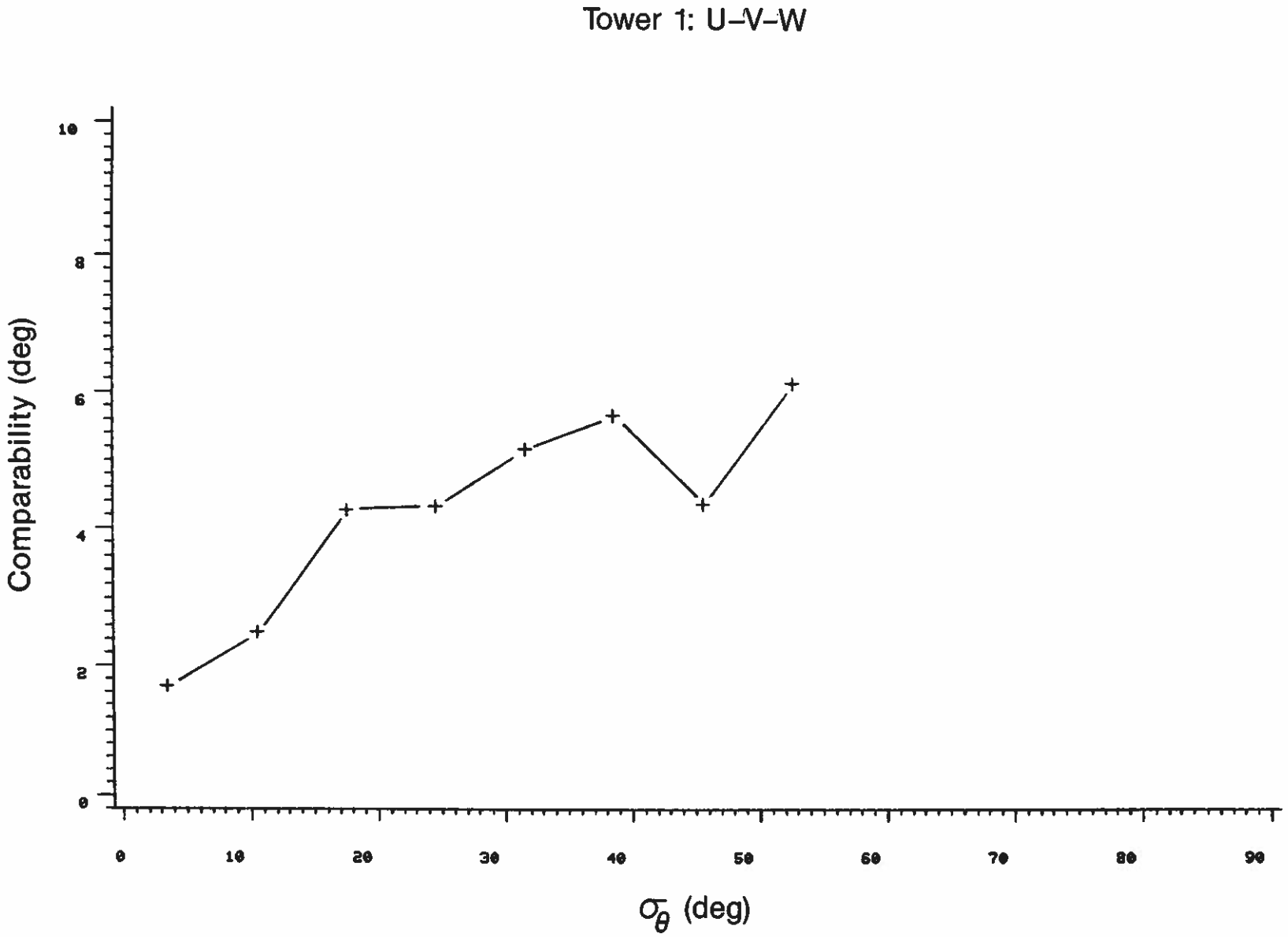

Figure 24. Comparability in σ_θ from U-V-W shown as a function of σ_θ.

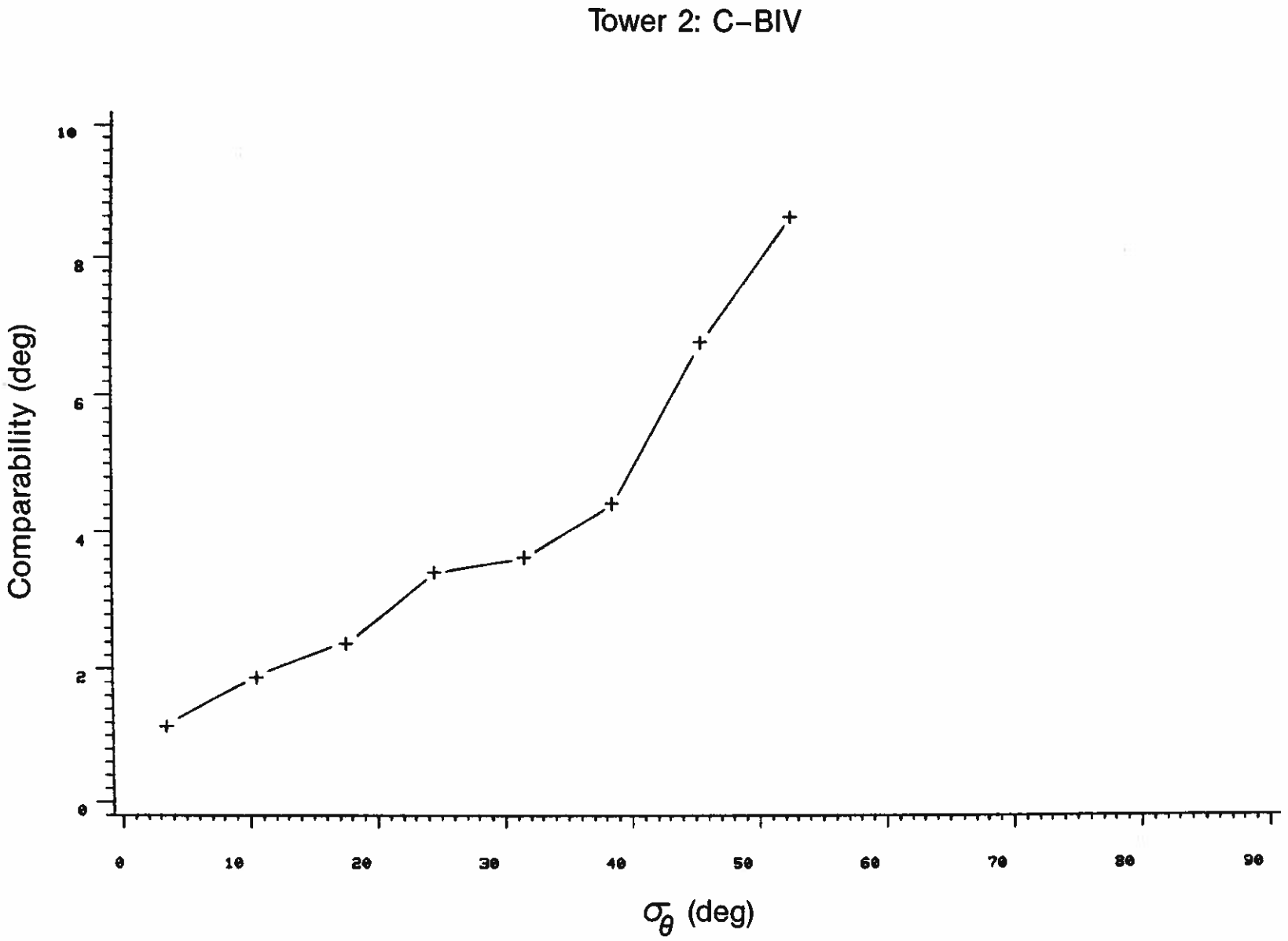

Figure 25. Comparability in σ_θ from C-BIV shown as a function of σ_θ.

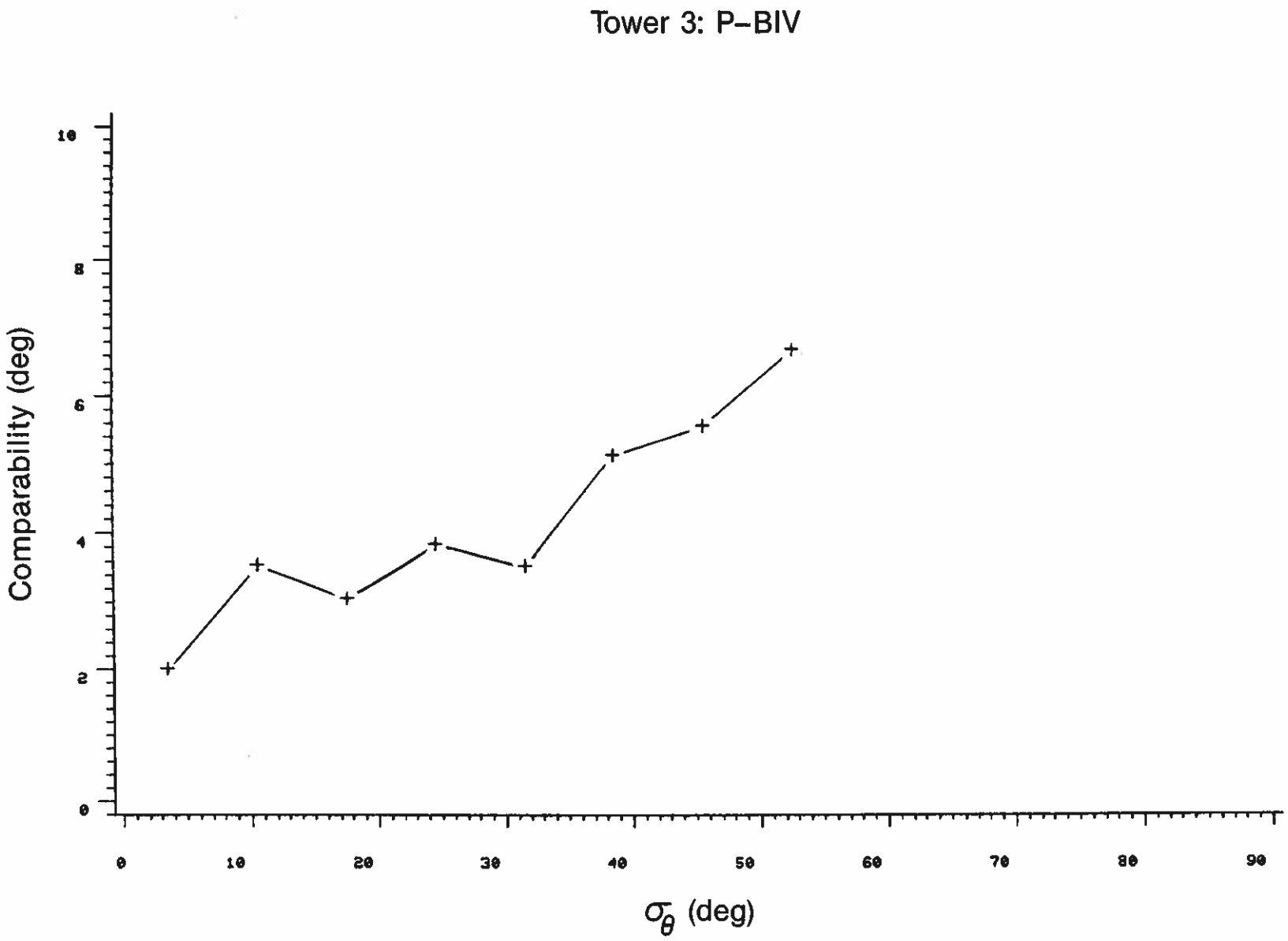

Figure 26. Comparability in σ_θ from P-BIV shown as a function of σ_θ.

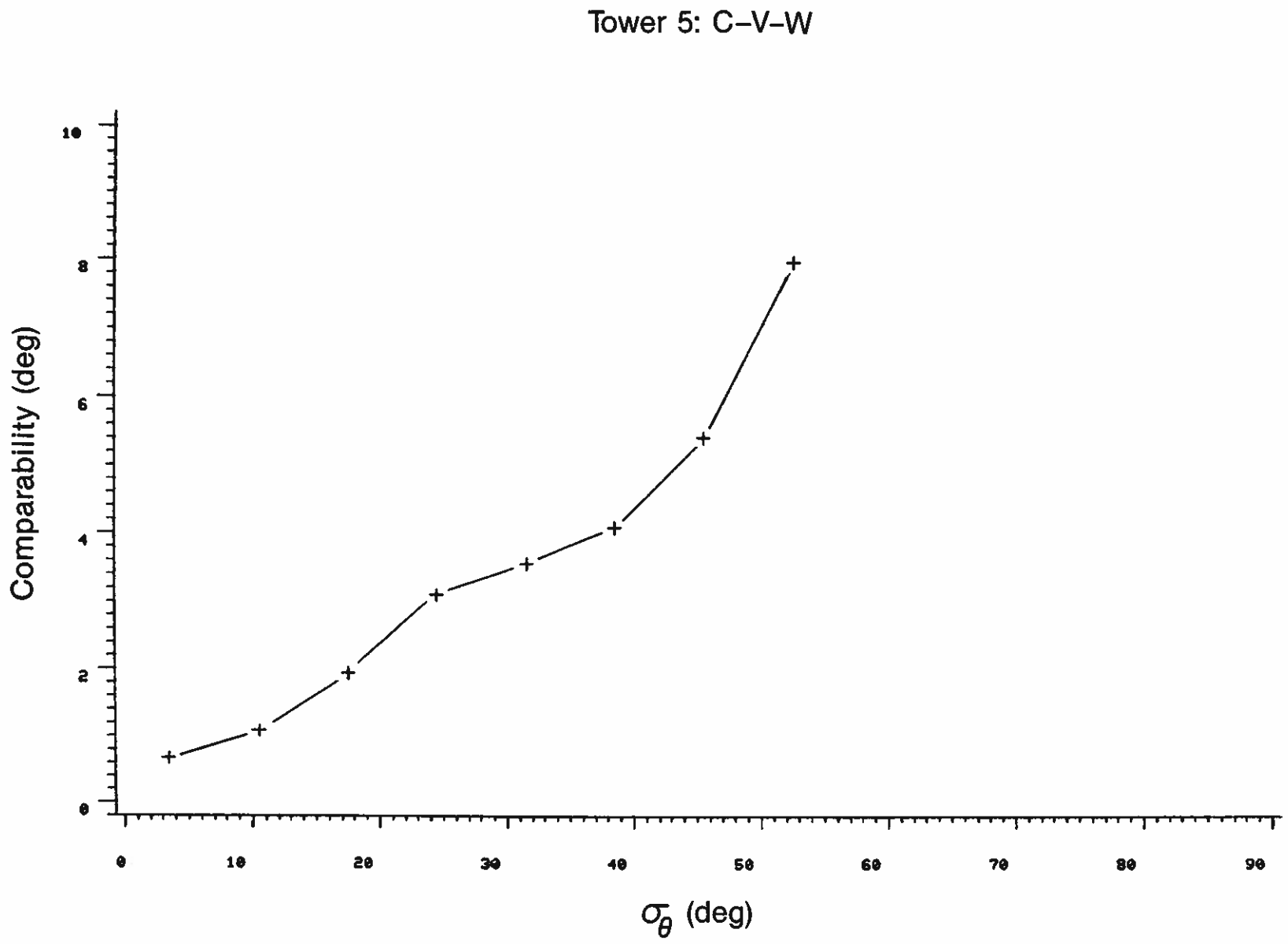

Figure 27. Comparability in σ_θ from C-V-W shown as a function of σ_θ.

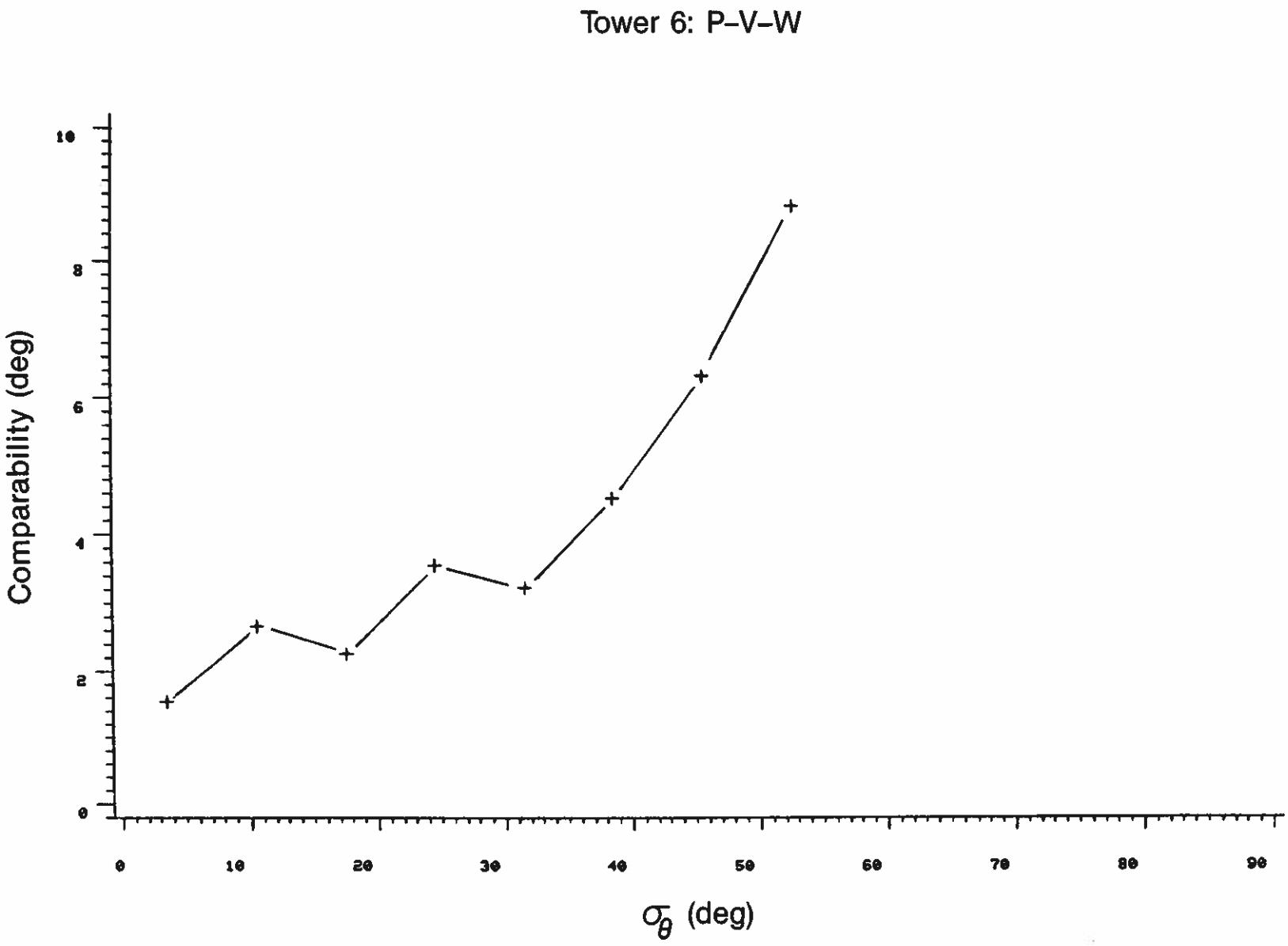

Figure 28. Comparability in σ_θ from P-BIV shown as a function of σ_θ.

7. COMPARISON OF σ_w VALUES

The vertical wind velocity, w, was measured with vertically oriented propellers, bivanes and the sonic anemometer. In the case of the bivanes, horizontal speeds measured by the cups (C-BIV) and the propeller (P-BIV) were used in combination with the inclination angles measured by the bivanes to compute the vertical velocity. On three towers (1, 5, and 6) identical propeller anemometers were used to measure vertical velocity. The reference anemometer (SONIC) measures w directly. Standard deviations, σ_w, were computed from the time series of w provided by each of the sensor systems.

Values for bias and comparability for σ_w are given in Table 7. The slight negative bias of the vertical propellers is to be expected; however, the positive bias of the bivanes indicates an overshoot, or underdamping. The close agreement in the magnitude of b and c for the propellers in U-V-W, C-V-W, and P-V-W is reassuring.

Table 7. Bias and comparability for σ_w

Instrument	b (m/s)	c (m/s)	N
U-V-W	-0.08	0.10	840
C-BIV	0.06	0.11	809
P-BIV	0.01	0.06	803
C-V-W	-0.07	0.08	782
P-V-W	-0.07	0.09	780

Daytime and nighttime values of b and c can be compared by use of Tables 8 and 9. Again it is clear that all instruments do slightly better under more stable conditions and that the bivanes show remarkably little bias at night.

Table 8. Bias and comparability for σ_w during the day

Instrument	b (m/s)	c (m/s)	N
U-V-W	-0.10	0.11	460
C-BIV	0.10	0.15	429
P-BIV	0.03	0.07	440
C-V-W	-0.07	0.09	428
P-V-W	-0.08	0.10	426

Table 9. Bias and comparability for σ_w at night

Instrument	b (m/s)	c (m/s)	N
U-V-W	-0.07	0.08	380
C-BIV	0.01	0.05	380
P-BIV	-0.01	0.04	363
C-V-W	-0.06	0.07	354
P-V-W	-0.06	0.07	354

Figures 29-33 show plots of σ_w comparability as a function of wind direction. A maximum near 94°, which is particularly pronounced in C-BIV, is caused by interference from the neighboring towers and possibly the structures around the BAO 300 m tower. Why this maximum is not seen in P-BIV is not clear.

Increases in wind speed increase the scatter in the measurements, but only at wind speeds above 5 m/s as seen in the comparability plots of Figs. 34-38. The largest scatter at the higher speeds is displayed by C-BIV. The scatter is significantly lower at all wind speeds for P-BIV.

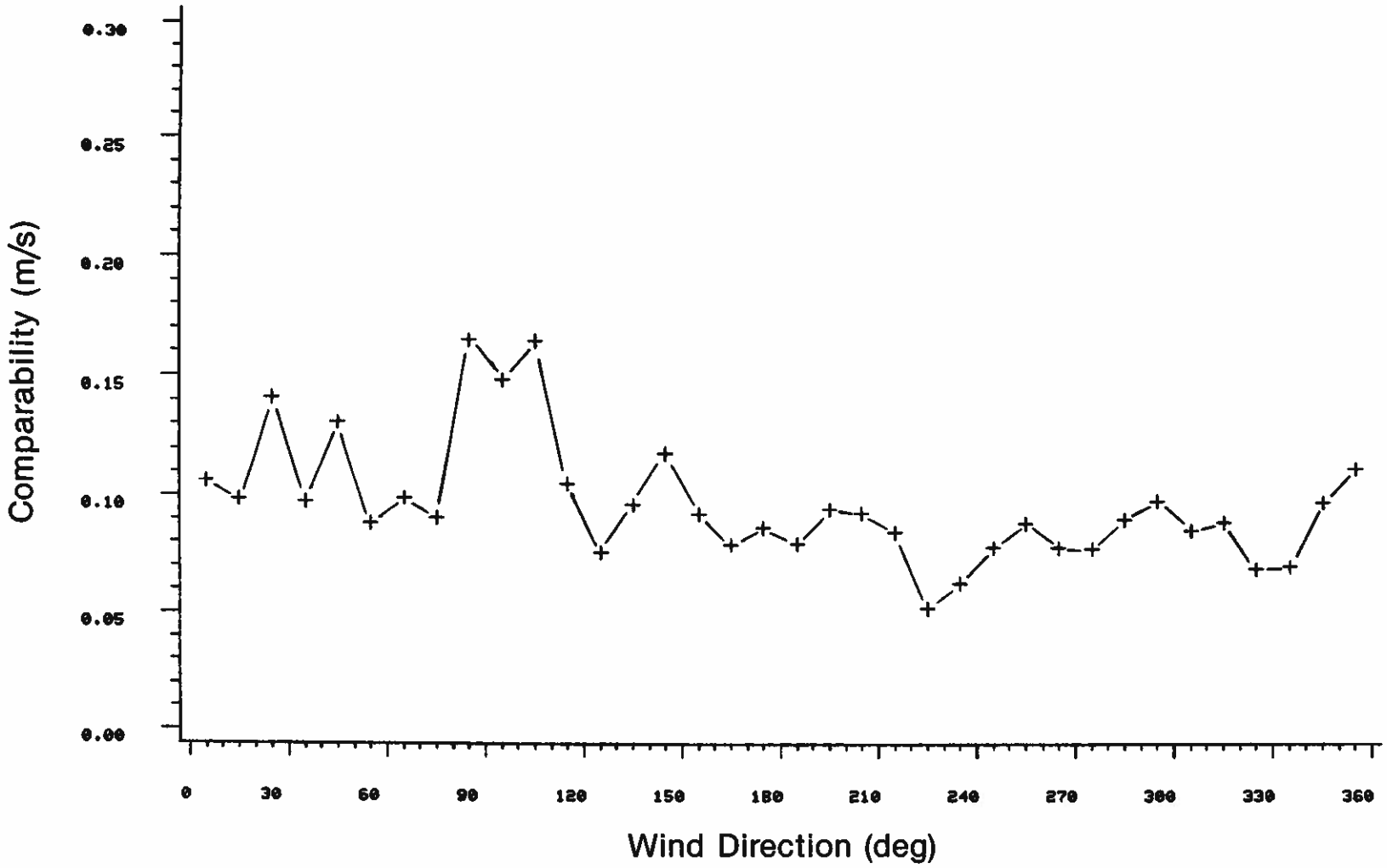

Figure 29. Comparability in σ_w from U-V-W shown as a function of wind direction.

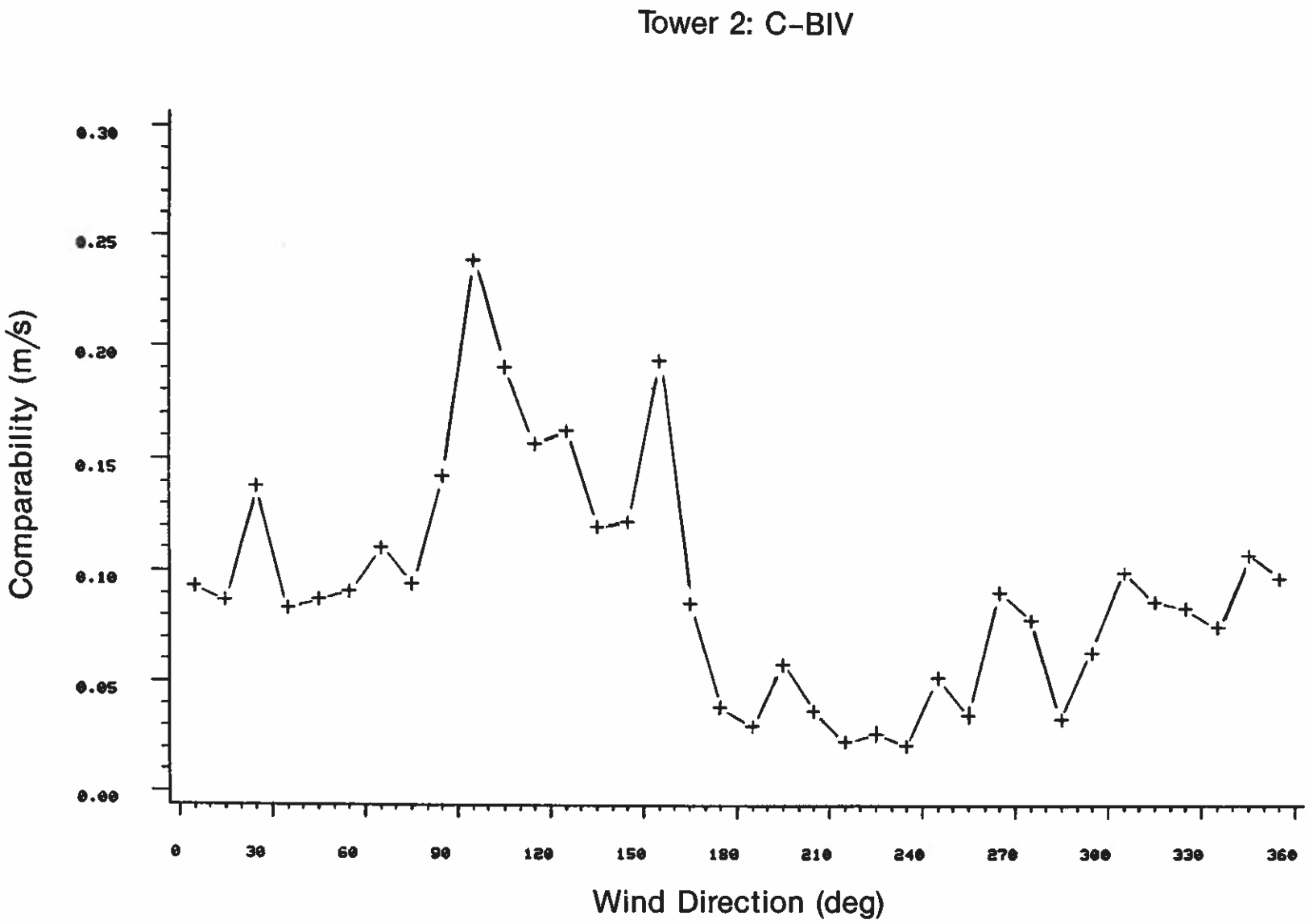

Figure 30. Comparability in σ_w from C-BIV shown as a function of wind direction.

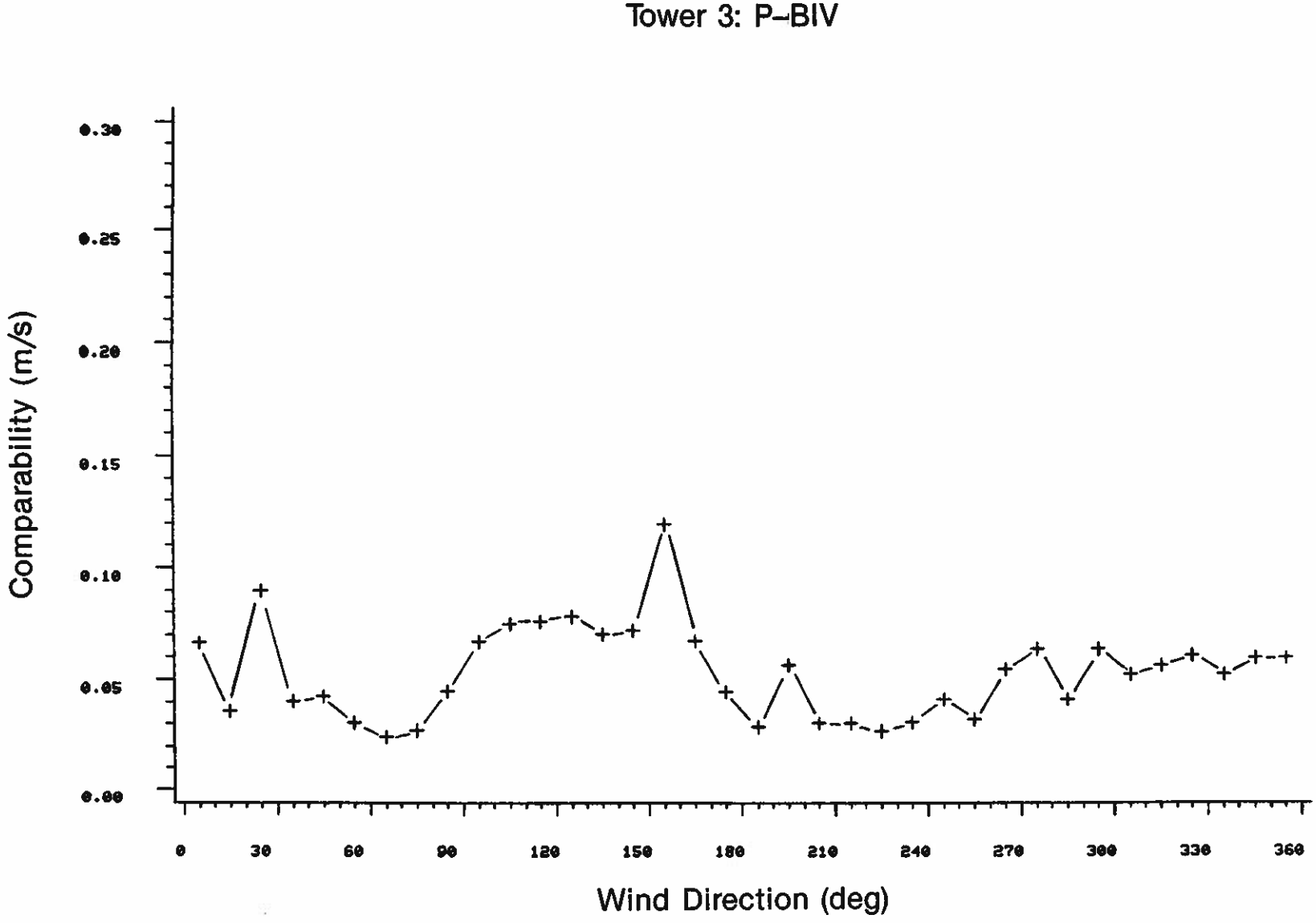

Figure 31. Comparability in σ_w from P-BIV shown as a function of wind direction.

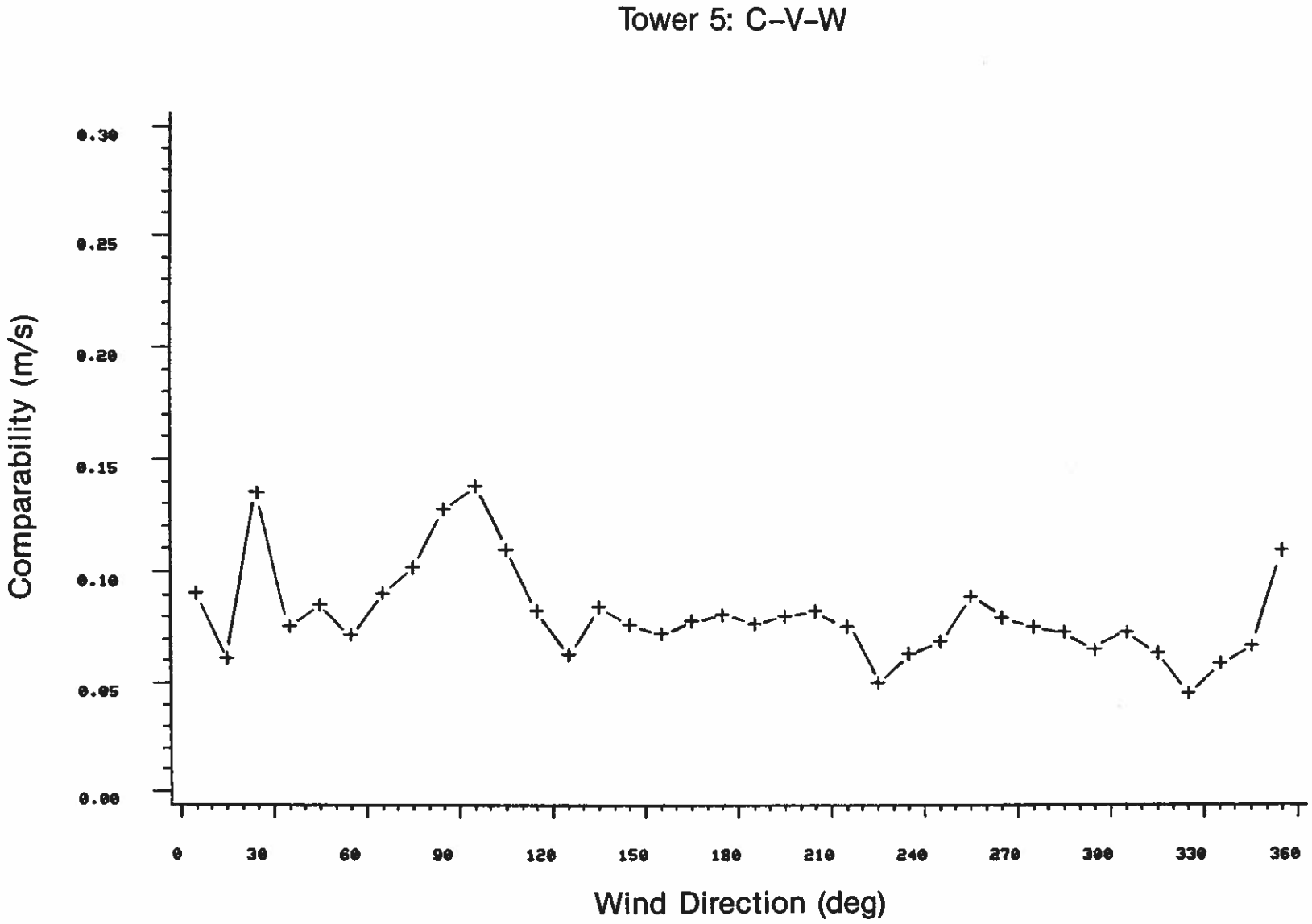

Figure 32. Comparability in σ_w from C-V-W shown as a function of wind direction.

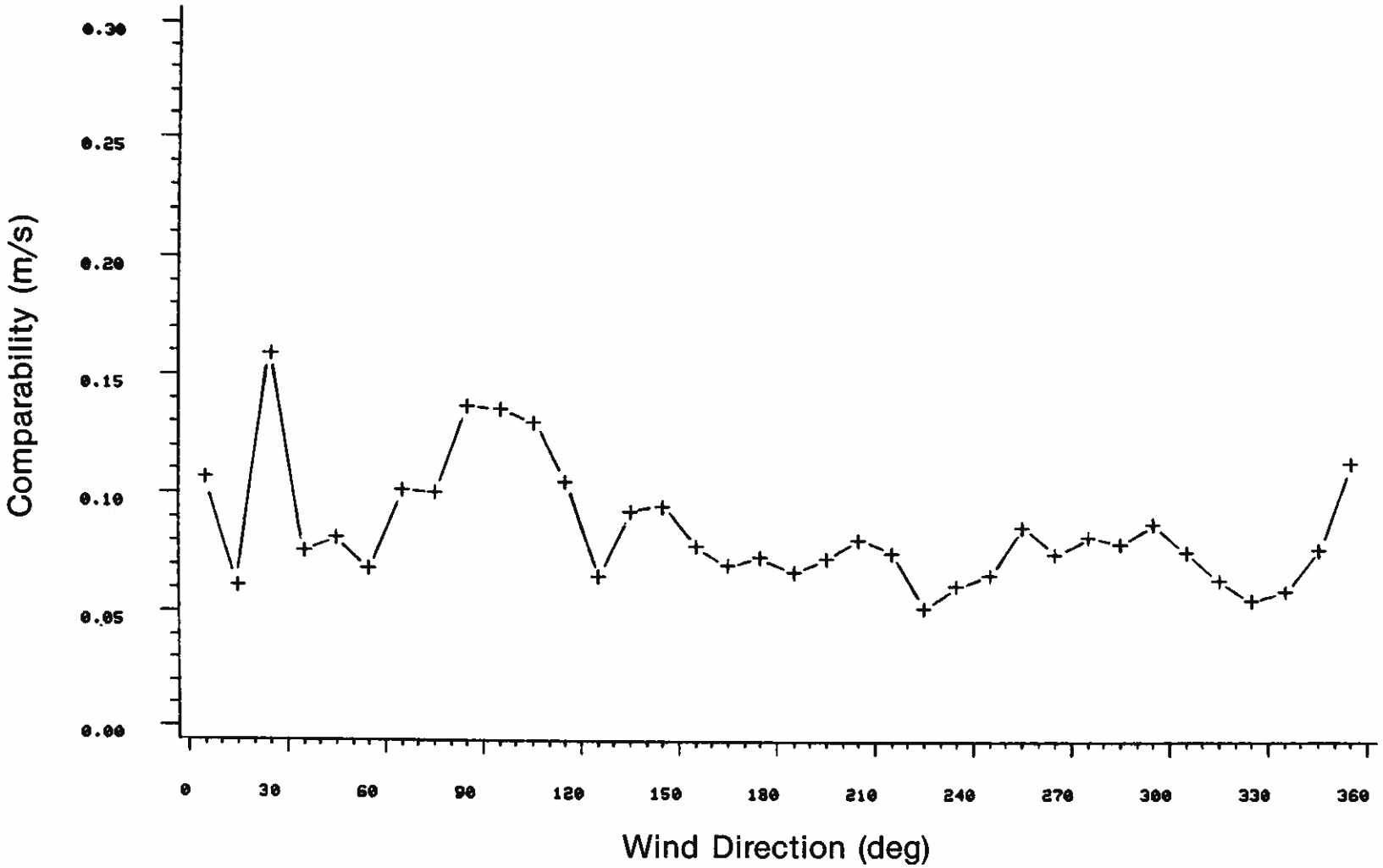

Figure 33. Comparability in σ_w from P-V-W shown as a function of wind direction.

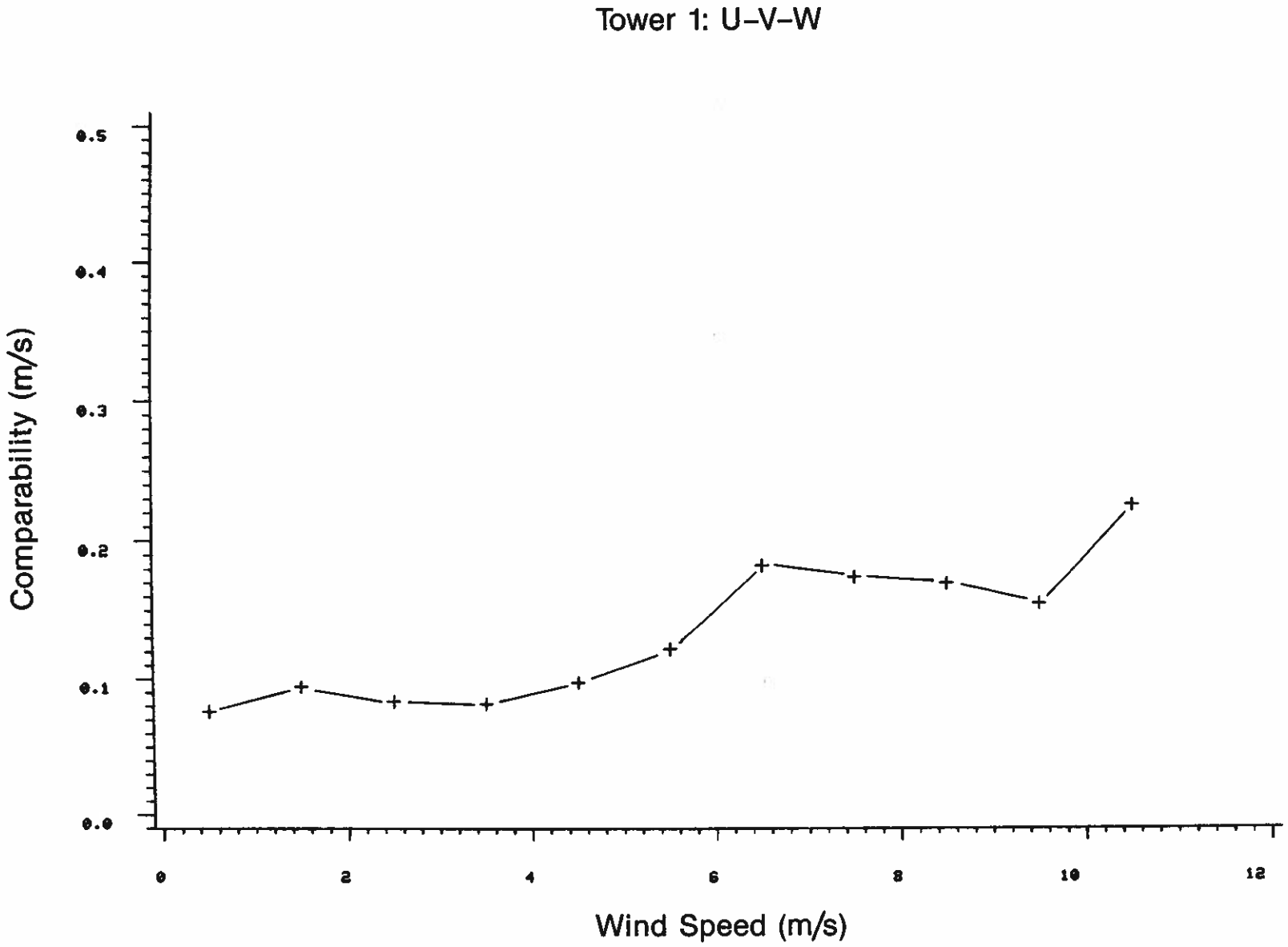

Figure 34. Comparability in σ_w from U-V-W shown as a function of wind speed.

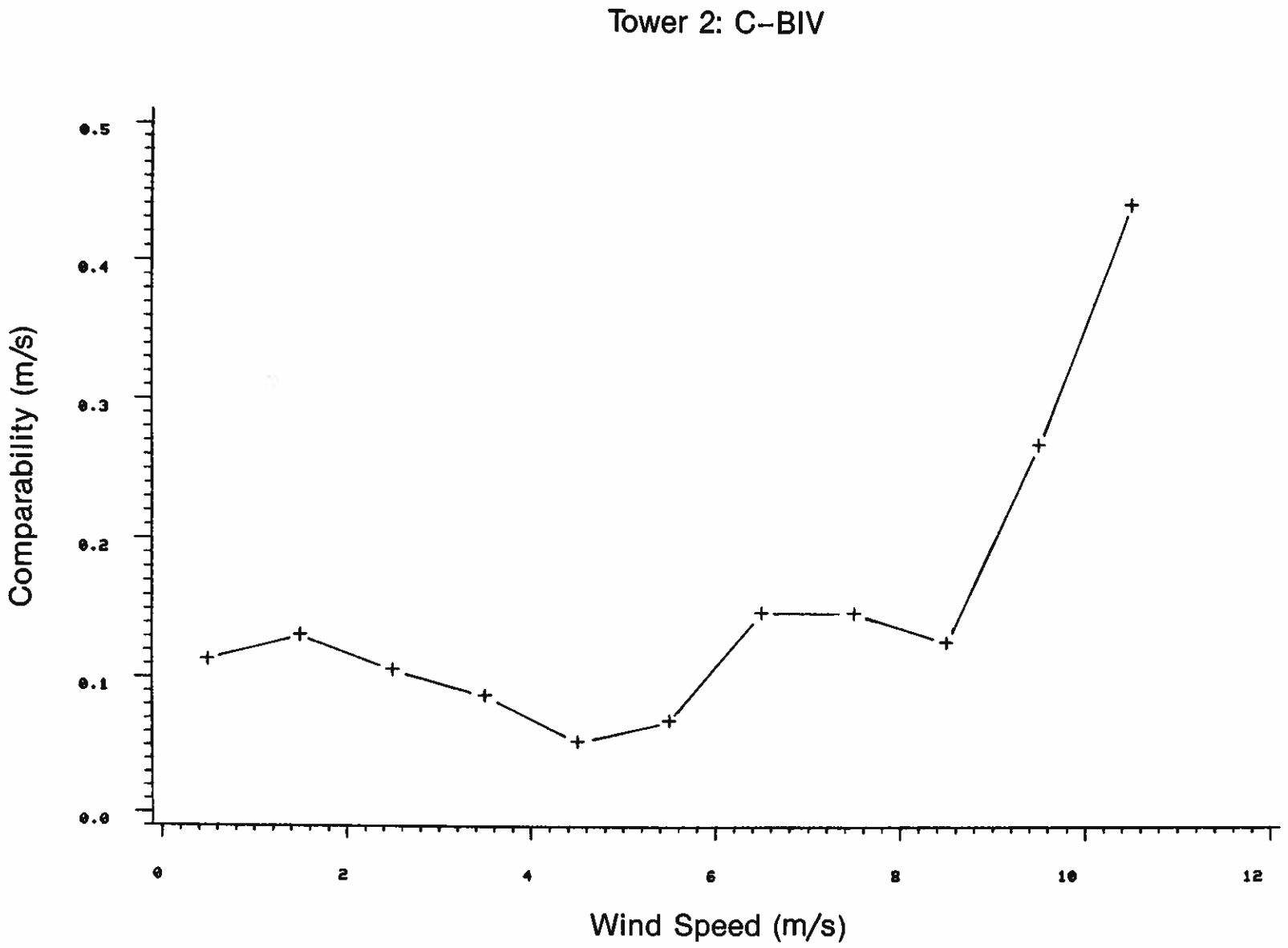

Figure 35. Comparability in σ_w from C-BIV shown as a function of wind speed.

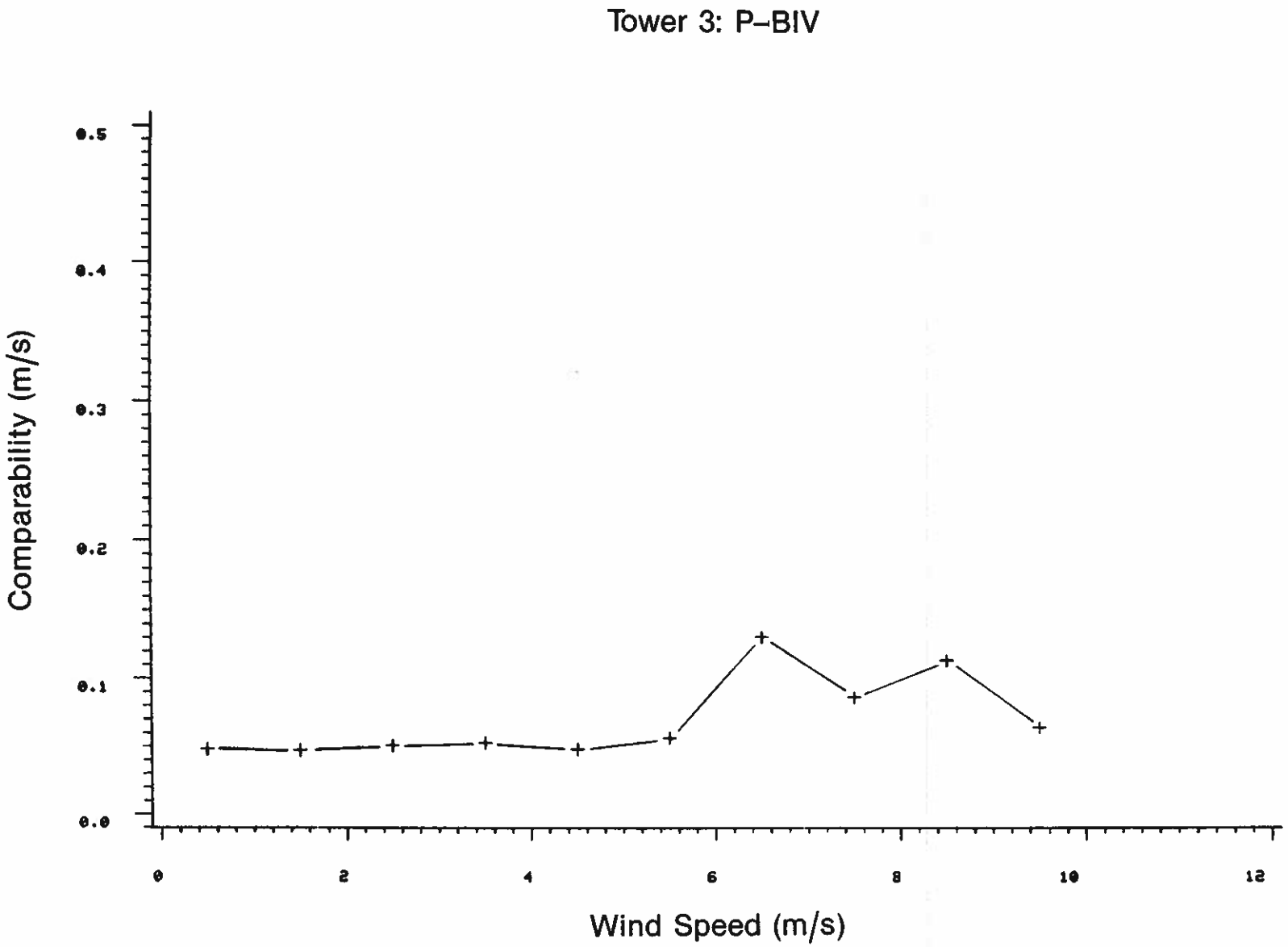

Figure 36. Comparability in σ_w from P-BIV shown as a function of wind speed.

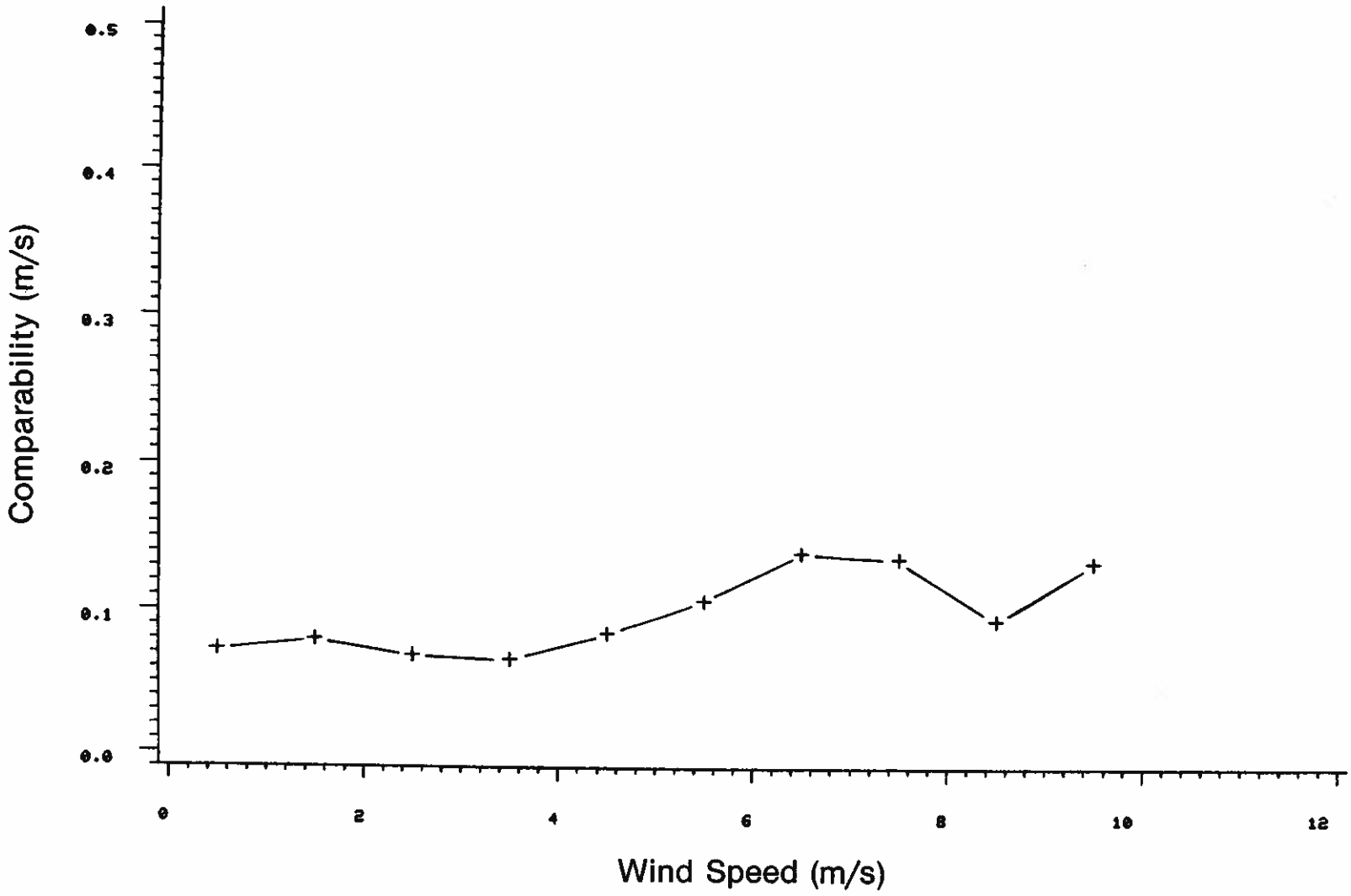

Figure 37. Comparability in σ_w from C-V-W shown as a function of wind speed.

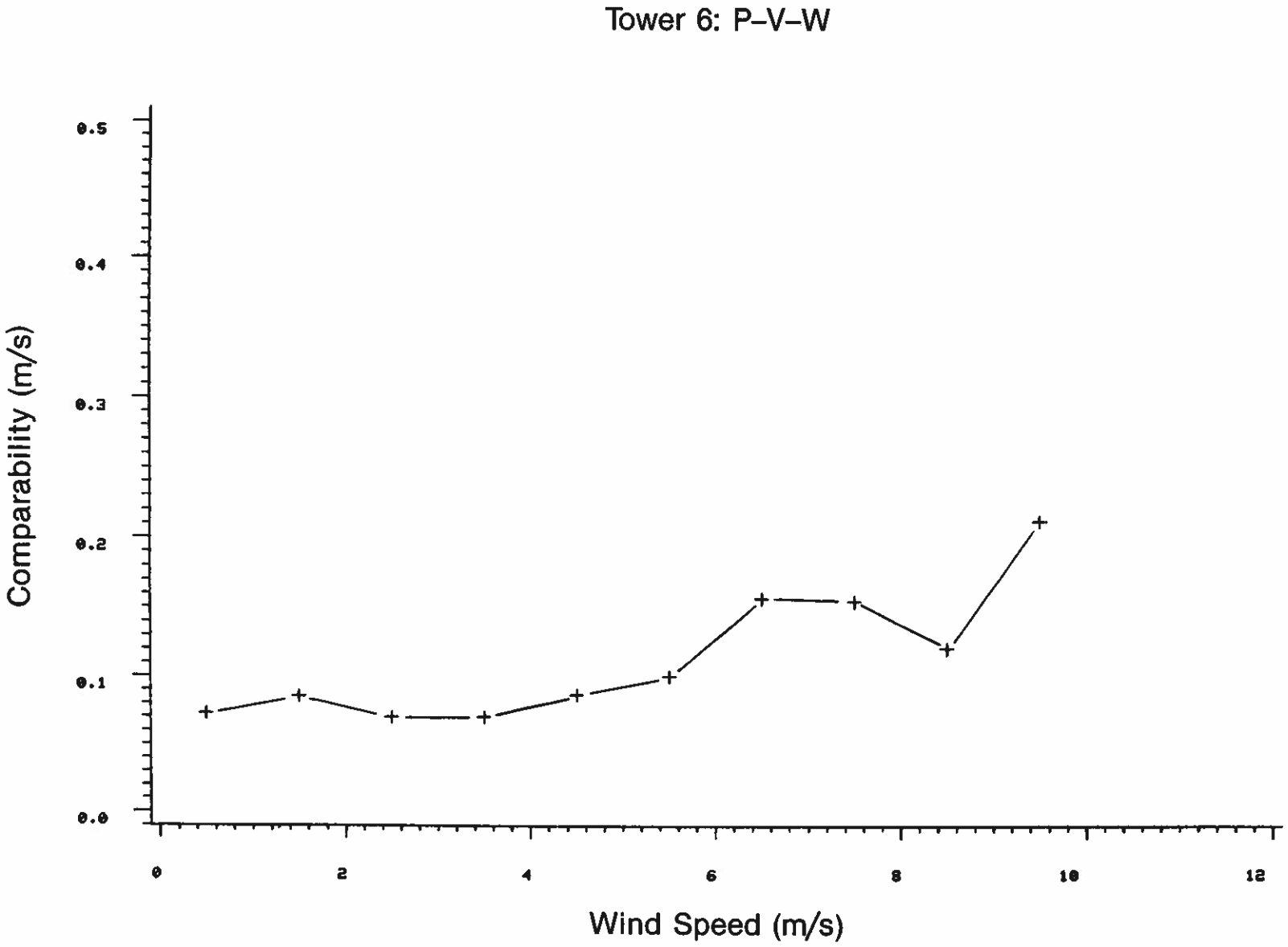

Figure 38. Comparability in σ_w from P-V-W shown as a function of wind speed.

8. COMPARISON OF σ_ϕ VALUES

The wind elevation angle (ϕ) was measured directly by the two bivanes and obtained indirectly from the wind components measured by the U-V-W system. These measurements and their standard deviations, σ_ϕ, were compared with the σ_ϕ computed from SONIC. Agreement is good according to the values in Table 10.

The slight positive bias of the lighter bivane is attributed to underdamping. That the U-V-W instrument agrees so closely with the bivanes is reassuring in view of the fact that it is used so frequently for turbulence measurements.

Table 10. Bias and comparability for σ_ϕ

Instrument	b (deg)	c (deg)	N
U-V-W	-0.30	2.07	890
C-BIV	0.65	1.80	804
P-BIV	-0.81	1.85	806

Comparisons of σ_ϕ measurements during the day and night are given in Tables 11 and 12. The differences shown here are interesting. C-BIV has a high positive bias during the day and a slightly negative one at night. The scatter as indicated by comparability is uniformly larger during the day than at night.

Table 11. Bias and comparability for σ_ϕ during the day

Instrument	b (deg)	c (deg)	N
U-V-W	-0.27	2.49	437
C-BIV	1.25	2.26	433
P-BIV	-0.83	2.14	435

Table 12. Bias and comparability for σ_ϕ at night

Instrument	b (deg)	c (deg)	N
U-V-W	-0.96	1.43	372
C-BIV	-0.05	1.02	371
P-BIV	-0.79	1.43	371

Figures 39-44, which plot σ_ϕ bias and comparability as functions of wind speed, bring a different perspective to the measurement. Although the U-V-W and C-BIV systems show only a small bias dependent on wind speed, the P-BIV has a definite negative bias at low wind speeds. This is probably due to the larger mass of P-BIV compared with the other two. All instruments show significant scatter at low wind speeds, but only C-BIV shows the scatter increasing again for speeds higher than 4 m/s (Fig. 43). The ϕ measurements are least dependable when the winds are light and variable; then the effects of bivane mass become more pronounced.

The σ_ϕ comparability is shown as a function of σ_ϕ itself in Figs. 45-47. All three instruments show an increase of c with σ_ϕ. Since large σ_ϕ values are associated with low wind speeds, the trends in these figures are not surprising.

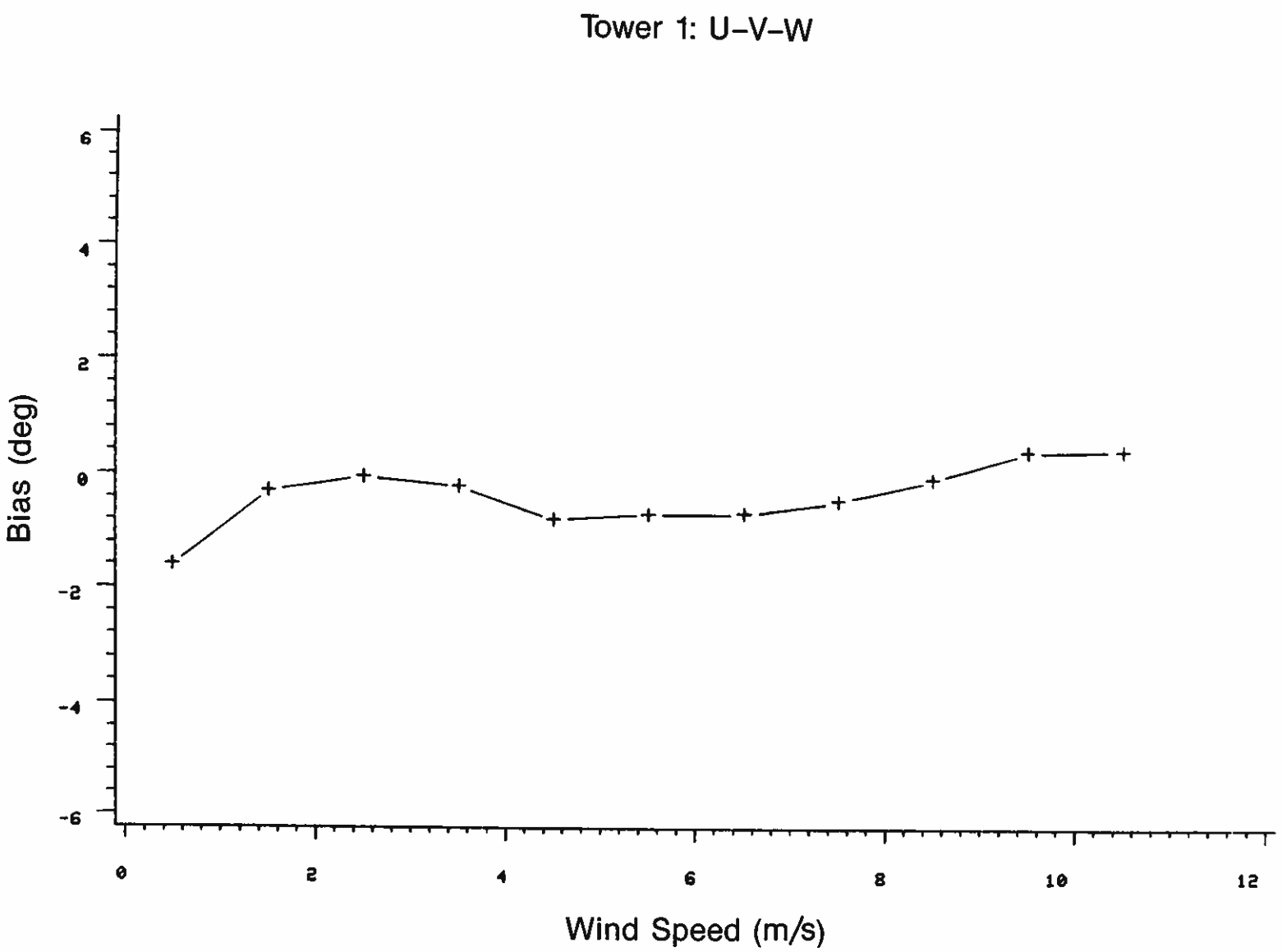

Figure 39. Bias in σ_ϕ from U-V-W shown as a function of wind speed.

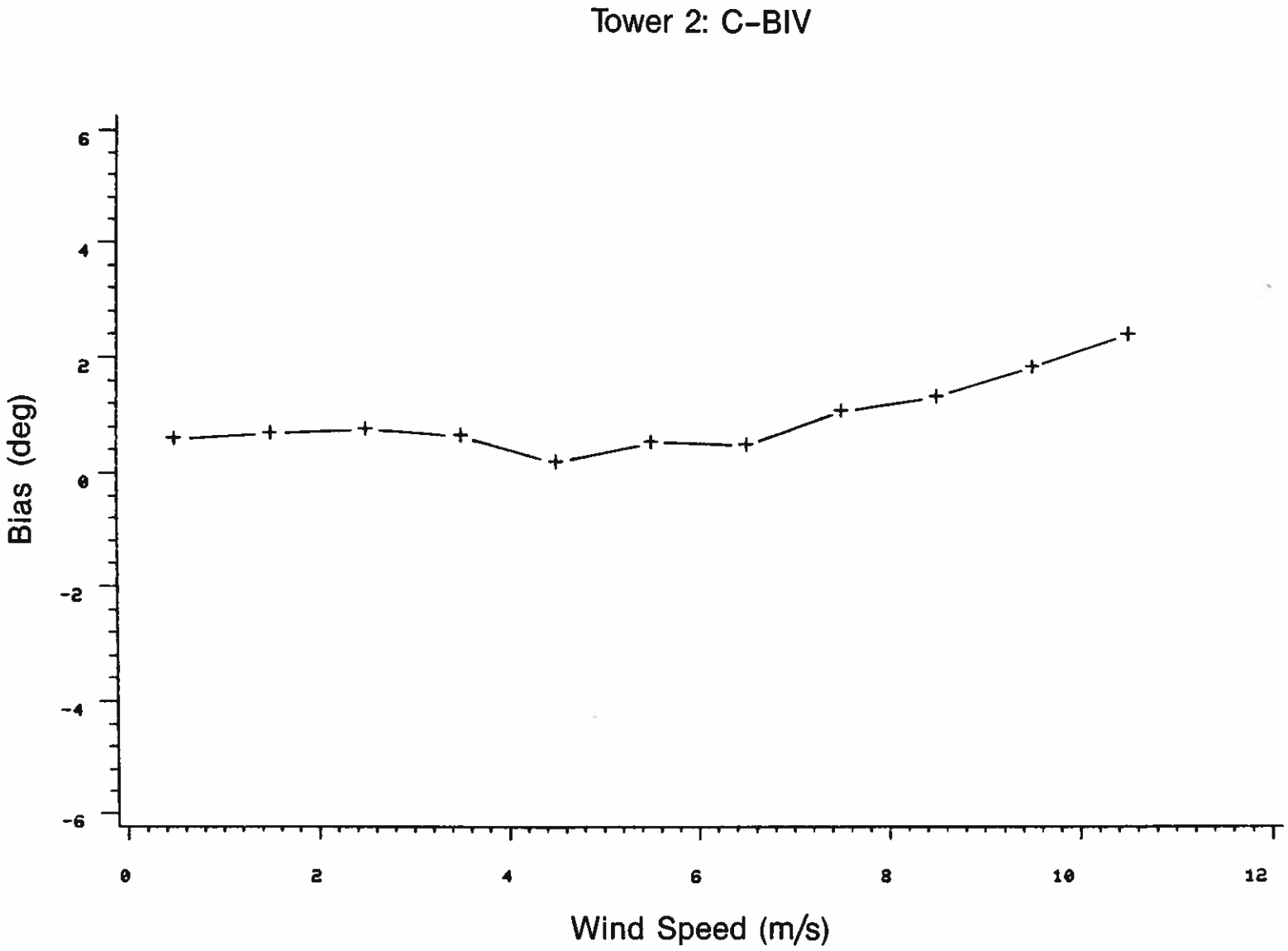

Figure 40. Bias in σ_ϕ from C-BIV shown as a function of wind speed.

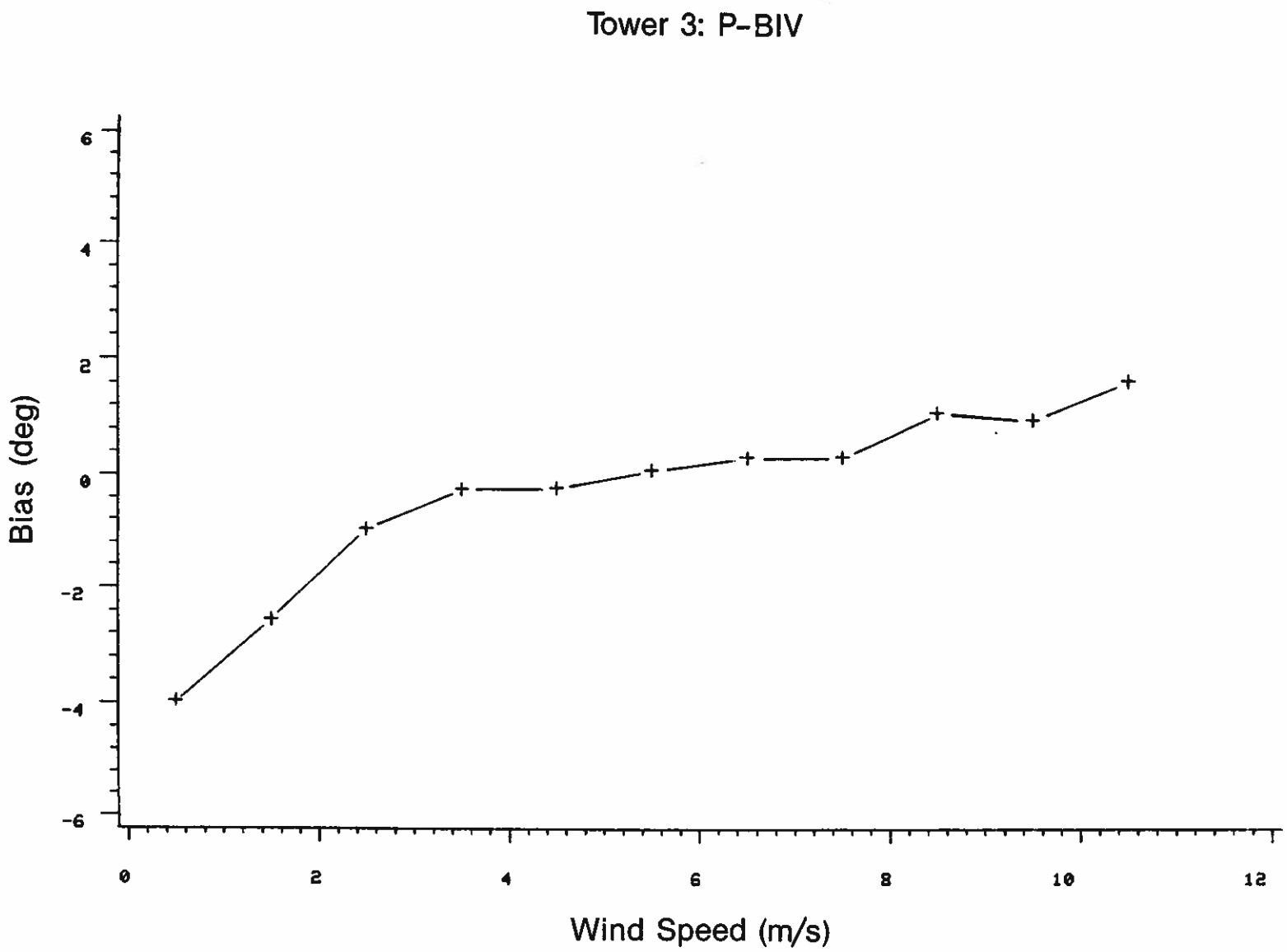

Figure 41. Bias in σ_ϕ from P-BIV shown as a function of wind speed.

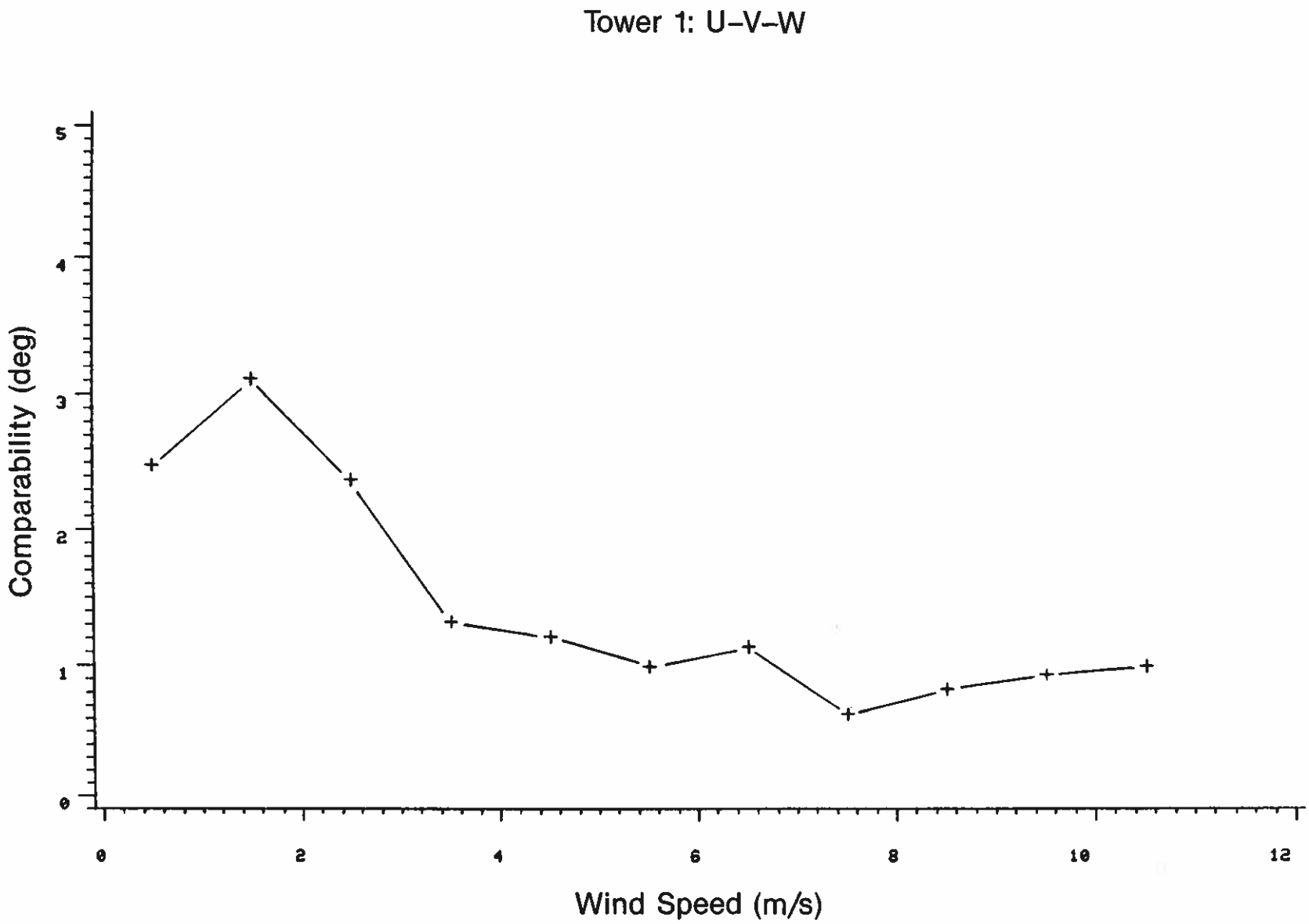

Figure 42. Comparability in σ_ϕ from U-V-W shown as a function of wind speed.

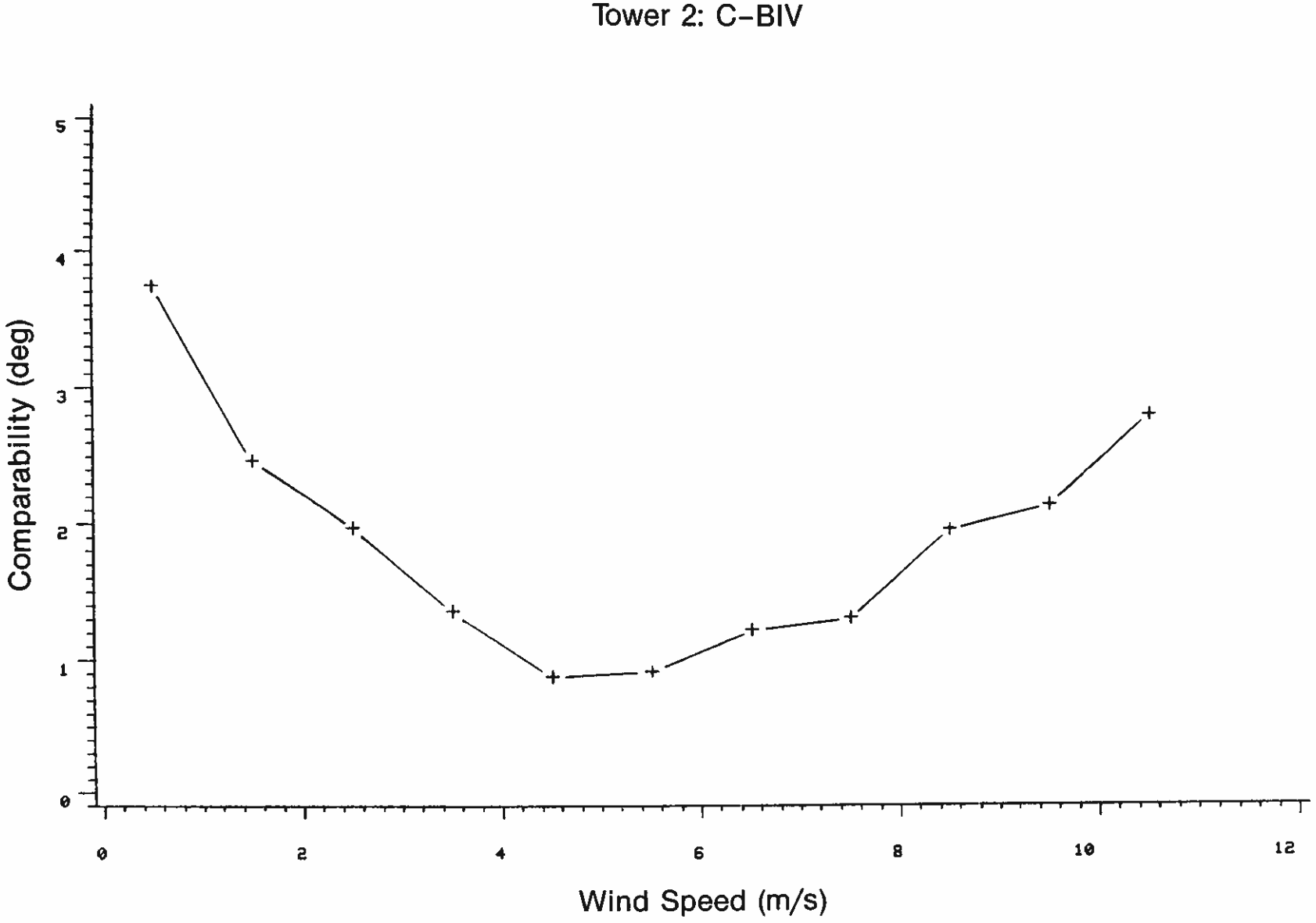

Figure 43. Comparability in σ_ϕ from C-BIV shown as a function of wind speed.

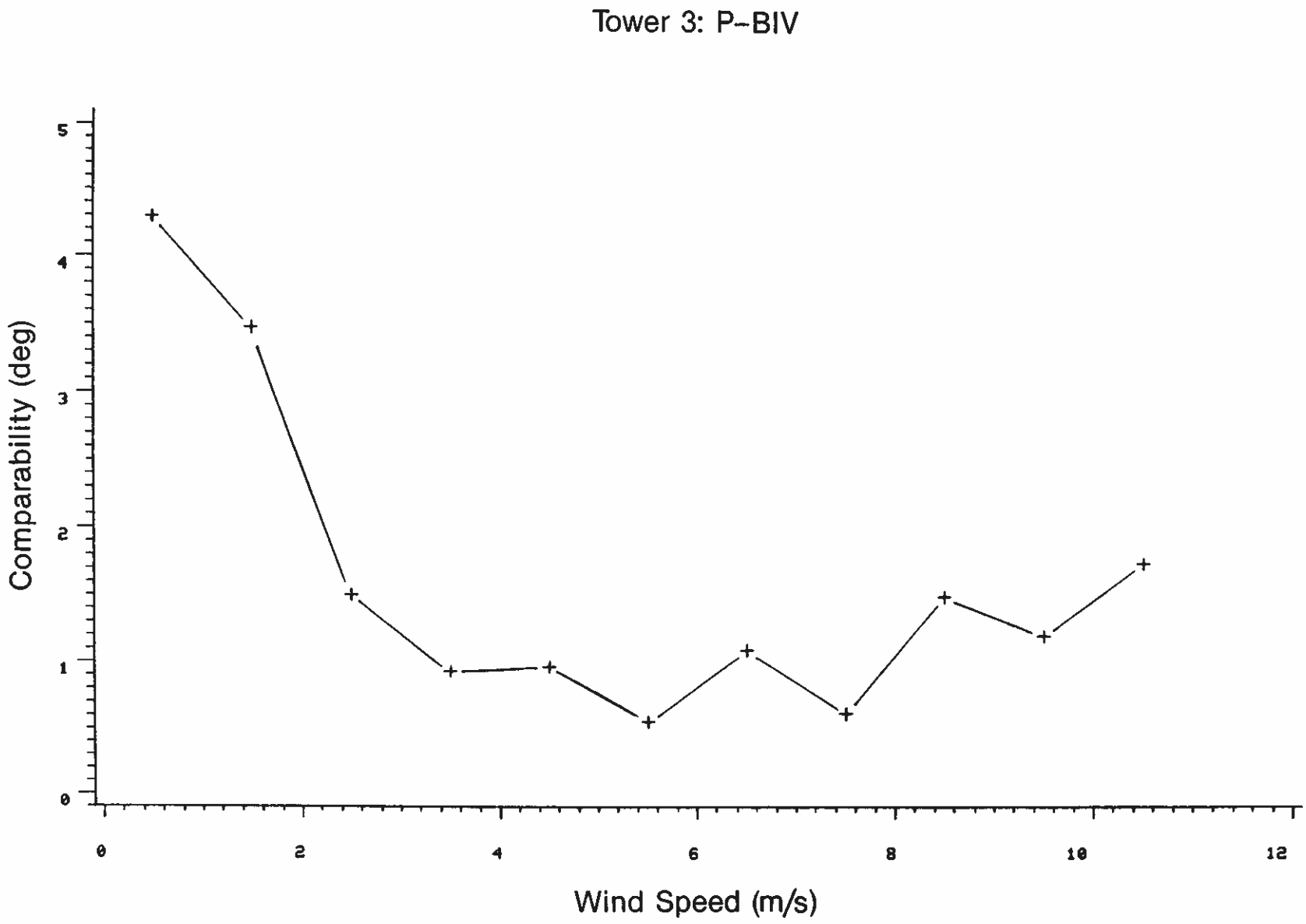

Figure 44. Comparability in σ_ϕ from P-BIV shown as a function of wind speed.

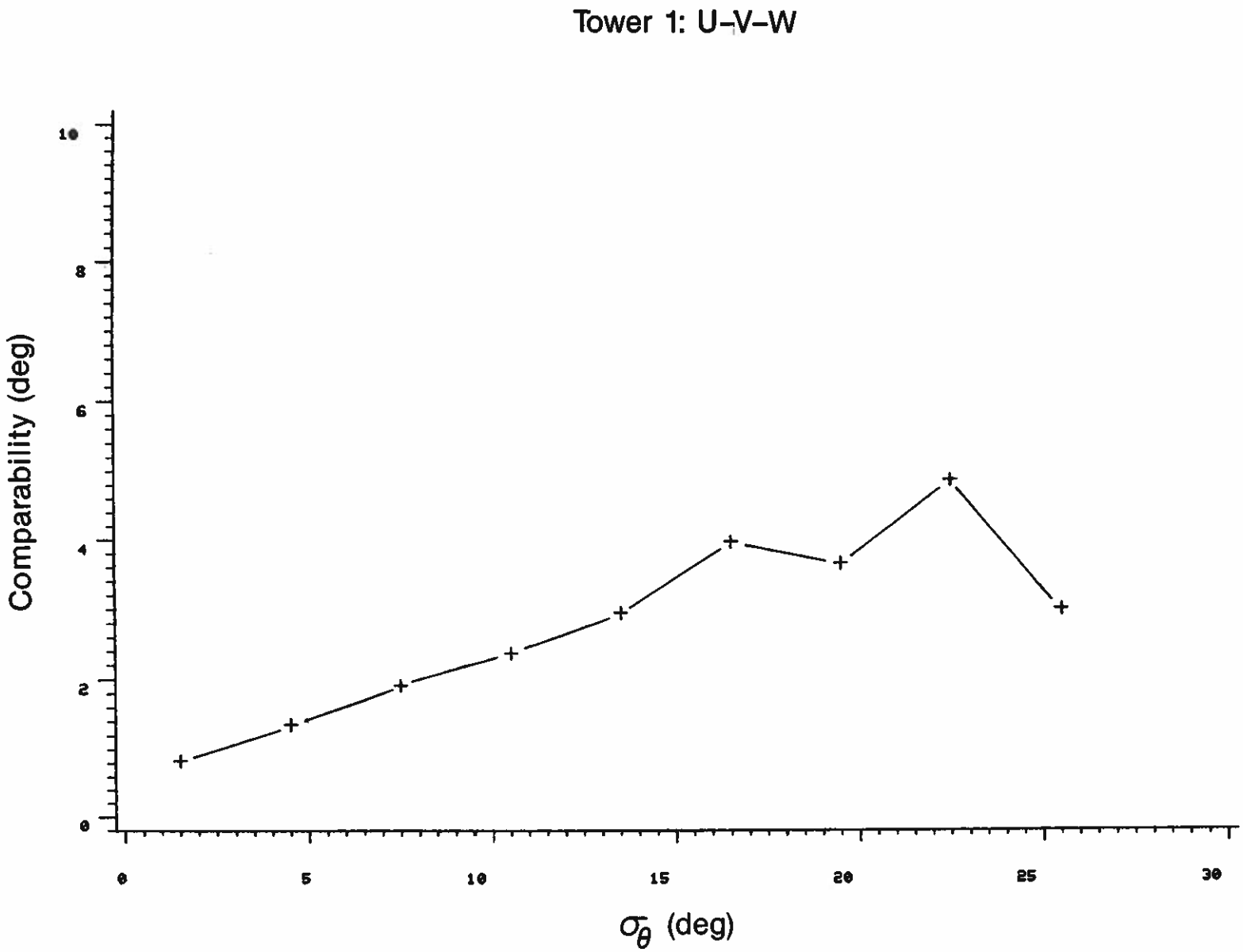

Figure 45. Comparability in σ_ϕ from U-V-W shown as a function of σ_θ.

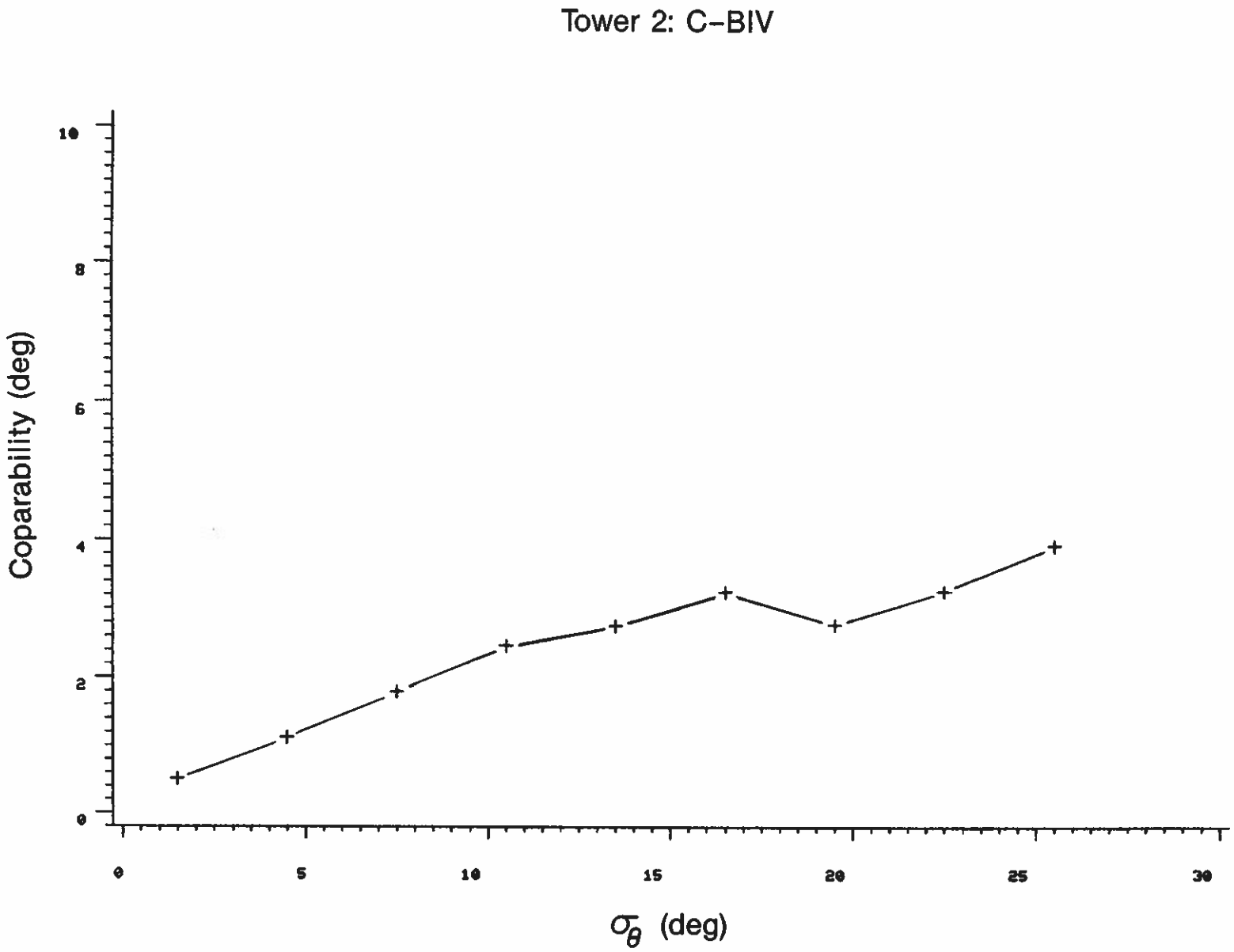

Figure 46. Comparability in σ_ϕ from C-BIV shown as a function of σ_θ.

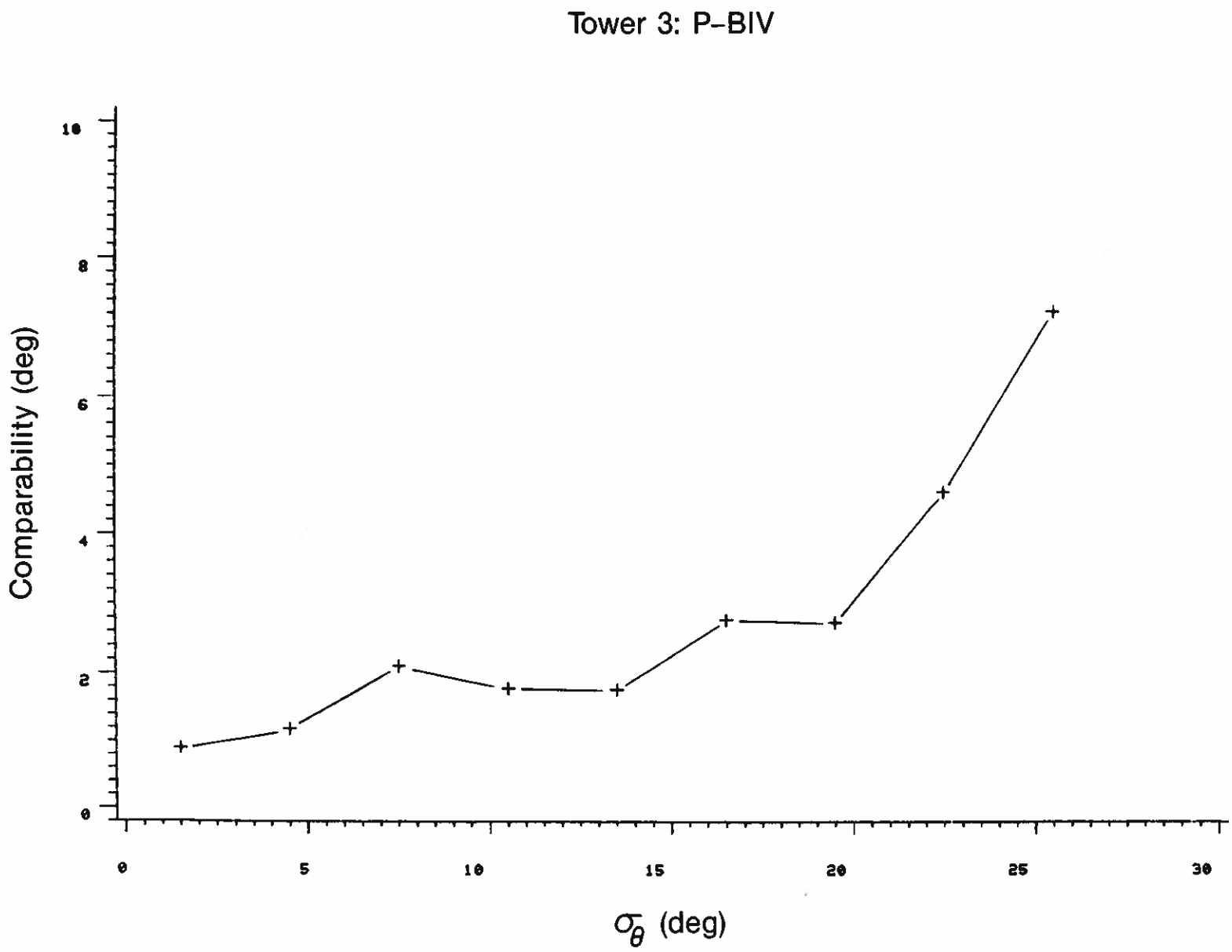

Figure 47. Comparability in σ_ϕ from P-BIV shown as a function of σ_θ.

9. COMPARISON OF SIGMA METERS

There are various devices on the market that purport to compute an effective standard deviation from input analog signals. These have frequently been used with meteorological equipment, usually wind vanes, to produce a σ_θ value for preselected averaging times. Early sigma meters processed analog signals, using variations on an R-C circuit, to estimate the standard deviation of the signal. With the availability of microprocessor chips, digital computation is now widely used. In this experiment two sigma meters, denoted A (analog) and D (digital), were tested. Several different input signals were used to see if any significant differences could be detected; in each case the two sigma meters saw the same input at the same time. Standard deviations estimated by the meters were compared with σ values computed by the BAO data logging system from the same input signals. The same data logging and averaging procedures used for the rest of this study were followed. No comparison is made with the sonic anemometer in this evaluation.

The results of this comparison (Table 13) indicate that for θ, ϕ, and w inputs the analog sigma meter significantly underestimates the standard deviation. Both systems show considerably more scatter for σ_θ than for σ_ϕ or σ_w, but the analog system shows scatter almost twice as large. The scatter is approximately equivalent for σ_ϕ; for σ_w the analog system performs slightly better than the digital in terms of both bias and scatter. Not surprisingly the performance of both systems deteriorates with increasing levels of turbulence, as is shown in Figs. 48 and 49. The reasons for this seem clear for

the analog system, but are less so for the digital. In any event, the trend toward more digital electronics and on-site digital data processing and logging should produce improvements in the digital meters and in the development of new algorithms for real-time analyses of meteorological data.

Table 13. Bias and comparability of standard deviations computed by the sigma meters and the wind sensors

Input Signal	Type of σ meter	b (deg)	c (deg)	N
θ(P-BIV)	A	-3.6	10.3	595
	D	-1.5	5.1	653
θ(C-BIV)	A	-3.8	10.8	354
	D	-1.2	5.5	354
ϕ(P-BIV)	A	-0.8	1.3	480
	D	0.7	1.3	479
ϕ(C-BIV)	A	-1.3	2.1	88
	D	0.6	1.9	88
w(U-V-W)	A	-0.05	0.06	157
	D	0.12	0.14	157

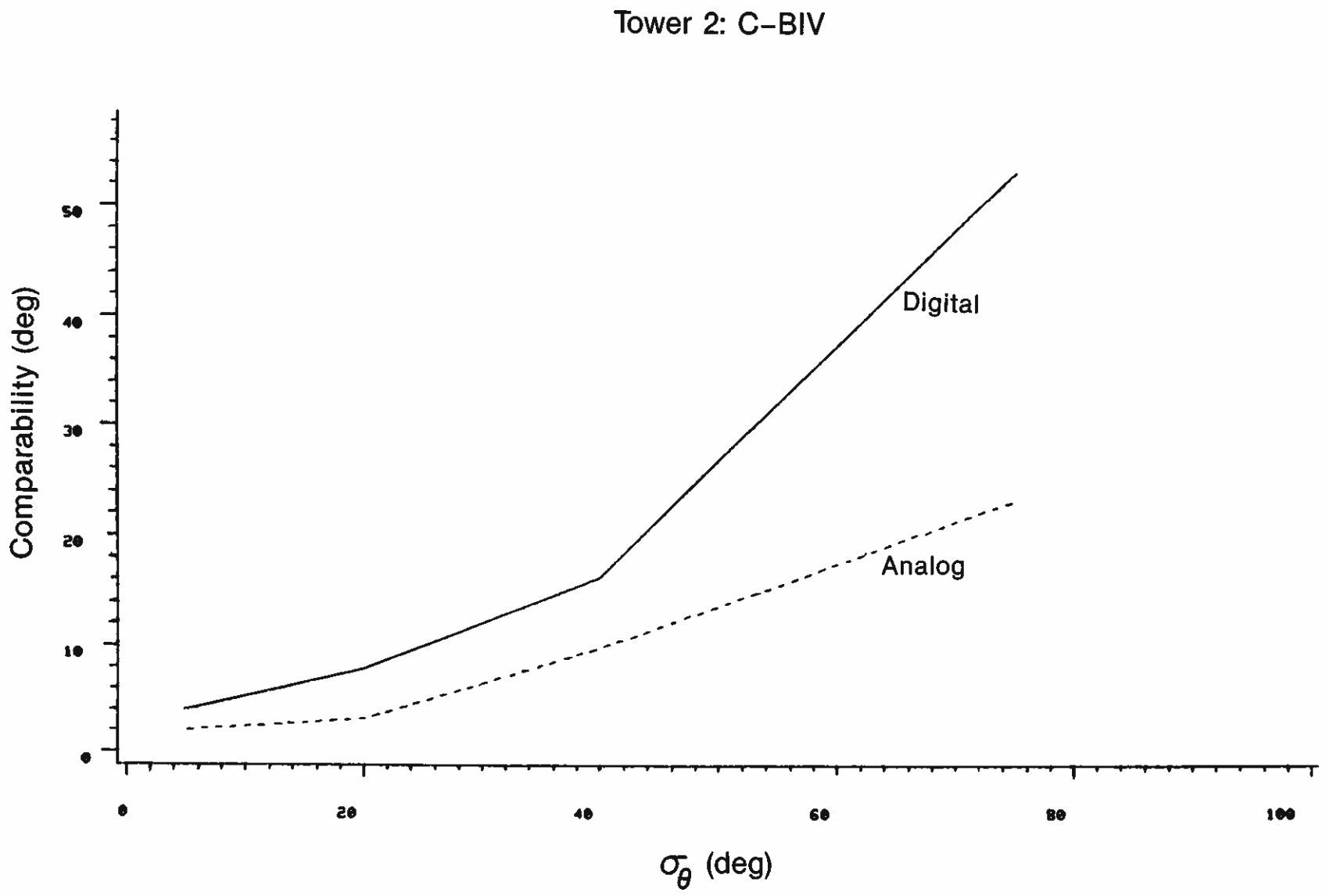

Figure 48. Comparability in σ_θ from the analog and digital sigma meters shown as functions of σ_θ.

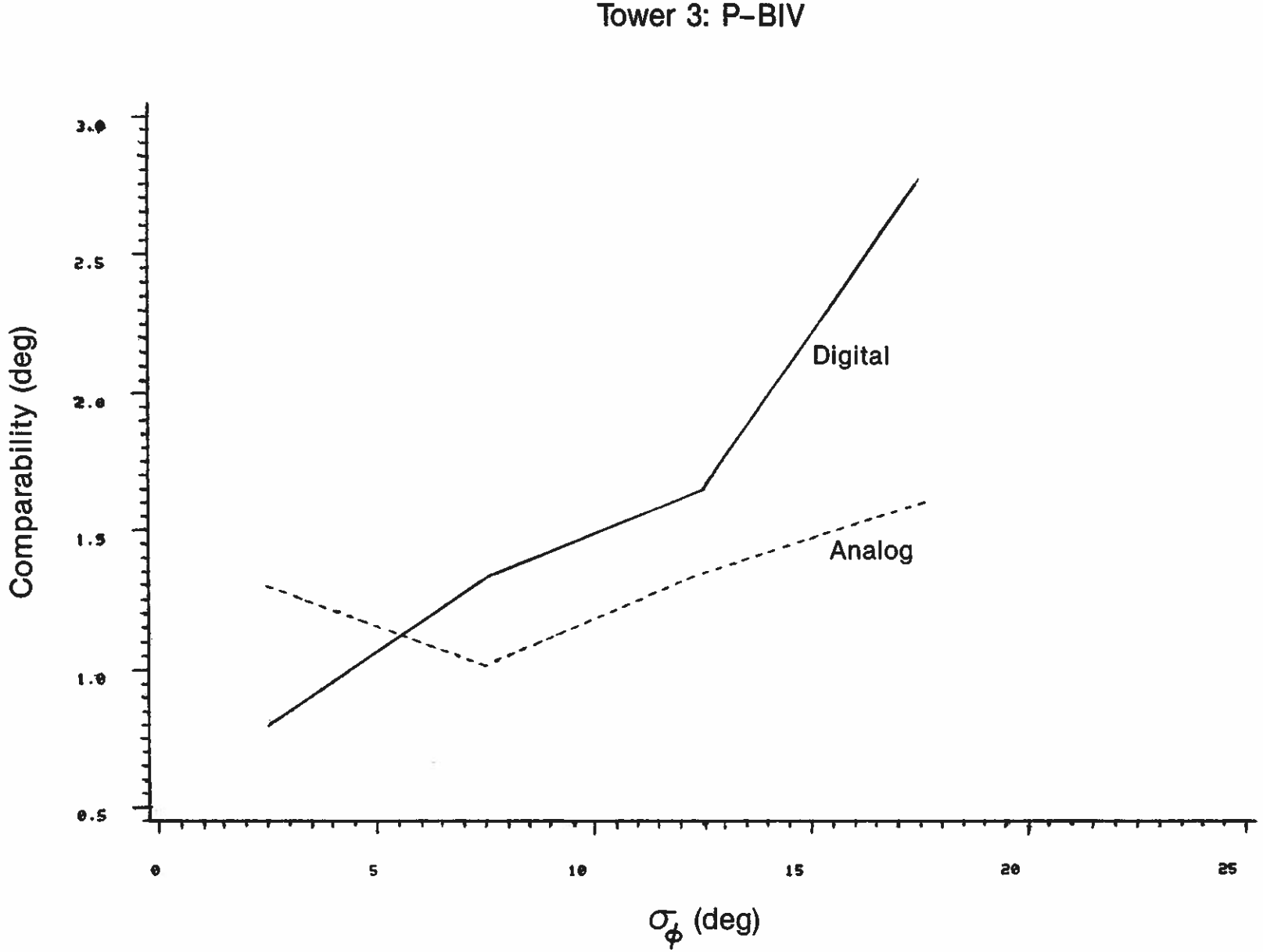

Figure 49. Comparability in σ_ϕ from the analog and digital sigma meters shown as functions of σ_ϕ.

10. SENSOR RESPONSE TO WIND FLUCTUATIONS

An important objective of this study was to determine how well our sensors respond to turbulent fluctuations in the flow. Published data on response lengths and distance constants enable us to derive response functions indirectly. The bias and comparability statistics presented in the foregoing pages offer additional clues. A direct approach is to compare spectra for typical flows from the candidate sensor and a reference sensor, such as the SONIC. Toward this end, we had recorded data from all our sensors at the full 10 samples/s rate on two days, 9 and 18 September. Time series from these records were subjected to the spectrum analysis procedures outlined by Kaimal and Gaynor (1983) and are used in the discussion that follows. Typical plots of frequency-weighted spectral intensities as functions of frequency, n, are presented in Figs. 50-52. Mean wind speeds, wind directions, and stability conditions for these periods presented are given in Table 14.

Table 14. Data summary for periods represented in Figs. 50-52

Date	Time (MST)	z/L	U(m/s)	θ(deg)
9 Sept. 82	1040-1200	-1.43	3.4	348
18 Sept. 82	1720-1840	0.05	6.5	192
18 Sept. 82	2000-2120	0.37	2.1	252

U: mean wind speed at 10 m
θ: mean wind direction at 10 m
z/L: stability parameter (height / Obukhov length) at 10 m

There is, in general, good agreement between the sensor and the SONIC spectra at middle and low frequencies. At the high-frequency end, the SONIC spectra fall off at a rate consistent with predictions for the inertial subrange, at a rate less steep than the sensor spectra (see Figs. 52-54). The sensor response starts to separate from the SONIC spectrum at approximately the same wavelength in all three stabilities. (We assume wavelength $\lambda \simeq U/n$, following Taylor's hypothesis.) The vertical arrows represent our best estimate of this separation point, which corresponds to wavelengths of 4.4 m for C-BIV, 7.0 m for P-BIV, and 32 m for C-V-W.

On closer examination, one finds a tendency in both bivanes to overestimate spectral contributions in the middle- to low-frequency range in unstable and neutral air, and to underestimate contributions in the middle- to high-frequency range in very stable air. For the vertical propeller, the underestimation in stable air is more extensive (Fig. 52), almost a factor of 2 across the entire spectral bandwidth. Intermittent stoppage of the propeller, when the wind drops below its response threshold, can produce such a depression in spectral levels. (The effect would be comparable to the effect of adding zeros to a time series. When time series are thus expanded, a correction factor is usually applied to restore the spectrum to its proper level.)

Transfer functions derived from composite plots of spectra from each sensor normalized by the SONIC spectra, are presented in Figs. 53 and 54. For variable x, the transfer function $T_x(\lambda)$ is defined as

$$T_x(\lambda) = \frac{[S_x(\lambda)]_{Sensor}}{[S_x(\lambda)]_{SONIC}} , \qquad (3)$$

where $S_x(\lambda)$ is the spectral estimate at wavelength λ. The light wind stable cases are not included in the composites, although they too would have fitted

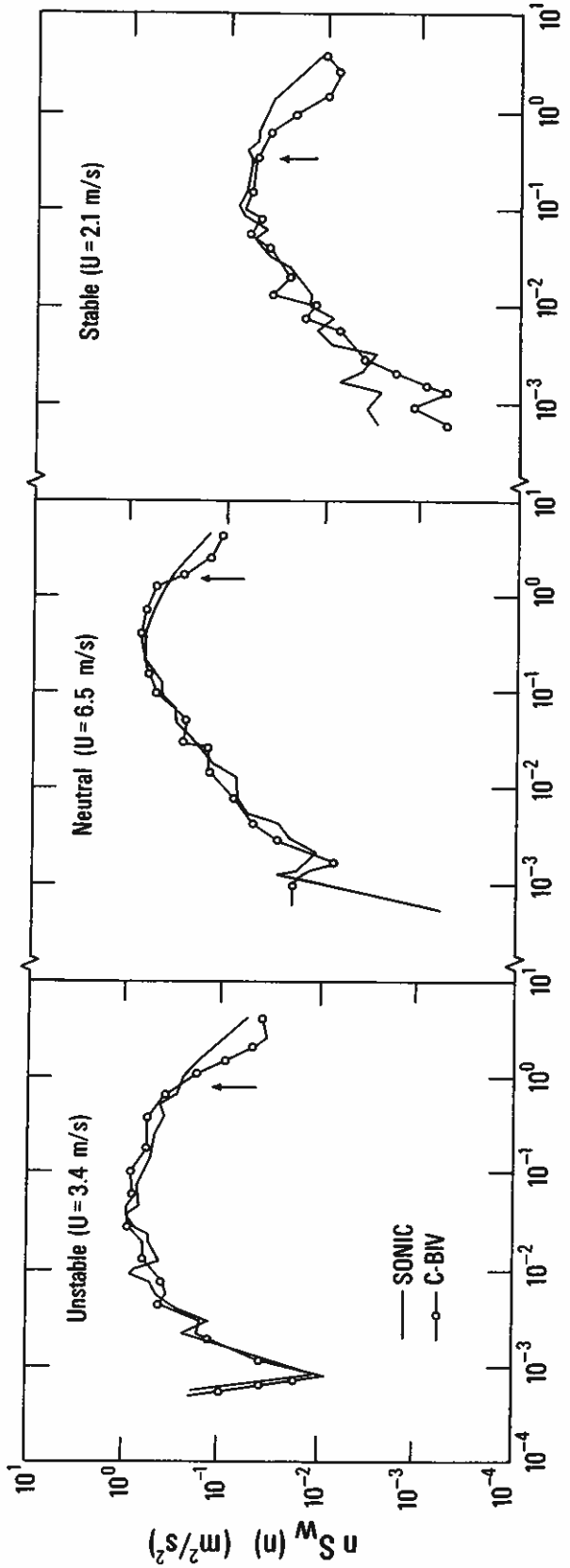

Figure 50. Spectra of w from SONIC and C-BIV for three stability conditions.

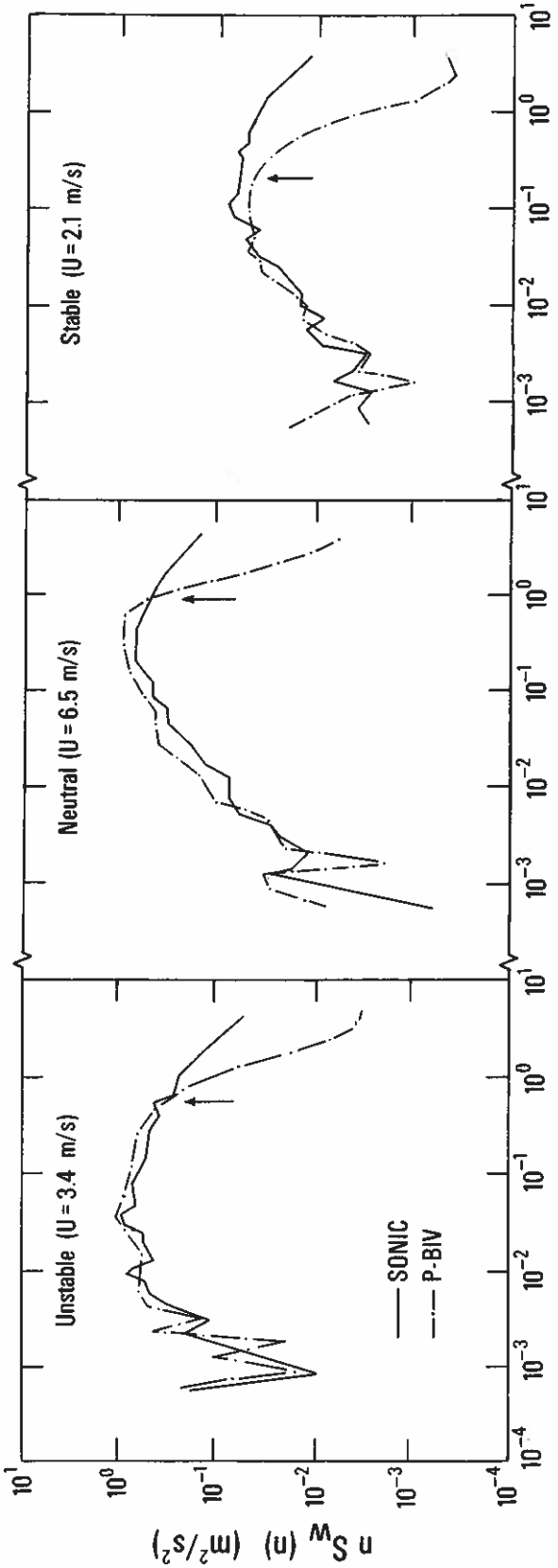

Figure 51. Spectra of w from SONIC and P-BIV for three stability conditions.

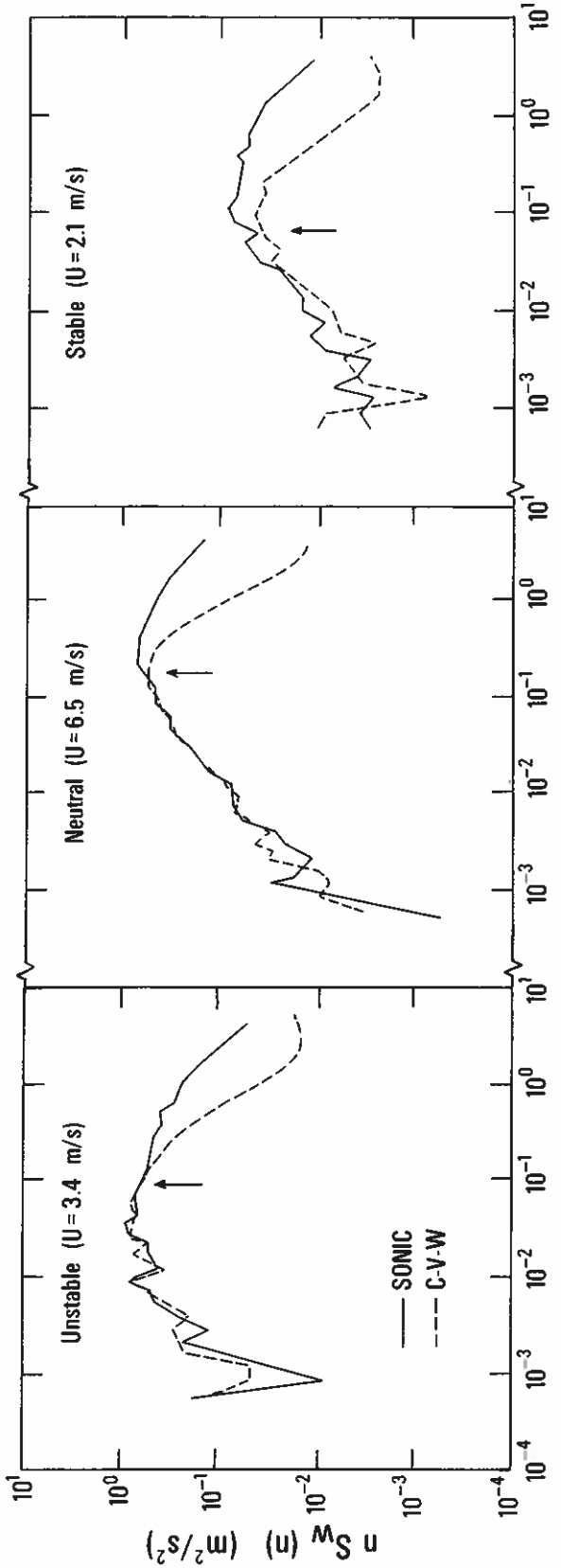

Figure 52. Spectra of w from SONIC and C-V-W for three stability conditions.

with only a small upward adjustment along the ordinate.

The overestimation in bivanes shows up very clearly in Fig. 53(a). Underdamping explains the increase near λ_c, the cut-off frequency, but the continued overestimation at lower frequencies remains a puzzle. Low-frequency energy in the horizontal fluctuations appears to be finding its way into the measured w component. Two possible paths come to mind: one through the gyro effect from the rotation of the propeller, and the other through 'cross-talk' from misalignment of the fins in the bivanes.

Leif Kristensen[1] (private communication) has investigated both those possibilities. His calculations show the gyro effect to be no more than 1% for the lightweight propeller in P-BIV. The misalignment effect, on the other hand, does not lend itself to a simple theoretical treatment. Kristensen's linear model, with two coupled second-order differential equations, could not account for the cross-talk produced by non-restoring forces on the fins. For now, we are left without a definitive explanation of the bivane's behavior.

Of the two bivanes, C-BIV has the better wavelength response, presumably because of its lighter construction. Dependence on the slower cup anemometer for its wind speed information has had little effect on C-BIV's w response. (This conclusion is supported by the fact that the transfer function for w follows ϕ and not the speed.) These favorable results notwithstanding, we had found earlier that C-BIV's bias for σ_w was the largest and P-BIV's the smallest (see Table 7 and Figs. 30 and 31), which shows that an enhanced high-frequency response does not necessarily imply better accuracy.

---

[1]Risoe National Laboratories, Roskilde, Denmark.

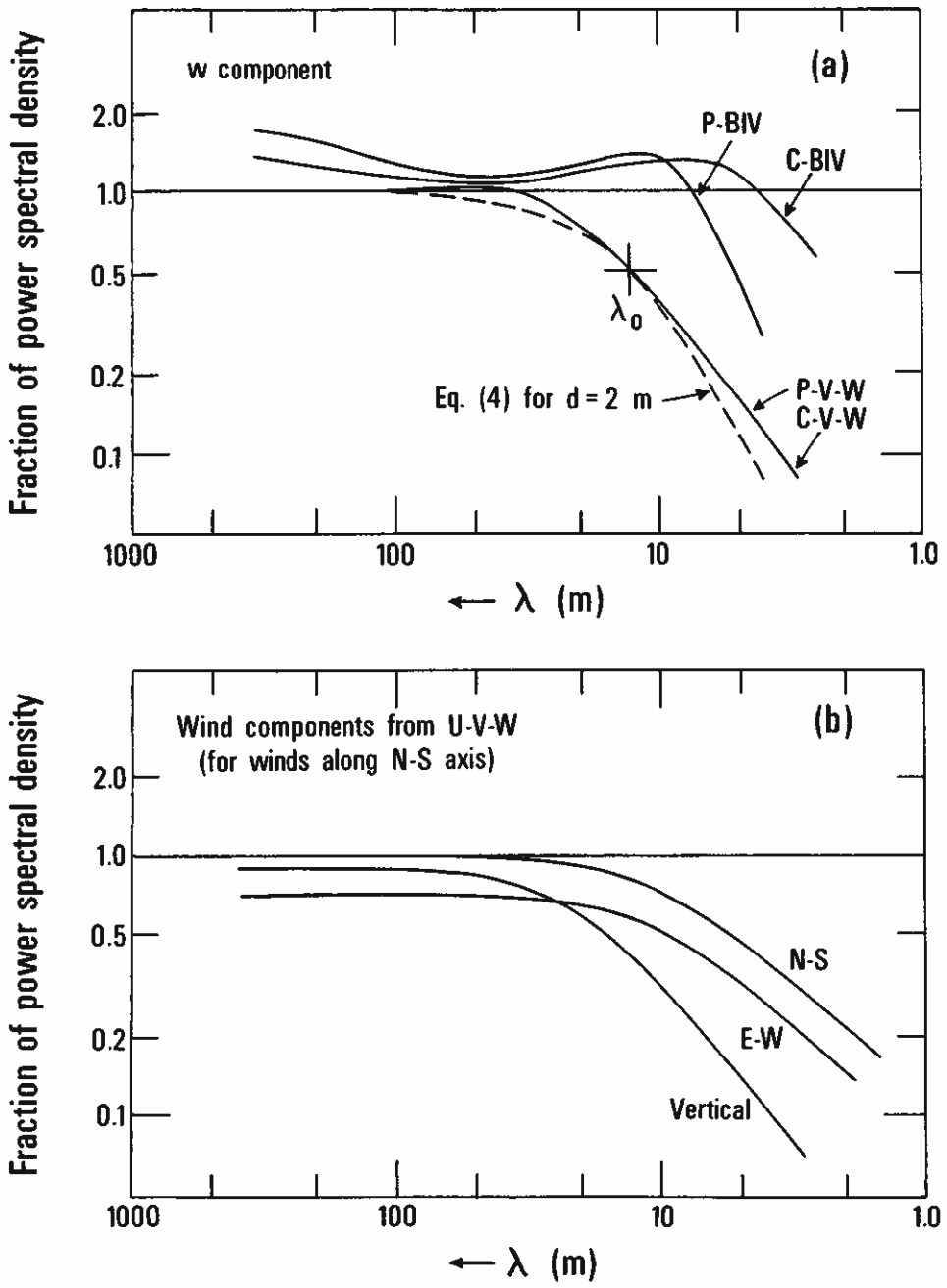

Figure 53. Transfer functions for (a) w response in C-BIV, P-BIV, C-V-W and P-V-W and (b) three-axis response in U-V-W.

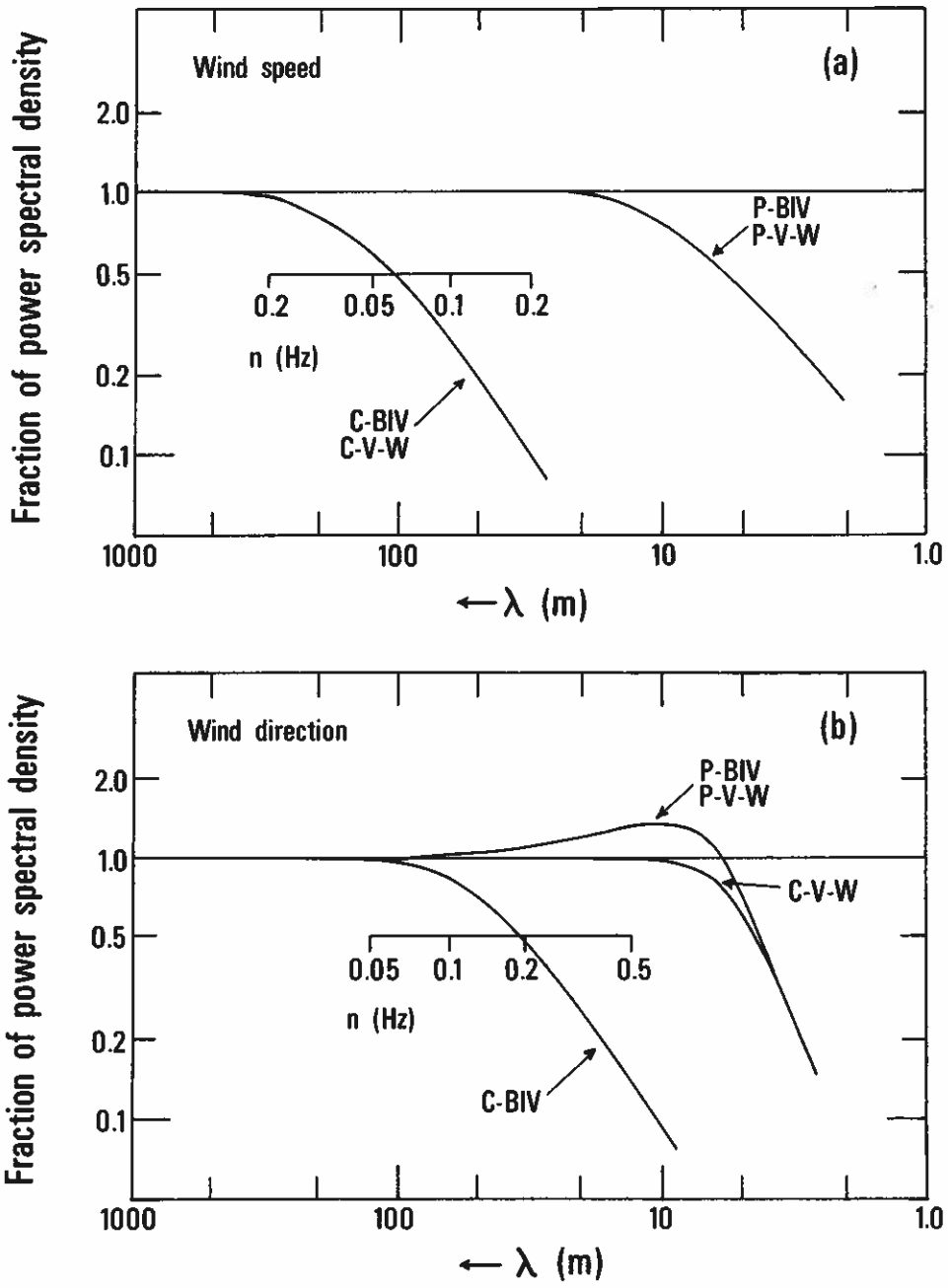

Figure 54. Transfer functions for (a) wind speed response and (b) wind direction response in the in situ sensors. Frequency scales apply only where sensor response is controlled by filtering in the translator circuit (see text). Frequency and wavelength scales match at U = 6.5 m/s.

The poor wavelength response of the w propeller (Fig. 53) is, at first glance, surprising, especially in view of the small distance constants (~1 m) reported from wind tunnel tests. But the discrepancy may not seem so serious if we recognize that (1) advertised distance constant is for flow in the axial direction, (2) distance constant increases from 1 to 2 m as the flow deviates from axial to 80° off axis (approaching infinity at 90°), and (3) factors as large as $4\pi^2$ can exist between the existing distance constant and the wavelength at which the sensor response begins to degrade.

The propeller response is often represented by a first order differential equation with a response function of the form

$$T(\lambda) = \frac{1}{1 + (2\pi d/\lambda)^2} , \qquad (4)$$

where $T(\lambda)$ is the power transfer function and d is the distance constant or the length of travel of the wind before the sensor attains 63% of a step wind change. This transfer function has a half-power wavelength, λ_o, at $\lambda = 2\pi d$ and a 98% power wavelength, λ_c, at $\lambda \approx 2\pi\lambda_o$. Thus,

$$\lambda_c = 2\pi\lambda_o = 4\pi^2 d \quad . \qquad (5)$$

The dashed curve in Fig. 53(a) represents Eq. (4) for a sensor with d = 2 m. This curve differs somewhat from the actual response curve for the propeller, but their respective λ_o's coincide. The predicted λ_c is larger by a factor of 2.5 than the observed λ_c (≈32 m). The attenuation in the observed w variance can still be significant. Daytime variances are smaller by a factor of 20% and nighttime variances by 50%, measured at 10 m height (see Table 15). These percentages are quite similar to the 30% and 60% attenuations, respectively, predicted by Horst (1973).

Table 15. Average of w variances (m^2/s^2) for unstable and stable conditions

Period (MST)	U-V-W	C-BIV	P-BIV	SONIC	C-V-W	P-V-W	N
0800-1540	0.208	0.326	0.332	0.286	0.226	0.225	24
1600-2300	0.024	0.065	0.053	0.063	0.031	0.032	22

N = number of 20 min variances averaged

The w propeller in U-V-W responded somewhat differently from the propellers in C-V-W and P-V-W. In Fig. 53(b), the w curve is slightly depressed, possibly due to a higher response threshold from bearing friction. For the E-W propeller, the observed depression can be attributed to a degraded response for winds that were predominantly N-S. The curve for the N-S sensor thus represents the true axial response of the propeller.

Figures 54(a) and (b) show the response functions for wind speed and wind direction. In both plots a frequency scale is inserted (positioned to match the λ scale at U = 6.5 m) to accommodate sensors that have roll-offs controlled by the time constants of the filters in their translator circuits. The response of the sensors themselves would have followed the λ scaling, but the filter time constant predominates in all cases. The reason for the nearly identical bias and comparability figures for C-BIV and C-V-W (Table 2) is now clear: the two systems have identical filters on them. Transfer functions for P-BIV and P-V-W are also identical, which is not surprising in view of their similar construction. Both systems show a λ_c of approximately 20 m, the same as for the N-S propeller in U-V-W.

As for wind direction, only C-BIV follows frequency scaling, because of the time constant of the filter that was inadvertently left in the θ translator. The filter in C-V-W's θ translator, on the other hand, was removed prior

to the experiment; C-V-W's response is therefore comparable with that of P-BIV and P-V-W. The effect of the filter on σ_θ measurement, as reflected in the bias values of Table 4, is not significant.

11. CONCLUSIONS

The results of the experiment demonstrate the best one can expect from conventional wind-monitoring systems, when careful attention is given to calibration and installation. Our findings can be summarized as follows:

1. Mean wind speed measurement seem the most reliable. They are subject to little, if any, overspeeding from the cup anemometers. However, mean wind direction measurements show scatter of about 5°, larger than expected.

2. Standard deviations σ_θ and σ_ϕ are measured with reasonable accuracy (scatter of ±3° in σ_θ, ±2° in σ_ϕ). The scatter increases linearly with magnitude up to a point (50° in σ_θ, 15° in σ_ϕ).

3. When transfer functions for w are compared, a clear difference emerges between the bivanes and the propellers. The bivanes tended to overestimate w but also responded to wavelengths as short as 4.4 m. The propellers did not overestimate w, but neither did they respond well to wavelengths shorter than 32 m. Intermittent stoppage of the propeller was probably responsible for the drop in spectral levels observed in the light wind stable case. The response to ϕ is the same as for w.

4. Sigma meter performance degrades with increasing turbulence. The digital meter shows smaller bias and less scatter than the analog meter in most cases.

REFERENCES

Busch, N. E., and L. Kristensen, 1976: Cup anemometer overspeeding. J. Appl. Meteor., 15, 1328-1332.

Hoehne, W. E., 1971: Standardized functional tests. NOAA Tech. Memo. NWST&EL-12, Sterling, VA. U.S. Department of Commerce. 23 pp.

Horst, T. W., 1973: Corrections for response errors in a three-component propeller anemometer. J. Appl. Meteor., 12, 1072-1075.

Izumi, Y., and M. L. Barad, 1970: Wind speeds measured by cup anemometers and influenced by tower structure. J. Appl. Meteor., 9, 851-856.

Kaimal, J. C., J. E. Gaynor, P. L. Finkelstein, M. E. Graves and T. J. Lockhart, 1984: An Evaluation of Wind Measurements by Four Doppler Sodars. BAO Report No. 5, Wave Propagation Laboratory, NOAA/ERL, Boulder, CO 80303. 110 pp.

Kaimal, J. C., and J. E. Gaynor, 1983: The Boulder Atmospheric Observatory. J. Appl. Meteor., 22, 863-880.

APPENDIX

Audit of Sensor Calibration

An audit was conducted in the vicinity of the Boulder Atmospheric Observatory (BAO) operated by NOAA on 3 and 4 September 1982 for Thomas J. Lockhart.

3 September 1982 Calibration of a Gill U-V-W propeller anemometer Model 27005, Serial 1005 equipped with 19 cm diameter polystyrene propellers.

The procedure used was to remove the propeller and rotate the shaft with a battery powered motor at approximately constant speed, monitored with a counter. The counter output was recorded and compared with the computer indicated speed. It was possible to monitor the voltage signal output of the interface which was sent to the analog-to-digital converter, and the raw digital count output by the ADC. It is a good practice to check calibration in as complete a manner as possible as was done here. In this way, one does not rely upon the calibration of the ADC or upon having the correct calibration in the computer. These happened to be correct because the BAO facility is very well run but it is not a good idea to rely upon these things. The raw count was converted by the computer to physical units by application of the following polynomial (used for both U and V):

$$y = 0.0061035\ x - 30$$

where x = raw count from the ADC and y = scaled data. Table 1 lists the counter values which were taken to be the calibration reference values and the scaled computer output (y values). The counter data were converted to meters/sec using the following equation:

$$s = 0.30\ k/60$$

where k is the counter output in revolutions/minute (RPM) and s is the speed in meters/sec. The constant 0.30 is the pitch of the propeller (0.30 meters/revolution) and the 60 converts the time base from minutes to seconds.

The BAO convention is that South and West components are taken to be positive.

The errors listed are the observed values minus the true values.

Note the W-component was not checked.

Table 1. Calibration of Gill U and V propellers. All speeds are in units of meters/sec. Observed data are as indicated by the computer. Times are MST. The direction of rotation is indicated as clockwise (CW) or counterclockwise (CCW).

Time	Observed	Calib.	Rotation	Comp.	Error
1342	1.51	1.50	CCW	U	0.01
1343	1.50	1.50	CCW	U	0.00
1358	1.50	1.51	CCW	U	-0.01
1359	1.51	1.51	CCW	U	0.00
1400	1.51	1.52	CCW	U	-0.01
1401	1.51	1.52	CCW	U	0.01
1402	1.50	1.51	CCW	U	-0.01
1403	1.49	1.51	CCW	U	-0.02
1406	-1.52	1.52	CW	U	0.00
1407	-1.52	1.52	CW	U	0.00
1408	-1.53	1.50	CW	U	-0.03
1409	-1.51	1.50	CW	U	-0.01
1410	-1.52	1.50	CW	U	-0.02
1411	-1.53	1.50	CW	U	-0.03
1414	-2.87	2.87	CW	U	0.00
1415	-2.88	2.87	CW	U	-0.01
1420	-1.45	1.52	CW	V	0.07
1421	-1.44	1.52	CW	V	0.08

4 September 1982 Calibration of the elevation angle of the MRI bivane and the R. M. Young bivane.

The bivanes were removed from the mast and set on their mounting plates. The elevation angle was set using jigs provided by the manufacturer. As above, the observed data presented in Table 2 are the computer output.

Table 2. Calibration of MRI and R. M. Young bivane elevation angles. Times are recorded to the nearest minute, all angles are recorded to the nearest degree.

Time	MRI Obs.	True	Error	R. M. Young Obs.	True	Error
				Adjusted R. M. Young bivane		
0803	0	0	0	0	0	0
0805	15	15	0	17	15	2
0808	30	30	0	32	30	2
0810	45	45	0	51	45	6
0812	0	0	0	1	0	1
0814	-15	-15	0	-15	-15	0
0816	-30	-30	0	-30	-30	0
0818	-45	-45	0	-39	-40	1
				Adjusted R. M. Young bivane		
0829				0	0	0
0830				15	15	0
0831				31	30	1
0832				50	45	5
0834				41	40	1
0835				1	0	1
0837				-15	-15	0
0838				-30	-30	0
0839				-39	-40	1

Note that the R. M. Young bivane was aligned before the calibration procedure was started and again before repeating the procedure. The adjustment of this bivane was difficult and appeared to shift. Also the Young calibration fixture was not as good as the MRI fixture. It was more difficult to use and

Table 3. Calibration of the R. M. Young bivane azimuth

Time	Observed	True	Error
0844	181	180	1
0845	210	210	0
0846	240	240	0
0847	269	270	-1
0848	299	300	-1
0849	329	330	-1
0850	350	350	0
0853	35	30	5
0854	64	60	4
0855	94	90	4
0856	123	120	3
0857	152	150	2

The two temperature sensors mounted on the mast assembly to measure temperature difference between the top and the bottom were removed and inserted into a thermal mass at about 0950. The thermal mass gradually warmed during the day and the results were monitored by the computer. The average difference was 0.09°C with the top sensor being the warmer. The sensors were well matched, with almost identical time constants.

In general, the calibration check went smoothly. It was evident that the sensors had all been carefully aligned and calibrated before the audit commenced. As noted above, the BAO facility is maintained very well and the computer system used to log the data was working well. This was an easy audit. However, it should be noted that there was considerable difficulty with the R. M. Young bivane. It was difficult to align and the calibration indicated considerable error. It is beyond the strict scope of this audit to speculate about probable long term calibration shifts but it would not be surprising to find that this bivane had shifted during the project.

This audit did not treat one aspect of the propeller anemometer performance, the cosine correction. R. M. Young data supplied with the propeller anemometers indicates that these propellers deviate from the desired cosine response. The worst case is when the wind vector is aligned about 45 degrees from the propeller axis. In that case the propeller underestimates the wind component by up to 20%. There was no indication that any cosine correction was being applied during the time of the audit. It would be possible, of course, to apply this correction later.

Audited by Fred V. Brock 

☆U.S. GOVERNMENT PRINTING OFFICE: 1985–576-000/20,004